Ultraviolet B and Blue Light - Induced Phototoxic Effects on Retinal Pigment Epithelium Using *In Vitro* Assays

by

Hyun-Yi Youn

A thesis

presented to the University of Waterloo

in fulfillment of the

thesis requirement for the degree of

Doctor of Philosophy

in

Vision Science and Biology

Waterloo, Ontario, Canada, 2008

©Hyun-Yi Youn 2008

Author's Declaration

I hereby declare that I am the sole author of this thesis. This is a true copy of thesis, including any required final revisions, as accepted by my examiners.

I understand that my thesis may be made electronically available to the public.

Abstract

It is well known that ultraviolet (UV) B (280-315 nm) and blue light (400-500 nm) radiation can produce phototoxic lesions in the neural retina and the retinal pigment epithelium (RPE). In the first section of this thesis, bovine lens cells (epithelium and superficial cortical fibre cell) and human retinal pigment epithelial (ARPE-19) cells were used to characterize *in vitro* changes following oxidative stress with UVB radiation in ocular lens optics and cellular function in terms of mitochondrial dynamics. In the second part, human retinal pigment epithelial (ARPE-19) cells and *in vitro* bioassays were used together to develop an *in vitro* approach for UV radiation-induced retinal toxicology research. In the third chapter, the *in vitro* approach developed above was used with intraocular lens (IOL) materials to evaluate the UV radiation blocking efficiency of commercially available IOL's. Lastly, narrowband blue light irradiation and *in vitro* assays were used to determine more precisely the wavelengths of blue light responsible for photochemical lesions of the retina as an effort to contribute to future IOL designs.

The results from mitochondrial dynamics of lens cells and RPE cells show significant decreases in mitochondrial movement after UVB irradiation in a dose dependent manner. Results obtained from four *in vitro* assays (Alamar blue assay, confocal microscopy for mitochondrial distribution and nucleic acids damage, phagocytotic activity assay) for evaluating the UVB-induced damage in ARPE-19 show significant decreases in cell viability as well as phagocytotic activity of RPE cells after UVB radiation. In addition, the results show that UV radiation can also induce the degradation of DNA/RNA and mitochondria of RPE cells in a dose dependent manner.

The results of the UV blocking efficiency test of commercially available IOL materials show very effective UV blocking ability, allowing no cellular damage at all, in comparison to an IOL uncovered control cell. The results of three different wavelengths of blue light exposure show that only 400 nm blue light radiation can cause significant damage to RPE cells, while 420 and 435.8 nm blue light radiation cause no cellular damage at all.

In conclusion, UVB and blue light radiation can cause phototoxic damage to the retinal pigment epithelium as a result of oxidative stress, and *in vitro* bioassays used for this research may offer a sensitive, and meaningful biomarker approach, not only for evaluating RPE function after oxidative and chemical stress, but also for evaluating IOL effectiveness.

Acknowledgements

I would like to thank my supervisor, Dr. Jacob Sivak for his great guidance, valuable advice, and total support. Dr. Sivak encouraged me to keep on pursuing my interest in scientific research.

I would like to also thank my committee members, Dr Anthony P. Cullen and Dr. Niels C. Bols for their help and guidance.

Thanks are also due to Dr. Ralph B. Chou and Dr. Vladimir Bantseev for their technical support.

I would like to acknowledge all my fellow graduate students from both the Sivak and Bols labs for providing a supportive research environment and donating their time to offer assistance and advice.

I would like to also express deep appreciation to my husband Sung-Wook Jeen, and my son Brian Yoonwoo Jeen for their love, endurance and support.

This research was supported by the Natural Sciences and Engineering Research council of Canada, and Bausch & Lomb, Inc., Rochester, NY, USA.

Table of Contents

List of Figures

List of Tables

List of Animations *

* Animations are available from the website.

http://www.annalsnyas.org/cgi/reprint/1091/1/17

List of Abbreviations

ACGIH	American Conference of Governmental Industrial Hygienist
ANOVA	analysis of variance
ARMD	age-related macula degeneration
ATCC	American Type Culture Collection
ATP	Adenosine-5'-triphosphate
BVD	back vertex distance
CCCP	carbonyl cyanide *m*-chlorophenylhydrazone
CFCs	chlorofluorocarbons
CLSM	confocal laser scanning microscope
DMEM	Dulbecco's Modified Eagle's Medium
DNA	deoxyribonucleic acid
DRP1	dynamin-related protein 1
dsDNA	double strand deoxyribonucleic acid
EDTA	ethylenediaminetetraacetic acid
FWHM	full width at half maximum
HEPES	N-2-hydroxyethylpiperazine-N'-2-ethanesulfonic acid
IOL	intraocular lens
ITS	insulin-transfferin-sodium selenite
NADH	nicotinamide adenine dinucleotide
PBS	phosphate buffered saline
PMMA	polymethyl methacrylate

PRA	Photochemical Research Associates
RCS	Royal College of Surgeons
RNA	ribonucleic acid
ROS	reactive oxygen species
RPE	retinal pigment epithelium
SEM	standard error of the mean
TMRE	tetra methyl rhodamine ethyl ester
TUNEL	terminal deoxynucleotidyl transferase biotin-dUTP nick end labeling
UV	ultraviolet
UVA	ultraviolet A
UVB	ultraviolet B
UVR	ultraviolet radiation

General Introduction

The neural retina detects the retinal image and transforms light energy into a communicable form of chemical energy. The retina is the innermost layer of the eyeball and it is made up of cells with vastly different functions. The outer monolayer is known as the retinal pigment epithelium (RPE), and inside of this is the inner neurosensory retina, which consists of photoreceptor cells, bipolar cells, ganglion cells, horizontal cells, amacrine cells, and interplexiform cells.

RPE cells are polarized epithelial cells. Long microvilli interdigitate on their apical surfaces with the outer segments of photoreceptor cells, whereas their basal surfaces, which are formed with many infoldings, are adjacent to Bruch's membrane.[1] The RPE is not directly involved in the neural events of vision, but it plays a critical role in the normal functioning and well-being of the photoreceptors.[2] RPE cells play a role in the phagocytosis of photoreceptor outer segment tips, and a major role in the regeneration of visual pigments.[1] Further, the presence of intracellular melanin granules is thought to increase photoreceptor efficiency by absorbing excess, scattered light.[1] RPE cells of many species also contain oil droplets in which vitamin A (retinol) is stored.[1] Vitamin A is a necessary metabolite for the visual cycle.

Optical radiation includes ultraviolet radiation (UVR, 100-400 nm), visible light (400-750 nm), and infrared radiation (750-10,000 nm).[3] UVR has been subdivided into UVC (100-280 nm), UVB (280-315 nm), and UVA (315-400 nm).[4] Visible light is

referred to as short- (blue, 400-500 nm), medium- (green, 500-620 nm), and long-wavelength (red, 620-750 nm) radiation.[5]

The depletion of ozone increases the levels of UVR, particularly UVB, reaching the Earth's surface.[4] Exposure to solar UVR has been implicated in skin and ocular pathologies. The cornea and the lens of the eye substantially filter and attenuate UVR that reaches the retina,[6] but depletion of the ozone layer, in combination with the increase in outdoor recreation and average span of life, may result in an increase in the accumulative lifetime exposure of the retina to UVR.[7] Also, the removal of the crystalline lens by cataract surgery may be associated with a substantial increase in the UVR that reaches retina.[8]

The term blue is often used for the broad range of optical radiation between 400 and 500 nm, and the blue-light hazard is defined as the potential for photochemical induced retinal injury resulting from radiation exposure at wavelengths between 400 nm and 500 nm.[9] It has been speculated that blue light may cause retinal damage or contribute to the development of age-related macular degeneration (ARMD).[10,11] Animal experiments show that retinal exposure to excessive levels of blue light induce photochemical damage of photoeceptor and RPE cells.[12,13]

Cataract, an opacification of the lens, is the most common cause of blindness in the world and there are currently no strategies to prevent it.[14] It is usually associated with aging. There are three major types of senile cataract: 1) nuclear cataract, or a cataract of the nucleus of the lens; 2) cortical cataract in the surrounding cortex; and 3) posterior subcapsular cataract, which occurs beneath the posterior capsule of the lens. Other

causes of cataract are associated with systemic diseases, such as diabetes,[15] galactosemia,[16] microwave or ionizing radiation,[17] trauma and the use of photosensitizing drugs,[18] and UV light.[19]

At present, there is no way to eliminate a cataract other than surgically removing it. Virtually everyone undergoing cataract surgery will have a plastic lens implant (intraocular lens, IOL) placed in the eye to replace the crystalline lens. IOLs were initially fabricated from polymethyl methacrylate (PMMA) without UVAbsorbing chromophores.[20] The dangers of retinal exposure to near-UVR transmitted by clear PMMA IOLs were recognized in 1978,[21] and IOL with UVR blocking chromophores bonded to optic polymers were introduced in the early 1980s.[22,23] However, some modern intraocular lenses still have inadequate UV and light protection.[24,25] Besides, nonfoldable PMMA IOLs that absorb blue as well as UVR were introduced in the 1990s,[26] and the first foldable (made of silicone or acrylic) blue light absorbing IOL were introduced in 2003.[27] Many clinical experiments and evidence from experimental studies show that IOLs increase light exposure of the retina.[8,24,28]

The focus of this dissertation is the development of an *in vitro* model of retinal UVR and blue light protection. An *in vitro* model of retinal UV and blue light protection is needed as results of the increase in energy accumulative lifetime exposure of the retina to UV radiation, the increased concern of blue light hazard, and the fact that crystalline lens protection is lost in cataract surgery without appropriate IOL protection.

The approach involves the exposure of a retinal cell culture to UVB and blue light radiation. After exposure, bioassays for cellular viability, mitochondrial damage and

dyamics, nuclei (DNA/RNA) damage, and phagocytotic activity are quantified using the Alamar blue assay, mitochondrial dynamics evaluation, confocal microscopy with two fluorescent (Rhodamine123 and Acridine Orange) staining methods, Hoechst assay, and phagocytotic activity assay.

Chapter 1

Mitochondrial "Movement" and Lens Optics Following Oxidative Stress from UVB Irradiation: Cultured Bovine Lenses and Human Retinal Pigment Epithelial Cells (ARPE-19) as Examples

Vladimir Bantseev[1], Hyun-Yi Youn[1]

[1]School of Optometry/Department of Biology, University of Waterloo, Waterloo, ON, Canada

Chapter 1 was published in Annals of the New York Academy of Sciences, December 2006 Vol.1091 (p.17-33). This was a collaborative effort between Hyun-Yi Youn and Dr. Bantseev in which Dr Bantseev provided the initial idea and effort related to the study of the dynamics of mitochondria while I contributed mainly to the RPE portion of the study. The paper was written by both of us.

1.1 Introduction

The key function of mitochondria is energy production through oxidative phosphorylation and lipid oxidation.[1] The process takes place within the mitochondrial inner membrane and includes five multi-subunit enzyme complexes. Several other metabolic functions are performed by mitochondria, including urea production and heme, non-heme iron and steroid biogenesis, intracellular Ca^{2+} homeostasis as well as interaction with the endoplasmic reticulum. For many of these mitochondrial functions, there is only a partial understanding of the components involved, with even less information on mechanisms and regulation.[2]

The vertebrate lens is a cellular structure responsible for fine focusing of light on the retina. The lens consists of two types of cells organised in distinct spatial patterns: the epithelial monolayer that covers the anterior surface and fibre cells that comprise the bulk of the lens. Cell division in the lens is restricted to the equatorially located epithelial cells which give rise to terminally differentiated fibre cells in a process that continues through life.[3] Early electron microscopy studies of mitochondria of vertebrate lenses showed an absence of mitochondria in lens fibre cells and the presence of very few, short mitochondria in the epithelial cells.[4] It became widely accepted that the lens epithelium plays the most important role in lens metabolism.[5] In recent years understanding of mitochondrial morphology and distribution has been enhanced by advances in confocal microscopy that permits imaging of living cells with the aid of fluorescent dye technology. Recent studies using specific fluorescent dyes and confocal microscopy of rat,[6] fish[7] and bovine lenses[8, 9] show that superficial cortical fibre cells contain numerous

metabolically active mitochondria, suggesting that the superficial cortical fibre cells play a much more active role in lens metabolism than previously suspected.

Recognition of the role of mitochondria in processes such as apoptosis and calcium homeostasis has sparked a renewed interest in mitochondrial research. As a by-product of respiration, the electron transport chain is known to be the major intracellular site for the generation of reactive oxygen species (ROS). Oxidative damage to the mitochondria has been experimentally demonstrated to cause an elevation in mitochondrially produced ROS.[10] Such mitochondrial changes have been manifested morphologically by the presence of short swollen mitochondria. Experimental lens damage has been found to correlate well with lens anatomy and with the integrity and activity of mitochondria found in the epithelium and superficial fibre layers of the lens.[8, 9]

The lens represents a very useful model to study mitochondria. Even though the mitochondria are restricted to a minute portion of the lens, namely the epithelial and superficial cortical fibre cells, they play an important role in maintaining lens transparency. Our previous studies have showed that following treatment with the mitochondrial uncoupler carbonyl cyanide *m*-chlorophenylhydrazone (CCCP), rat[6] and bovine[8] lenses developed opacities. Similarly bovine lenses treated with sodium dodecyl sulfate[9] showed a decrease in mitochondrial length and numbers and at the same time developed opacities, suggesting that mitochondria and lens optical quality are correlated. Our recent study, using confocal microscopy, was undertaken to image the movement of live mitochondria of bovine lens epithelial and superficial cortical fibre cells.[11] Using the mitochondria-specific dye tetra methyl rhodamine ethyl ester (TMRE), mitochondrial movement was acquired using confocal laser scanning microscopy by imaging the intact

lens equatorial region for 3 to 5 minutes. Bi-directional dynamic movement of mitochondria with frequent reversals was observed in both epithelial and superficial cortical fibre cells of live bovine lenses. In the epithelium, this movement was up to 5μm/min whereas in the superficial cortex the observed movement was up to 18.5μm/min. The movement was abolished following treatment with CCCP. Whether the movement is true motion, or movement of TMRE across a mitochondrial network representing change in the distribution of potential across the inner membrane, presumably allowing energy transmission across the cell from regions of low to regions of high ATP demand, remains unclear.

Several epidemiological studies have showed a correlation between UV radiation and cataract development.[12] Once the lens is removed, the intraocular lens may not offer sufficient protection[13] and the retina may receive an increased amount of UV radiation. Earlier[14] and more recently[15] experimental investigations showed that UV irradiation affects the optics of bovine lenses. The retinal pigment epithelial cells, having the same embryonic origin as neurosensory retina have been recently used as an *in vitro* retinal model to study the molecular mechanisms following UV radiation.[16] Cellular and molecular mechanisms of UV damage on lens or retinal tissue are still not clear. Moreover, less is known as to how the mitochondria are affected. The purpose of this study was to characterize *in vitro* changes following UVB radiation in terms of mitochondrial dynamics of bovine lens epithelium and superficial cortical fibre cells and human retinal pigment epithelial (ARPE-19) cells.

1.2 Materials and Methods

All chemicals were obtained from Sigma Chemical Co. (St. Louis, MO), unless indicated otherwise. Mitochondria-specific fluorescent dye Rhodamine-123 was obtained from Invitrogen Canada Inc. (Burlington, ON).

1.2.1 Bovine Eye Dissection and Lens Culture

Bovine eyes, obtained from a local abattoir, were dissected and the lenses were excised within 1-5 hours post-mortem under sterile conditions, as described previously.[9] Briefly, the lenses were suspended on a bevelled washer (14 mm inner diameter) in a three-part chamber (made from glass, silicon rubber and a metal base) filled with 21ml of culture medium consisting of Medium 199 with Earle's salts, 100 mg/L L-glutamine, 3% dialysed fetal bovine serum, 2.2 g/L sodium bicarbonate, 5.96 g/L HEPES and 1% antibiotics (100 units/ml penicillin and 0.1 mg/ml streptomycin). Lenses were then pre-incubated at 37^0C with 95% air and 5% CO_2 for 24 hour prior to experimental use to ensure that lenses damaged during dissection were excluded from the study.

1.2.2 Human Retinal Pigment Epithelial Cell Culture

The human ARPE-19 cell line, originally obtained from American Type Culture Collection (ATCC), was kindly provided by Dr. R. Tchao, University of the Sciences in Philadelphia. ARPE-19 cells were plated in glass bottom culture dishes (MatTek

Corporation, Ashland, MA) at low density and cultured in DMEM/Ham's F-12 50:50 mixture supplemented with L-glutamine and 15mM HEPES (Mediatech, Herndon, VA), 10% fetal bovine serum (Hycolone, Logan, UT), and insulin-transferrin-sodium selenite media supplement (ITS supplement). The cell line was then grown to be at least 70% confluent in a humidified incubator with 95% air and 5% CO_2 at 37^0C. To maintain the optimal growth conditions, the physiological solution was changed every 24 hours.

1.2.3 UVB Irradiation of Cultured Bovine Lenses and ARPE-19 cells

Exposure to ultraviolet radiation (UVB) was produced by filtering banks of UV fluorescence tubes in a custom designed UV irradiation unit with 95% air and 5% CO_2 as described previously.[15] Briefly, before irradiation, the UV source was calibrated with an Instaspec II diode-array spectroradiometer (Oriel Corporation, Stratford, CT). Cultured bovine lenses and at least 70% confluent ARPE-19 cell monolayer were then irradiated at 37^0C with 1.0 and 0.5 J/cm^2 of broadband UVB (290 - 320 nm), with the calculated biologically effective radiant energy levels of 0.445 and 0.223 J/cm^2, respectively. The UV source was positioned directly above the lenses or cells. In order to minimize absorption of the radiation by the medium, during irradiation the medium was removed except for a 1.0 mm layer that covered either the bovine lenses or the ARPRE-19 cells. Following the radiation, the previously removed medium was replenished immediately with fresh warm stock.

1.2.4 Analysis of Lens Optical Properties-Spherical Aberration

Lens optical quality (spherical aberration) was assessed using the Scantox™ *in vitro* automated laser scanning system developed at the University of Waterloo before exposure and daily for 14 days after the irradiation at approximately the same time each day. In order to provide optimal conditions, the culture medium was changed every 48 hours. The Scantox™ *in vitro* automated laser scanning system consists of a collimated laser source that projects a laser beam onto a plain mirror mounted at 45^0 on a carriage assembly. This mirror reflects the laser beam directly up through the scanner table surface and through the lens under examination. The mirror carriage is connected via a drive screw to a positioning motor. This positioning motor turns the drive screw and thereby moves the laser in user-defined steps across the lens in an automated fashion. A digital camera captures the actual position and slope of the laser beam at each step. When all steps have been made, the captured data for each step position is used to calculate the back vertex distance for each position and the difference in that measurement between beams. A series of 22 laser beams, passed at increments of 0.5mm, for a total range of 11mm are projected through the lens. The results for this part of the study involved 9,900 objective optical measurements (30 lenses, 15 scan points, 22 beams).

1.2.5 Confocal Laser Scanning Microscopy

To investigate mitochondrial morphology and movement, the mitochondria-specific fluorescent dye Rhodamine 123 was used. Rhodamine 123 is a lipophilic cell-permeable, cationic non-toxic fluorescent dye that specifically stains live mitochondria.

Rhodamine 123 is accumulated specifically by the mitochondria in proportion to membrane potential. At various time intervals the morphology, distribution and movement of the mitochondria were analysed immediately (n=3 for each group), and after treatment at 7 (n=3 for each group) and 14 days (n=3 for each group) in bovine lenses. For ARPE-19 cells, the analysis was carried out immediately (n=2 glass bottom culture dishes for each group) or 1 (n=2 for each group) and 2 days (n=2 for each group) days after radiation. For confocal microscopy, samples were loaded with Rhodamine 123, by bathing them for 15 minutes at room temperature in either 10ml serum-free M199 (bovine lenses) or 3ml serum-free DMEM/Ham's F-12 50:50 mixture (ARPRE-19 cells) containing 20μm Rhodamine 123, and rinsed. For confocal microscopy imaging, bovine lenses were then immobilised in 1% agarose on glass bottom plates as described previously,[11] whereas ARPRE-19 cells were imaged in glass bottom plates without agarose. Time series of bovine lens epithelial and superficial cortical fibre cells as well as ARPE-19 cells were acquired with a Zeiss 510 (configuration Meta 18) confocal laser scanning system (Carl Zeiss Inc., Toronto Canada) equipped with an inverted Axiovert 200M microscope and a high numerical aperture 40-x water-immersion C-Apochromat objective (NA 1.2). The combination of a 488nm Argon laser and 505 long pass emission filters were used to visualise Rhodamine 123 fluorescence. Subsequent image analysis (such as the number and length of mitochondria and rate of movement) was achieved using commercial LSM510 VisArt and Physiology software packages (Carl Zeiss Inc., Jena, Germany) and Image Analysis toolbox of MatLab 7.1 software package (MathWorks Inc., Natick, MA). The representative length of mitochondria was measured from one end of the most visible structure to the other end using the measure function of

the software. The rate of movement (expressed in μm/min) was determined by noticing the initial position (position zero) of moving mitochondria in the first X, Y gallery of time series, to the final movement observed during the time series by measuring the length in microns (μm).[11]

1.2.6 Statistical Analysis

Statistical analyses were carried out using either one- (number and length of the mitochondria) or two-way repeated (lens optics) measures of ANOVA, calculated by SAS® 9.1 statistical software (SAS Institute Inc., Cary, NC). Data were considered significantly different at probability levels equal to or less than 0.05. The difference was recorded numerically with all results expressed as mean ± standard error of the mean (SEM).

1.3 Results

1.3.1 Bovine Lens Optical Function

In total, 30 bovine lenses were scanned, divided into three groups: controls and UVB irradiated, at 1.0 and 0.5 J/cm^2. The lenses were scanned before radiation and daily for 14 days using the automated scanning laser system, Scantox™. Figure 1 shows representative individual scans consisting of 22 laser beams scanned across that of a control (A), 1.0 (B) and 0.5 J/cm^2 (C) treated lenses at day 14 after irradiation. The control group showed little change in the amount of spherical aberration. By examining the data over time across all groups, a latent dose-dependant increase in the amount of spherical aberration (back vertex distance variability) over time was found (Fig. 2). A significant increase in the amount of spherical aberration became evident in the 1.0 J/cm^2 irradiated group lenses starting on day 11 ($p<0.05$). By day 14 in both irradiated groups the amount of spherical aberration was significantly higher then that of controls ($p<0.05$). Moreover, at day 14 the 1.0 J/cm^2 treated group showed an exponential increase in the amount of spherical aberration (over 2.5 times higher value) in comparison that that of the 0.5 J/cm^2 group.

1.3.2 Mitochondrial morphology and movement of controls

In this study the mitochondria of both bovine lenses and APRE-19 cells were stained with specific fluorescent dye, Rhodamine 123. In the epithelium of bovine lenses

strikingly different mitochondrial morphologies could be seen ranging from short, dot-like structures less then 1μm long, to elongated threads, up to 10μm long. When the dot-like mitochondria could be found dispersed throughout the cytoplasm, the elongated dense threads appeared to surround the individual nuclei, filling the bulk of the epithelial cells (Fig. 3A). Occasionally, branching could be seen on those elongated threads. In contrast, in the superficial cortex while short, dot-like mitochondria less then 1μm long were seen, more elongated and not as dense up to 74μm long threads of mitochondria could be seen (Fig. 3B). While occasional branching in these long threads could also be seen, as in the epithelium, the mitochondria were not as dense, and were roughly aligned along the long axis of the superficial cortical fibre cells. The morphology of the mitochondria of ARPE-19 cells was also heterogeneous, with some mitochondria measuring less then 1μm while others were up to 15μm long (Fig. 3C). Frequently branches in those thread-like structures could be seen. While in some cells dense threads of mitochondria could be seen arranged radially around the nuclei, in other cells the threads could be seen loosely arranged throughout the cytoplasm processes without particular reference to the nuclei. Using a MatLab semi-automated image analysis approach we were able to determine the number and the average length of the mitochondria, with values for controls and treated lenses and ARPE-19 cells listed in Table 1.

In order to establish a control base-line, prior to UVB irradiation, the mitochondria of bovine lens epithelial and superficial cortical fibre cells and ARPE-19 cells were monitored by capturing Rhodamine 123 fluorescence over time using confocal laser scanning microscopy. These events were summed for 4 minutes of data acquisition

with 120 frames on average. In the epithelium of bovine lenses the most obvious and rapid movement was seen in the short, dot-like mitochondria. This movement, around the nuclei, was up to 8μm/min (Animation 1). In the superficial cortex apparent movement along the long axis of the cells could be seen in both dot-like short and elongated mitochondria with up to 5μm/min and up to 25μm/min, respectively (Animation 2). In both the lens epithelium and superficial cortex movement of the mitochondria was bi-directional. Similarly, bi-directional movement of short and elongated mitochondria was seen in the ARPE-19 cells measuring up to 3μm/min and 12μm/min, respectively (Animation 3). Moreover, as part of the movement branching was noted in many mitochondria.

1.3.3 UVB Irradiation-Induced Morphological Changes and Alterations in Size and Movement of the Mitochondria

At both UV energy levels studied, morphological changes and alterations in movement of the mitochondria were monitored immediately, 7 and 14 days after irradiation of bovine lenses. Because of rapid cell division, changes in ARPE-19 cells changes were monitored immediately, 1 and 2 days after UVB irradiation. Changes were compared to controls of each group. Immediately following 1.0 J/cm^2 irradiation of lenses perinuclear-arranged threads of mitochondria could be seen resembling that of controls in the epithelium, whereas in the periphery of the cell, numerous short and swollen, nodule-like mitochondria could be seen in contrast to the controls (Fig. 4A, Table 1). Despite the close resemblance to controls, no movement of the mitochondria in

the epithelial cells was seen. Moreover, Rhodamine 123 bleaching was observed 2 min after data acquisition (Animation 4). In the superficial cortical fibre cells while the size of mitochondria was similar to that of controls, small numerous vacuoles scattered throughout cytoplasm could be seen (Fig. 4B, Table 1). Movement of the mitochondria in the superficial cortical fibre cells was only seen occasionally in dot-like and the shorter mitochondria (Animation 5). In the 0.5 J/cm^2 group, change in the lens epithelium was similar to that of 1.0 J/cm^2 group lenses, with perinuclear-arranged threads of mitochondria resembling that of controls (Table 1). In the periphery, numerous short and swollen, nodule-like mitochondria could be seen (data unavailable). Occasional movement of dot-like mitochondria could be seen in the epithelial cells (data unavailable). In the superficial cortex of 0.5 J/cm^2 – exposed lenses, the changes were similar to the 1.0 J/cm^2 group lenses and was limited to the presence of small numerous vacuoles (data unavailable). While longer thread-like mitochondria showed occasional movement in some lenses, short dot-like mitochondria were seen moving readily in multi-directional, burst-like patterns (data unavailable).

Drastic morphological changes were observed in the lens epithelium 7 days after 1.0 J/cm^2 irradiation. Only a few cells and large vacuoles were seen (Fig. 4C). In the remaining cells only diffuse Rhodamine 123 fluorescence was seen. In the superficial cortex, fewer and shorter mitochondria, as well as large vacuoles, could be seen (Fig. 4D). However, the remaining mitochondria were not moving. In the 0.5 J/cm^2 group lenses 7 days after irradiation, while distinct epithelial cells could be seen, Rhodamine 123 fluorescence was very diffuse (data unavailable). In the superficial cortical fibre cells numerous small vacuoles could be seen while the mitochondria resembled that of controls

(data unavailable). The major change was the lack of movement of the mitochondria. Moreover, complete Rhodamine 123 bleaching was evident immediately after data acquisition.

By 14 days after 1.0 J/cm^2 treatment few bovine epithelial cells could be seen. No mitochondria were seen. Large vacuoles scattered throughout the cytoplasm were seen in the superficial cortex. In the 0.5 J/cm^2 group lenses 14 days after irradiation, distinct epithelial cells could be captured. However, large prominent vacuoles were seen. While in some lenses only diffuse Rhodamine 123 fluorescence was seen, in other samples mitochondria, shorter then that of controls, could be seen. The remaining mitochondria exhibited quick burst-like movement over a very short distance (less than 1μm). Moreover, Rhodamine 123 bleaching was evident 3 min after data acquisition. In the superficial cortex small vacuoles could be seen scattered throughout the cytoplasm. Mitochondria appeared shorter then that of controls. Occasionally, swollen, nodule-like mitochondria were seen. However the major change, as compared to 7 days after treatment, is the fact that some movement of the mitochondria over a short distance could be seen, especially in small, dot-like structures.

In the ARPE-19 cells immediately following 1.0 J/cm^2 irradiation very diffused Rhodamine 123 fluorescence could be captured and only a few dot-like, short mitochondria were seen (Fig. 4E). No movement was seen and Rhodamine 123 photobleaching was observed immediately after the start of data acquisition (Animation 6). Overall shortening of the mitochondria could be seen immediately after 0.5 J/cm^2 irradiation, with only few branched mitochondria seen (Fig. 4F). Those shorter mitochondria were not moving and Rhodamine 123 bleaching was observed 3 min after

data acquisition (data unavailable). In ARPE-19 cells for both 1 and 2 days after 1.0 and 0.5 J/cm^2 irradiation only a few cells lacking mitochondria remained, exhibiting only diffuse Rhodamine 123 fluorescence (data unavailable).

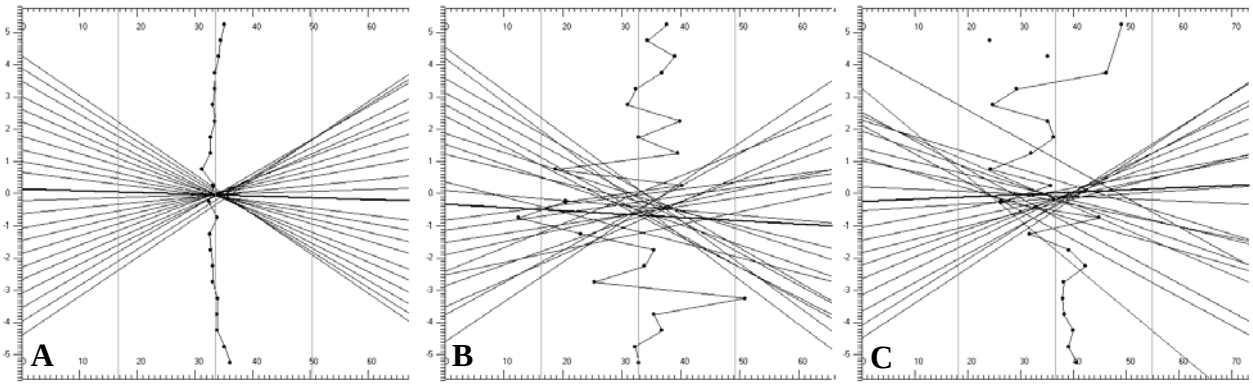

Figure 1. Representative individual scans comparing optics of control to that of 1.0 and 0.5 J/cm^2 14 days after UVB irradiation.

Lens optical quality was assessed using the automated laser scanning system, as described in Methods. UVB dependent increase in the amount spherical aberration, as shown by a broken line, was seen in 1.0 (B) and 0.5 J/cm^2 (C) irradiated lenses as compared to control (A). The x-axis (mm) indicate the back vertex distance and the y-axis (mm) indicate the position of the laser beam across the lens.

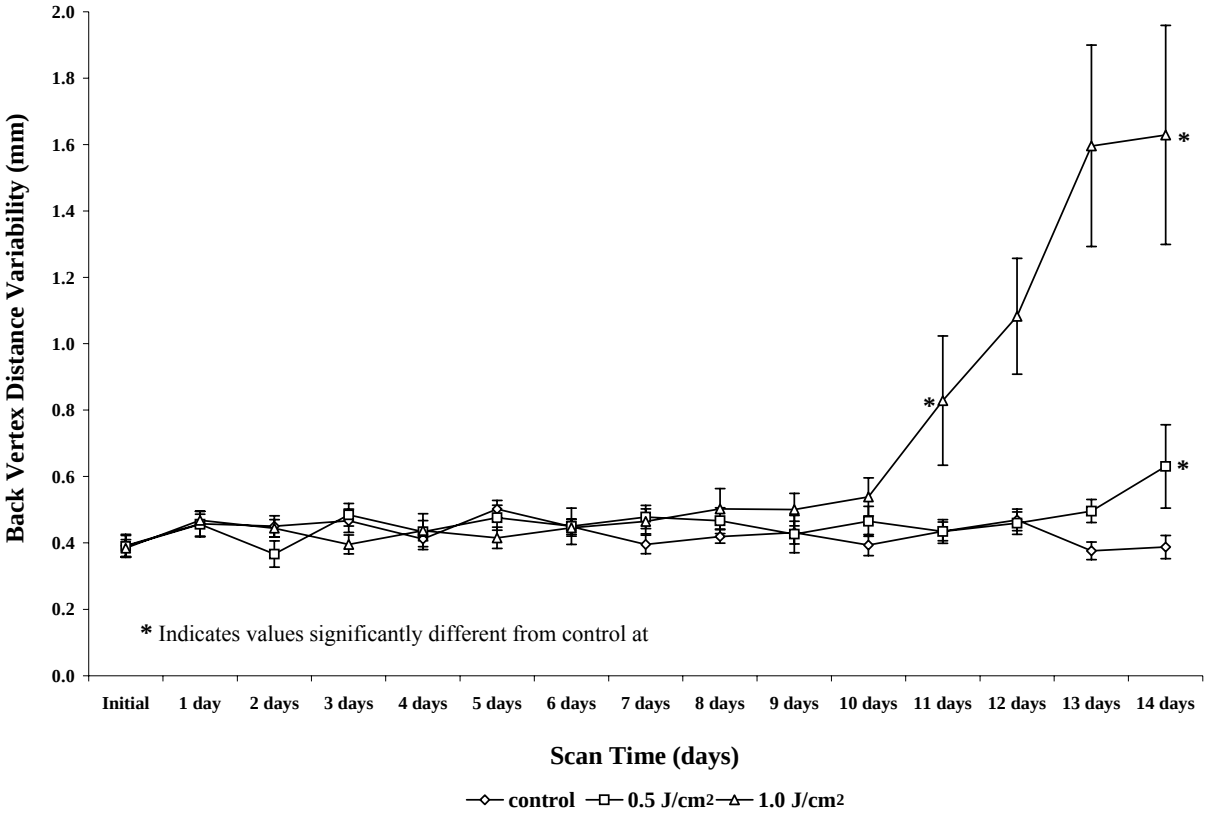

Figure 2. Comparative effect of UVB irradiation over time on optics of bovine lenses.

A latent dose-dependent increase in the amount of spherical aberration (back vertex distance variability, mm) was seen. Compared to controls, a significant increase ($p<0.05$) in 1.0 J/cm^2 group lenses was noted on day 11. Spherical aberration continued to increase and by the end of the experiment the difference was significant in both group lenses.

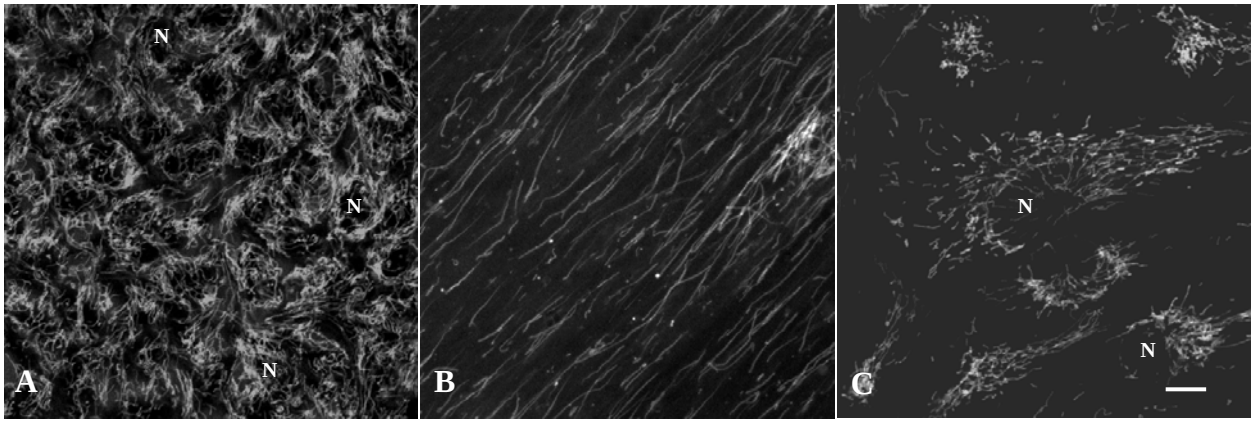

Figure 3. Representative confocal micrographs showing the distribution and morphology of the mitochondria of controls.

Bovine lenses and ARPE-19 cells were loaded with Rhodamine 123 and viewed under confocal microscope as described in Methods. The mitochondria of bovine lens epithelium are shown in A and superficial cortex in B, whereas the mitochondrial of ARPE-19 cells are shown in C. Bar = 10μm

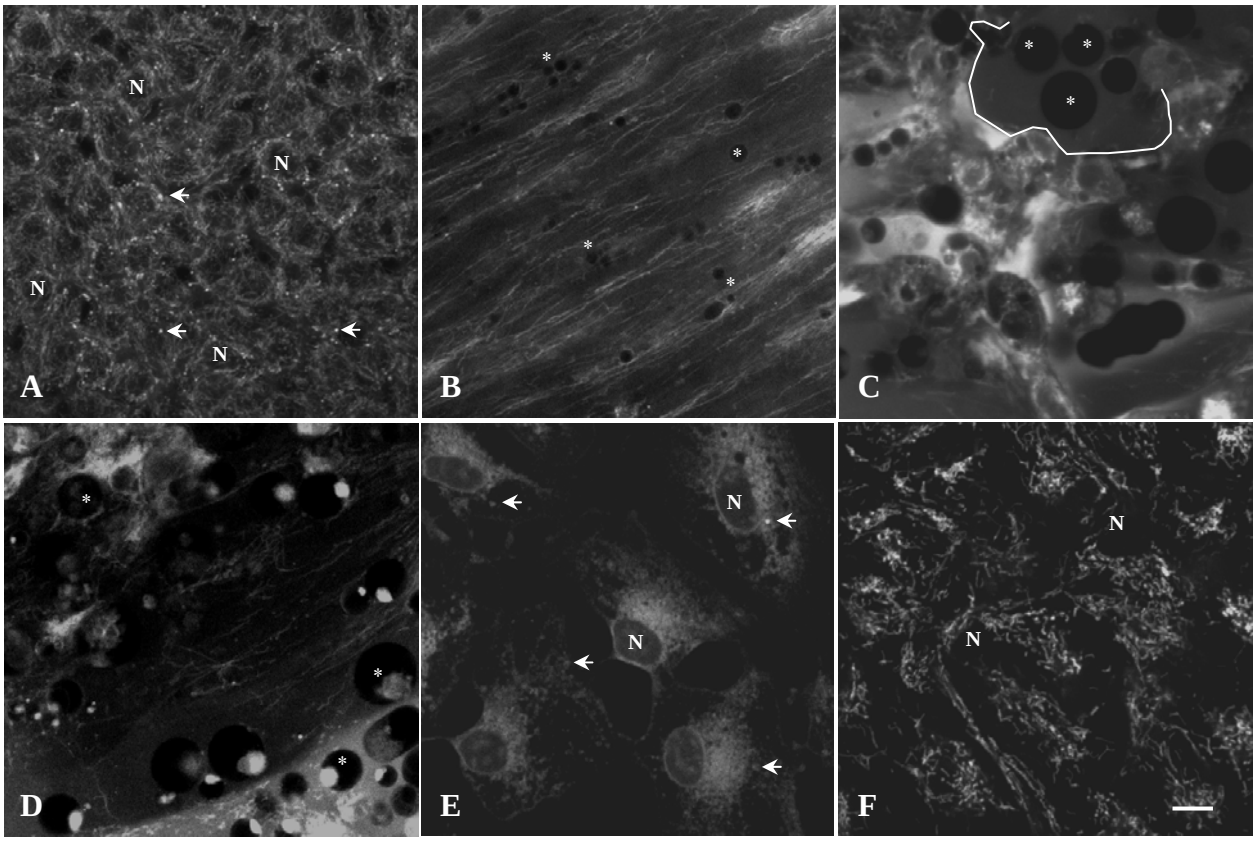

Figure 4. Representative confocal micrographs showing UVB irradiation-induced morphological changes and alterations in size of the mitochondria.

Compared to controls short swollen nodule-like mitochondria (indicated by arrows) were seen in epithelium of bovine lenses immediately after 1.0 J/cm2 irradiation (A). In the superficial cortex the immediate effect of 1.0 J/cm^2 was expressed by a presence of small numerous vacuoles (B, indicated by asterisks). Only few cells and large vacuoles (solid line) were seen in the epithelium of bovine lenses 7 days after 1.0 J/cm^2 (C). In the superficial cortex at the same time fewer and shorter mitochondria as well as vacuoles (asterisks) were seen (7 days after 1.0 J/cm^2, D). In the ARPE-19 cells immediately after 1.0 J/cm2 only few dot-like short mitochondria (indicated by arrows) were seen (E). In the 0.5 J/cm^2 overall shorter mitochondria were seen (F). Bar = 10μm

Table 1. Comparative list of changes in the average mitochondrial length (μm ± SEM) over time in epithelium and superficial cortical fibre cells of control (untreated) and 1.0 or 0.5 J/cm^2 UVB irradiated bovine lenses and ARPE-19 cells.

Treatment	Control (range)	1.0 J/cm^2 (range)	0.5 J/cm^2 (range)
Immediate (epi)	2.54 ± 0.03 (1-10)	2.03 ± 0.02 (0.4-7)*	1.84 ± 0.02 (0.4-6)*
7 days (epi)	2.83 ± 0.05 (0.7-13)	N/A	2.0.4 ± 0.03 (0.4-7)*
Immediate (fib)	6.25 ± 0.26 (1-74)	3.38 ± 0.12 (0.4-29)*	3.38 ± 0.13 (0.4-44)*
7 days (fib)	4.63 ± 0.17 (0.4-53)	3.34 ± 0.14 (0.4-28)*	4.56 ± 0.18 (0.5-46)
Immediate ARPE-19	3.08 ± 0.095 (0.6-36)	N/A	2.77 ± 0.06 (0.7-13)*

* Indicates values significantly different from control at $p<0.05$

ANIMATION CAPTIONS

Animation 1. Movement of mitochondria in the epithelium of control bovine lenses. Movement of mitochondria in epithelium of bovine lenses, loaded with Rhodamine 123 was captured over time as described in Methods. In the epithelium of control bovine lenses the movement could be seen in both short and longer structures. Such an example of longer mitochondria is outlined by an arrow. More rapid movement of shorter mitochondria is highlighted by a circle whereas occasional branching is highlighted by a square.

Animation 2. Movement of mitochondria in the superficial cortex of control bovine lenses. Overall movement of mitochondria in the superficial cortex of control bovine lenses was faster than in that of epithelium. However this movement was also seen in short, dot-like structures, as outlined by a circle and also in elongated mitochondria (highlighted by an arrow).

Animation 3. Movement of mitochondria in control ARPE-19 cells. Similar to bovine lens epithelium and superficial cortex movement of short and elongated mitochondria was seen in control ARPE-19 cells. An example of such movement is highlighted by arrows. Moreover, as part of the movement branching was noted in many mitochondria as outlined by circle and a square.

Animation 4. The immediate effect of 1.0 J/cm^2 UVB irradiation on movement of mitochondria in epithelium of bovine lenses.

Immediately following 1.0 J/cm^2 irradiation the phenotype of the mitochondria in epithelium was similar to controls. However no movement of the mitochondria was seen. Moreover, rapid Rhodamine 123 bleaching was observed.

Animation 5. The immediate effect of 1.0 J/cm^2 UVB irradiation on movement of mitochondria in superficial cortex of bovine lenses.

Immediately following 1.0 J/cm^2 irradiation while elongated mitochondria resembled that of controls, occasional movement was only seen in dot-like mitochondria (highlighted by a square and arrows).

Animation 6. Lack of movement of mitochondria in ARPE-19 cells immediately following 1.0 J/cm^2 UVB irradiation.

Immediately following 1.0 J/cm^2 irradiation no movement of mitochondria could be seen, with only a few dot-like, short mitochondria were seen.

* Animations are available from the website.

http://www.annalsnyas.org/cgi/reprint/1091/1/17

1.4 Discussion

Exposure to solar ultraviolet (UV) radiation has been implicated in skin and ocular pathologies, including cataract.[12] The gradual depletion of stratospheric ozone due to chlorofluorocarbons (CFCs), aircraft pollutants and other industrial pollutants substantially increases the levels of ultraviolet (UV) radiation, particularly UVB, reaching the Earth's surface.[17] While the cornea loses its refractive function once removed from the eye, the lens, cultured in physiological solution, continues to maintain its cellular makeup and original refractive function. Similarly, cultured ARPE-19 cells represent an *in vitro* model of neurosensory retina.

The major and most novel consequence of the UVB irradiation reported in this study is the cessation of mitochondrial movement. While our recent study showed the movement of mitochondria in bovine lenses,[11] to our knowledge this is the first study describing movement of mitochondria in ARPE-19 cells. The mechanism of organelle movement is not known in bovine lenses or ARPE-19 cells. In neurons, transport is thought to occur along microtubules, presumably involving kinesin-related proteins and cytoplasmic dynein.[18] This movement can be inhibited by stabilizing microtubules with drugs like nocodazole.[19-21] A recent study of rat lens showed the existence of a microtubule-based motor system containing both kinesin and dynein in the elongating fibre cells.[22] The presence of this system was attributed to the transportation of Golgi complexes to their target regions during increased cell growth accompanying elongation of the secondary fibre cells. A large number of microtubules were regularly arranged into bundles parallel to the long axis of fibre cells, a morphological observation similar to that

of the distribution of the mitochondria seen in the superficial cortical fibre cells (Fig. 3B) and this may represent the machinery responsible for the observed rapid mitochondrial movement in the superficial cortex of bovine lenses. Movement is also an ATP-dependent process, and the depolarization of mitochondria combined with the potential impairment of function associated with the calcium load could deplete local ATP concentrations quite rapidly. Thus, a number of different mechanisms could contribute to the cessation of movement. The mechanisms responsible for the alteration in movement may also underlie the shape change. If the rod-like structure associated with normal mitochondria is essentially a function of the organelle being stretched out on a cytoskeletal structure, the dissolution of that structure could result in the rounding that we report here.

The second finding of this study is related to the highly variable morphology and distribution of mitochondria seen in that of controls and also the observed morphological changes and alterations in size of the mitochondria following irradiation (Table 1). The observation in the controls may be related to the dynamic state of the mitochondria. In growing cells mitochondria are frequently found as extremely dynamic structures with tubular sections dividing in half, branching, and fusing presumably to form a complex network.[23] Moreover, there is an emerging appreciation that the decrease in the size of the mitochondria may be associated with early cell injury and that these changes are related to the offset of normal fusion and fission of the mitochondria.[24] In several *in vitro* models of apoptosis it has been reported that normal elongated mitochondria become fragmented.[25, 26] Fragmentation of mitochondria following treatment may be a consequence of the association of proteins such as dynamin-related protein 1 (DRP1)

with mitochondria. Over expression of this protein, responsible for mitochondrial fission in neurons, causes fragmentation,[26, 27] whereas a dominant-negative form of DRP1 decreases sensitivity to mitochondrially mediated apoptosis.[26]

Alterations in mitochondrial morphology in neurons[28] and astrocytes[29] in response to calcium loading has also been reported. These authors found that mitochondria changed from elongated rod-like to short spherical morphology following treatment. In these studies the authors concluded that one of the possible mechanisms in the observed shape change was caused by mitochondrial permeability transition. In a previous study it was proposed that the elongated, thread-like or reticulated form of mitochondria is beneficial on the basis of studies in cardiac myocytes.[30] Thus, because of the cable properties of mitochondria, the proton motive force generated by the electron transport chain can be effectively distributed across the reticulum and thus facilitate ATP synthesis. This advantage is hypothetical at this point because whether the mitochondria are able to generate a spatially limited proton motive force is unclear. In the present study, the consequence of the alteration in morphology for mitochondrial function appears to correlate with observed increase in the amount of spherical aberration in bovine lenses, whereas the connection is much less clear for ARPE-19 cells. Our previous studies using the mitochondrial uncoupler carbonyl cyanide *m*-chlorophenylhydrazone (CCCP) resulted in concentration-dependent fragmentation of mitochondria and an increase in the amount of spherical aberration of bovine lenses.[8] The current results and our previous studies[8, 9] have suggested that modified mitochondrial function may have a direct consequence on lens optics.

A latent UVB dose-dependent increase in the amount of spherical aberration seen in bovine lenses confirms earlier observations.[14, 15] This latent effect of oxidative stress from UVB irradiation on loss of sharp focus was first evident at the 11 days scan point, where an over 2-fold increase in BVD variability in the 1.0 J/cm^2 irradiated group lenses was seen. By day 14 in both irradiated groups the amount of spherical aberration was significantly higher then that of controls ($p<0.05$). While the difference in the amount of calculated biologically effective radiant energy levels was linear between the two groups (0.445 and 0.223 J/cm^2, respectively), at day 14 the 1.0 J/cm^2 treated group showed an exponential increase in the amount of spherical aberration (over 2.5 times higher value) in comparison that that of the 0.5 J/cm^2 group.

As mentioned in the introduction, the vertebrate lens is a cellular structure that consists of two types of cells organised in distinct spatial patterns: the epithelial monolayer that covers the anterior surface and fibre cells that comprise the bulk of the lens. Cell division in the lens is restricted to the equatorially located epithelial cells which give rise to terminally differentiated fibre cells in a process that continues through life. The newly formed fibre cells overlie the pre-existing cells in a process that continues throughout life, resulting in a steady increase in tissue volume. The oldest cells, which at one time were the embryonic lens, form the lens nucleus, or central zone. Loss of ageing or damaged cells is impeded because of their central location and because of the complete enclosure of the lens by the acellular capsule. The observed latency in the optical response may be explained, at least partially, by the lens' unique morphology and its rate of growth as described above. Similar results were seen in the study of age and toxic treatment of rat lenses where delayed optical change was seen in older lenses in

comparison to younger once.[31] Moreover, the younger lenses showed the ability to recover from toxic damage while the older ones did not.[31]

It is interesting to consider the role of oxidative stress from UVB irradiation on lens optics and mitochondria and how these may be an expression of early cell injury. The effects are clearly produced by UVB exposures that are above the normal threshold. However, the changes in shape and movement of the mitochondria that we observe are very similar to the effects of CCCP. This is notable, because we have demonstrated recently that the application of CCCP results in both mitochondrial rounding and movement cessation.[11] Based on the observation of a short dot-like mitochondria one can conclude that rounding of mitochondria or their temporary immobilization does not inevitably lead to injury. However, it is interesting to note that the lens is capable of recovery, both in terms of lens optics and the normal morphological phenotype of mitochondria, following low concentrations of CCCP treatment.[11] This suggests that the recovery of mitochondrial function aids in the restoration of lens optical function. Thus, in this experimental paradigm, the alteration of mitochondrial morphology would be considered a symptom rather than a cause of cell injury. Indeed, this raises the possibility that either shape or movement change could be an attempt to protect the cell from injury, although what exactly is accomplished by this maneuver remains to be established.

In summary, the main findings of this study are that UVB irradiation causes a cessation of mitochondrial movement in both bovine lenses and ARPE-19 cells. It also produces a latent change in lens optics and a rapid and substantial remodeling of mitochondrial morphology. Morphological changes and alterations in size and movement of the mitochondria could be detected immediately and over time following UVB

irradiation. These findings suggest that oxidative stress might alter the normal movement of mitochondria to cellular destinations where ATP synthesis is required and thus impair not only cellular function but also lens optics. More broadly, these experiments clearly establish an unappreciated dynamic equilibrium that exists between the distribution of mitochondria within cells and their biological function. Under conditions of oxidative stress or chemical treatment one might anticipate that impaired mitochondrial function would alter the ability of mitochondria to move and thereby prevent the normal distribution of mitochondria within either lens epithelium and superficial cortex or ARPE-19 cells. While cellular repair mechanisms may exist at or below threshold levels of UVB radiation, under conditions of chronic stress over a life time, the oxidative stress could stop new mitochondria from being delivered to distal parts of the superficial cortical fibre cells and ARPRE-19 cells, or possibly even prevent the retrieval of dysfunctional mitochondria to the cell body for degradation, either of which may result in cell damage. When one considers the number of endogenous toxins that the ocular surface is exposed to (such as oxidative stress) as well as accidental exposure to xenobiotics that may impair mitochondrial function and dissipate the mitochondrial membrane potential, it seems likely that the alteration of the movement and morphology of mitochondria is likely to be a broadly important phenomenon associated with lens and ARPE-19 cells injury.

Chapter 2

In Vitro assays for evaluating the ultraviolet B-induced damage in cultured human retinal pigment epithelial cells

Hyun-Yi Youn[1], Vladimir Bantseev[1], Niels C. Bols[2], Anthony P. Cullen[1], Jacob G. Sivak[1]

[1]School of Optometry/Department of Biology, University of Waterloo, Waterloo, ON, Canada

[2]Department of Biology, University of Waterloo, Waterloo, ON, Canada

Chapter 2 was published in the Journal of Photochemistry and Photobiology 2007 Vol.88 (p.21-28). All the data collection and analysis were performed by Hyun-Yi Youn, who was also the primary author. Drs. Bantseev, Bols and Cullen provided technical support and advice. Dr. Sivak provided supervisory and editorial assistance throughout.

2.1 Introduction

The neural retina detects the retinal image and transforms light energy into a communicable form of chemical energy. The outermost layer of the retina, the retinal pigment epithelium (RPE) is derived embryologically from the same neural tube tissue that forms the neurosensory retina. Although the neurosensory retina differentiates into several layers of neurons, the RPE remains a melanin-pigmented monolayer that takes on the characteristics of a secretory epithelium [1]. The RPE is not directly involved in the neural events of vision, but it is critical for the normal functioning and well-being of the photoreceptors [2].

Solar UV radiation, having wavelengths from approximately 200 to 400 nm, is capable of penetrating the ozone layer and only UVB and UVA (280 ~ 400 nm) reach the terrestrial surface [3]. The depletion of ozone increases the levels of UV radiation, particularly UVB (280~315 nm), reaching the Earth's surface [4]. Exposure to solar UV radiation has been implicated in skin and ocular pathologies. It is well known that visible and ultraviolet (UV) radiation can produce photochemical lesions in the neural retina and the RPE. For example, in studies of morphometric cellular changes of human RPE cells after exposure to UV radiation (200 ~ 400 nm), *in vivo* examination of anesthetized rat retina after UV and green light irradiation (320 ~ 600 nm), and DNA damage of human RPE cells caused by broadband UVA (315 ~ 400 nm) and UVB (280 ~315 nm) radiation [5-9]. The role of UV exposure in retinal damage has been well established, including retinal degeneration due to the lipid peroxidation [7,10,11]. The cornea and the lens of the eye substantially filter and attenuate UV radiation that enters the eye, so that only a

very small proportion reaches the retina [12]. Also, cataract development with age will reduce the amount of UV radiation exposed to the retina due to the opacification of the crystalline lens. However, depletion of the ozone layer, in combination with the increase in outdoor recreation and average span of life, may result in an increase in the accumulative lifetime exposure of the retina to UV radiation [8]. Also, the removal of the crystalline lens by cataract surgery may be associated with a substantial increase in the UVR that reaches the retina [13]. While manufacturers of intraocular implants have responded to the need to filter UV wavelengths, the cut-off wavelength at the blue end of the spectrum is still a matter of dispute. In fact, a human RPE cell line has been used for many *in vitro* study of UV-induced damage [8,9] as well as blue light damage [14,15] to the retina.

The objective of this study is to evaluate the broadband UVB-induced damage in cultured human retinal pigment epithelial cell, and to develop an *in vitro* model of retinal UV protection. An *in vitro* model of retinal UV protection is needed as a result of the increase in energy accumulative lifetime exposure of the retina to UV radiation and the fact that crystalline lens protection is lost in cataract surgery without appropriate intraocular lens protection. Thus, an *in vitro* model will also be useful for testing the safety and efficacy of intraocular lens material in protecting the retina from UV damage. This work involves the exposure of a retinal cell culture to UVB radiation. Cellular viability, mitochondrial damage, nucleic acid damage, and phagocytotic activity are quantified after exposure, using the Alamar blue assay, confocal laser scanning microscopy with two different fluorescent stains, and a phagocytotic activity assay.

2.2 Materials and Methods

2.2.1 Human retinal pigment epithelial cell culture

The human ARPE-19 cell line was derived from the eyes of a 19-year-old male donor. Human RPE cell line ARPE-19, originally obtained from American Type Culture Collection (ATCC), was provided by Dr. R. Tchao, University of the Sciences in Philadelphia. ARPE-19 was plated at low density and cultured in DMEM/Ham's F-12 with L-glutamine and 15mM HEPES (Mediatech, VA, USA). The medium also contained 10% fetal bovine serum (Hycolone, UT, USA), and insulin-transferrin-sodium selenite media supplement (ITS supplement) (Sigma, MO, USA). The cell line was then maintained in a humidified incubator in an atmosphere of 95% air and 5% CO^2 at 37°C and the culture medium was changed every 48 hours. The cells were plated in T75 or T150 flasks (Falcon, NJ, USA), and allowed to grow until the cultures were confluent. After a confluent monolayer appeared (at least 70% confluent), subculturing was carried out using a dissociating agent such as Trypsin/EDTA solution (Cascade Biologics, OR, USA). Subculturing is usually performed during the log phase when the cells are at their healthiest and are able to adapt to the new environment most efficiently [47].

2.2.2 UVB irradiation of cultured RPE cell

Exposure was produced by filtering banks of UVB fluorescence tubes (cat. No F15T8/UVB; Microlites Scientific, ON, Canada) in a custom designed UV irradiation

unit with 4% CO^2 and 96% membrane filtered air. The spectral distribution of the UVB fluorescent tubes used extends from 290 nm to about 370 nm wavelengths, with a peak at around 315 nm. However, since it was found that the contribution of the wavelengths within the 320 to 370 nm waveband was only 0.1%, this was ignored. Before irradiation, the UV source was calibrated with an Instaspec II diode-array spectroradiometer (Oriel Corporation, CT, USA). After two to three days of pre-incubation at 37°C, 4% CO^2/ 96% air to form a confluent cell monolayer, the cells were irradiated with 0.2, 0.1 and 0.05 J/cm² of broadband UVB (280 -315 nm). The UV source was positioned directly above the cell. In order to minimize absorption of the radiation by phenol red in the medium, the medium above the cell was removed during UV exposure. A thin layer of medium, 1.0 mm thick was left and thus, a minor phenol red effect may have influenced the results. Exposure time was calculated with the formula: $H_\lambda = t \times E_\lambda$, where H_λ is the energy level indicated as exposure per unit area (J/cm²), *t* is the exposure time (second), and E_λ is the irradiance (W/cm²) (ACGIH, 2000). The irradiance, measured with a calibrated Instaspec II diode-array spectroradiometer, was 0.000306 W/cm^2, and the exposure times were 10 min 54 sec, 5 min 27 sec, and 2 min 44 sec, respectively. The solar broadband UVB irradiance level in June 1999, measured in Waterloo, ON, Canada, was 0.000276 W/cm^2 [48]. Thus, the irradiance level used for this study is comparable to solar spectral irradiance. For comparison to other studies, it was necessary to calculate the biologically effective UVB (280 –315nm) dose of the three radiant energy levels. The calculation was carried out using the American Conference of Governmental Industrial Hygienist (ACGIH) spectral weighting functions using the formula:

Biologically effective dose = $\sum_{290}^{320} H_\lambda \times \Delta_\lambda \times S_\lambda$, where H_λ is the actual radiant exposure

(J/cm²) at a specific wavelength as obtained from the spectroradiometer, Δ_λ is the wavelength interval (nm), and S_λ is the UVR spectral weighting function or relative spectral effectiveness (unitless) [16]. The calculated biologically effective radiant energy levels were 0.089, 0.045, and 0.022 J/cm², respectively.

2.2.3 Alamar Blue assay

The Alamar Blue assay, a fluorometric indicator of cellular metabolic activity, was obtained from MEDICORP Inc. (Montreal, Quebec, Canada). The Alamar Blue assay is a proprietary assay designed to quantify cell proliferation, cytotoxicity and viability. For experimental use, the Alamar Blue was diluted into the culture medium without serum to 8% (v/v). The assay solution was prepared immediately before each use to avoid possible precipitation. For fluorescence measurements, the cells were transferred into a sterile flat bottom multi-well cell culture plate. Cell density was adjusted to 1×10^5 cells/ml for 48-well plates [17] and 5×10^4 cells in 500 $\mu\ell$ of medium were added to each well. The cells were then allowed to grow for two to three days in an incubator to form a confluent cell monolayer. After the irradiation, the culture medium was carefully aspirated from each well, and the cells were rinsed once with culture medium. Then 100 to 150 $\mu\ell$ of 8% Alamar blue working solution was added to each well, and the cells were further incubated in an incubator for one hour to allow the dye to be taken up by the cells. After the incubation, fluorescence measurements were performed with the CytoFluor™ II fluorescence multi-well plate reader (PerSeptive Biosystems Inc., MA). Prior to measurements, the excitation / emission wavelengths

settings on the CytoFluor™ plate reader were adjusted to 530 /590 nm, with the sensitivity gain set at 50, and temperature at 37ºC.

2.2.4 Confocal microscopy

Confocal scanning laser microscopy (Carl Zeiss LSM) and three fluorescent stains (Hoechst 33342, Rhodamine 123, and Acridine Orange) (Molecular Probes, OR, USA) were used to observe the effects of UVB radiation on RPE cell morphologic features. Hoechst 33342 nucleic acid stain is a popular cell-permeant nuclear stain that emits blue fluorescence when bound to dsDNA [18]. Rhodamine 123 is a cationic, lipophilic, water-soluble oxonium chloride salt that stains mitochondria in living cells in a membrane potential-dependent fashion [19]. Acridine Orange is a cell-permeant nucleic acid binding dye that emits green fluorescence when bound to dsDNA and red fluorescence when bound to ssDNA or RNA. In the present study, 1×10^5 cells in 1.5ml of culture medium were seeded into collagen coated glass bottom culture Petri dishes (MatTek Corp., MA, USA). After culturing the cells for 48 hours and achieving 80 to 90% confluence, the cells were then stained for mitochondria and nucleic acid using Rhodamine 123 (20mM) and Hoechst 33342 (10mg/ml) for 20 min at 37ºC. Other cells were also stained for dsDNA and ssDNA (as well as RNA), using Acridine Orange (10mg/ml) for 20 min at 37ºC. A Zeiss confocal laser scanning microscope (CLSM) 510 system attached to an Axiovert 100 microscope with a 40× water-immersion C-Apochromat objective was used to observe and record the effects of the three different dyes.

2.2.5 Phagocytotic activity assay

Confocal scanning laser microscopy (Carl Zeiss Inc., Jena, Germany) and fluorescent microspheres (Molecular Probes, OR, USA) were used to observe the effects of UVB radiation on RPE cell phagocytotic activity. ARPE-19 were seeded in collagen coated glass bottom culture Petri dishes (MatTek Corp., MA, USA) with a density of 1.3×10^5 cells in 2ml of culture medium. After adhering overnight at 37°C with 5% CO_2, 7×10^{10}, fluorescent microspheres of 0.1μm diameter were added at a total volume of 2ml/Petri dish. Red fluorescent carboxylate-modified microspheres (580/605 nm) were used. After 24 hours incubation, the medium with microspheres was removed and then the adherent cells were washed carefully with fresh medium twice to remove uningested particles before observation. The micospheres in the cells were observed using the confocal microscope, and the intensity of the fluorescent was measured using the Image Analysis toolbox of Matlab 7.1 software package (MathWork Inc., MA, USA).

2.2.6 *Statistical analysis*

Statistical calculations were completed using a two-way repeated measures analysis of variance (ANOVA). A probability value of less then or equal to 0.001 was considered significant.

2.3 Results

2.3.1 Cell viability

The Alamar Blue assay readings were presented as percent cell viability relative to the non-UVB exposed cells at three time points: 1 hour, 24 hours and 48 hours after irradiation. The results for UVB exposed RPE cells showed dose – dependent decreases in cell viability in comparison with the control cells (Figure 1). The measurements for 0.1 and 0.2 J/cm^2 exposed cells at the 24-hour time point presented the lowest percentage, showing similar loss of cell viability (49.6±5.0% and 47.4±1.0%, respectively), while cells irradiated with 0.05 J/cm^2 at the 1-hour time point (90±10.7%) were the least damaged, showing no significant difference in cell viability, in comparison with non-irradiated control cells ($p=0.1241$). However, cells exposed with UVB at the energy level of 0.05 J/cm^2 were significantly different from controls at 24 and48 hour time points ($p < 0.001$), and also there was no cellular recovery during the entire culture period. Cells exposed to both 0.1 and 0.2 J/cm^2 showed time and energy level – dependent decreases in cellular viability at the both 1 and 24 – hour time points. However, there was some cellular recovery at the 48-hour time points for both energy levels, showing increased percent cell viability at 48-hours in comparison to 24-hours (Figure 1). The Alamar blue assay results for all three energy levels (0.05, 0.1, and 0.2 J/cm^2) at the 48-hour time point clearly showed energy level – dependent decreases in cell viability (87.3±4.1%, 71.0±5.1% and 52.7±2.8%, respectively).

2.3.2 Confocal microscopy

2.3.2.1 Mitochondrial distribution and Rhodamine 123 + Hoechst 33342 fluorescence

After irradiation, cell groups (both control and treated) were first stained with both Hoechst 33342 (double strand DNA) and Rhodamine 123 (mitochondria). Non-irradiated cultured RPE cells exhibited no morphological changes during the entire culture period (first column of Figure 2). Overall, increasing the energy level of UVB radiation induced progressive morphological changes, increasing degradation of mitochondria (Figure 2). Cells treated with UVB at energy level of 0.05 J/cm^2 showed no significant morphological changes (both mitochondria and DNA) during the entire culture period and appeared to be similar to the control cells (second column of Figure 2). Numerous mitochondria could be seen surrounding individual nuclei, and mitochondrial distribution was in accordance with cellular viability as observed using the Alamar blue stain for 0.05 J/cm^2 UVB - exposed cells (Figure 1). However, the 0.05 J/cm^2 – treated cells showed shorter mitochondria (arrows of second column and first row of Figure 2), mostly around the nuclei, while the control cells showed longer mitochondria (arrows of first column and first row of Figure 2) which were distributed evenly. The cells exposed to 0.1 J/cm^2 showed similar mitochondrial distribution to the cells treated with 0.05 J/cm^2 at the 0-hour time point (third column of Figure 2). However, 0.1 J/cm^2 exposed cells showed fewer mitochondria than the 0.05 J/cm^2 exposed cells at 24-hour time point. After 48 hours, 0.1 J/cm^2 exposed cells showed an increase in mitochondrial distribution and the distribution agrees with the results for viability of the cells as observed using the

Alamar blue stain for 0.1 J/cm^2 exposed cells (Figure 1). The confocal images for the 0.2 J/cm^2 UVB treated cells showed severe damage to the mitochondria during the entire culture period (fourth column of Figure 2). The results for 0.2 J/cm^2 and 0.1 J/cm^2 exposed cells at 48 hours also showed reduced cell populations in comparison with the control group.

2.3.2.2 Nucleic acidic distribution and Acridine Orange fluorescence

Previous efforts with Hoechst 33342 used to evaluate the nucleic acids were not successful. The effects were not clear since the nuclei look fuzzy due to poor resolution (blue fluorescence in Figure 2). Therefore, another group of cells (both control and treated) were stained only with Acridine Orange (dsDNA and ssDNA/RNA, respectively) after the irradiation.

Non-irradiated cultured RPE cells exhibited no nucleic acidic damage during the entire culture period (first column of Figure 3). Overall, increasing the energy level of UVB radiation induced progressive nucleic acidic damage, showing reduced fluorescence, especially on single strand DNA or RNA (Figure 3). Cells treated with UVB at energy level of 0.05 J/cm^2 showed no significant changes (both dsDNA and ssDNA/RNA) at the 0-hour time point, a result similar to that for the control cells (second column, first row of Figure 3). However, in the 0.05 J/cm^2 group, dsDNA (green fluorescence) in the nucleus appeared to be degraded at the 24-hour time point, showing up as a non-fluorescent (black) portion, while ssDNA/RNA were still not significantly degraded (red fluorescence) (second column, second row of Figure 3). The 0.1 J/cm^2 UVB-exposed

group of cells showed a similar pattern as that of non exposed cells at the 0-hour time point (third column, first row of Figure 3). However, after 24 hours, both 0.1 J/cm^2 and 0.2 J/cm^2 groups of cells showed less fluorescence for both green (dsDNA) and red (ssDNA/RNA).

2.3.3 Phagocytotic activity

Phagocytotic activity is being presented as mean fluorescence of the ingested microspheres (9 different confocal images). Ingestion of red fluorescent microbeads (excitation 580nm, emission 605nm) of RPE cells was shown in the confocal microscopy results (original magnification ×40 oil, ×2 zoom) (Figure 4). The control cells have significantly greater capacities for uptake than the 0.1 and 0.2 J/cm^2 UVB-exposed cells ($p<0.001$), while the 0.05 J/cm^2 UVB-exposed cell group showed no significant difference from the control cell group ($p=0.3815$) (Figure 5). Overall, phagocytotic activity assay data for UVB-exposed RPE cells showed dose – dependent decreases in phagocytotic activity in comparison with the control cells (Figure 5).

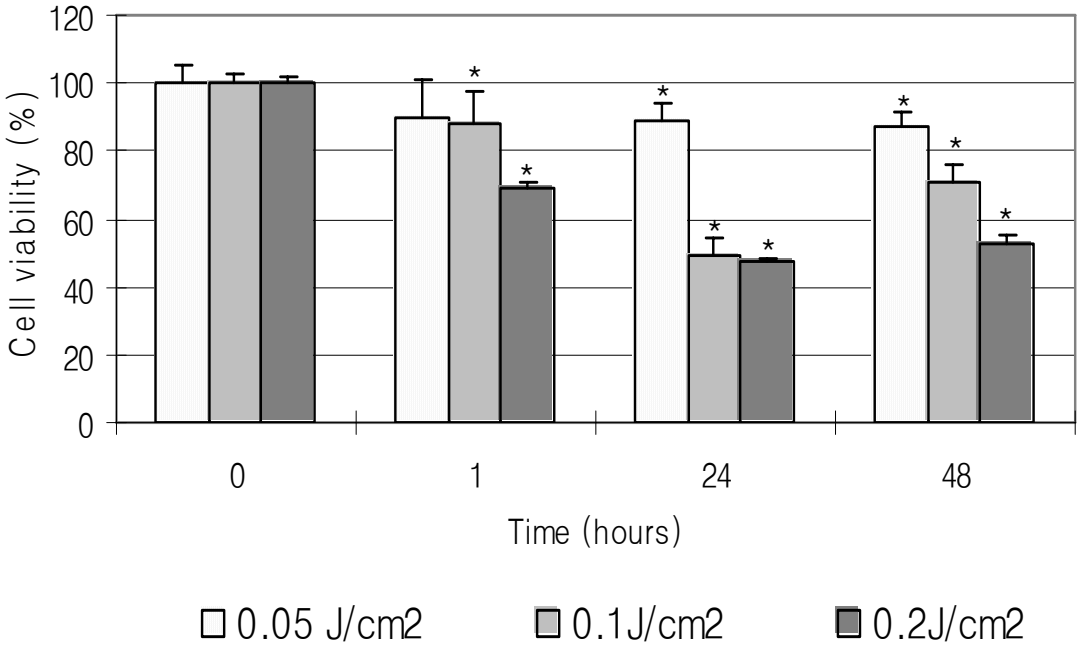

Figure 1. Cell viability (%) as a function of time (0, 1, 24, and 48 hours) for ARPE-19 cells irradiated with broadband UVB (0.05, 0.1, and 0.2 J/cm2) as revealed by the Alamar blue assay. Cell viability was expressed as a percent of non-UVB exposed cells (% of control). * indicates significant differences as compared to controls ($p < 0.001$).

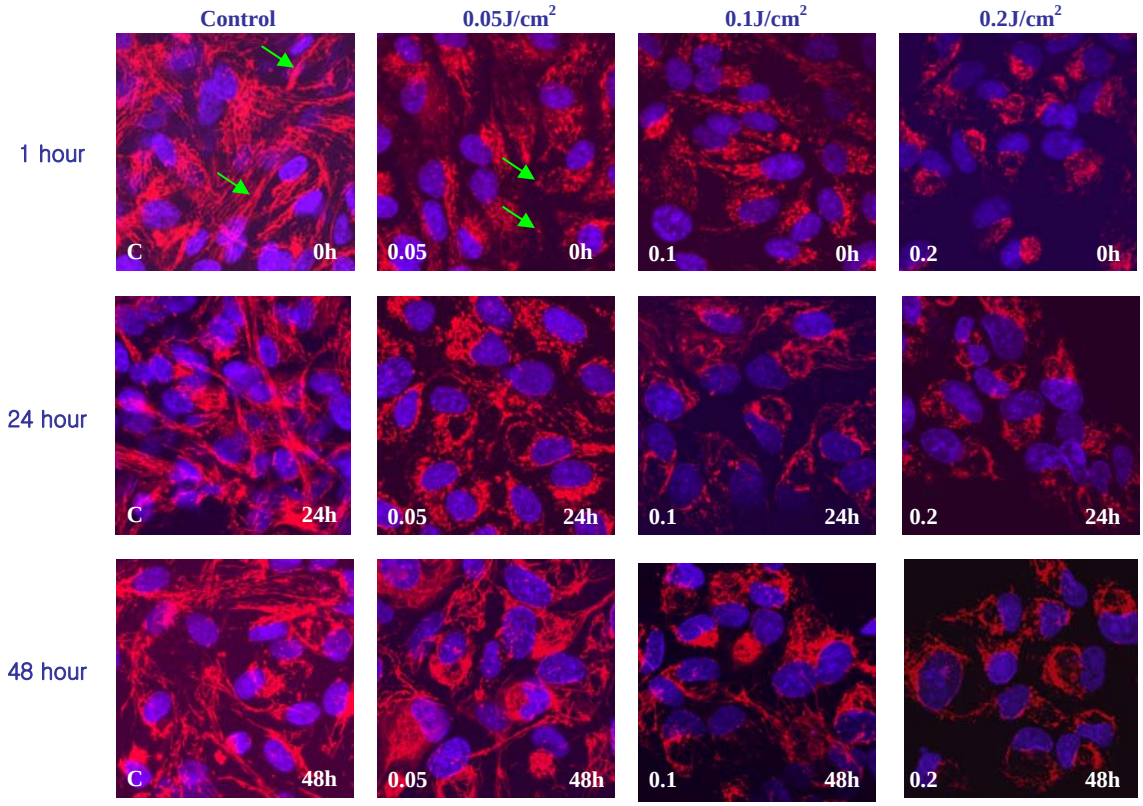

Figure 2. Representative confocal laser scanning micrographs showing the effect of UVB (0.05, 0.1, and 0.2 J/cm2) at T1, T24 and T48 on distribution of the Rhodamine 123 stained mitochondria (red) and Hoechst 33342 stained nuclei (blue) in ARPE-19 cells.

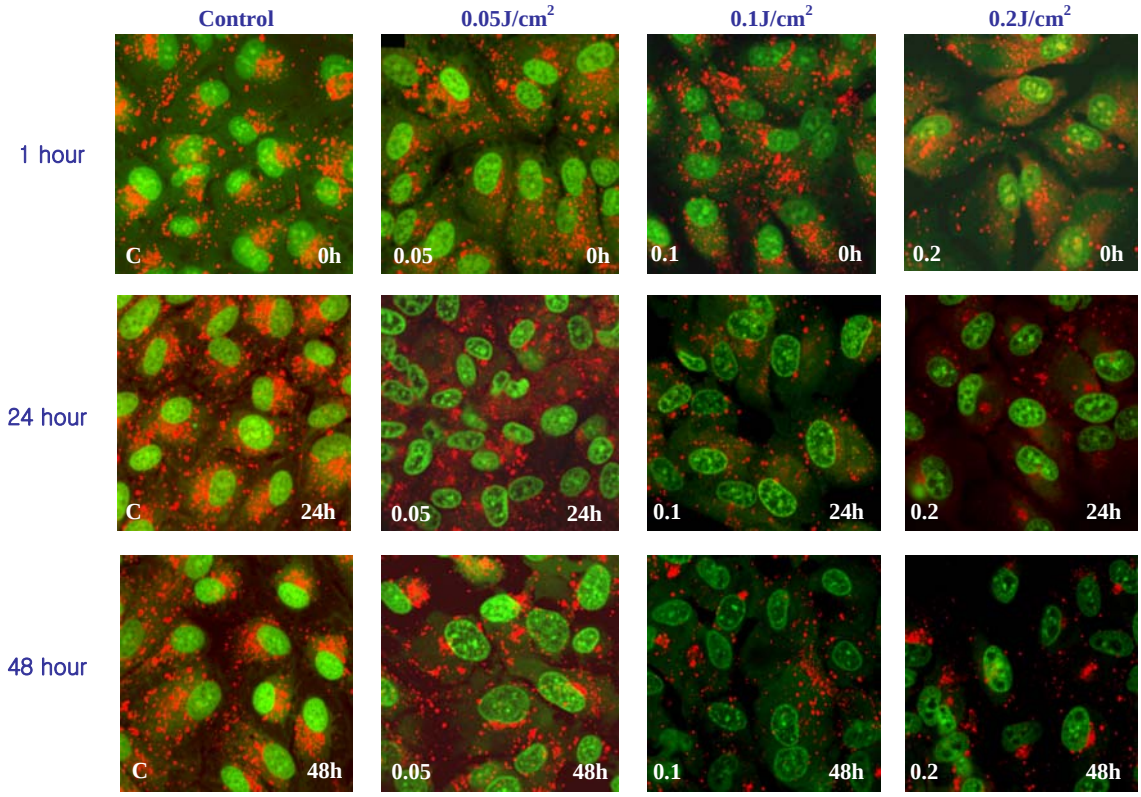

Figure 3. Representative confocal laser scanning micrographs showing the effect of UVB (0.05, 0.1, and 0.2 J/cm2) at T1, T24 and T48 on distribution of the dsDNA (green) and ssDNA (red) in ARPE-19 cells stained with Acridine Orange.

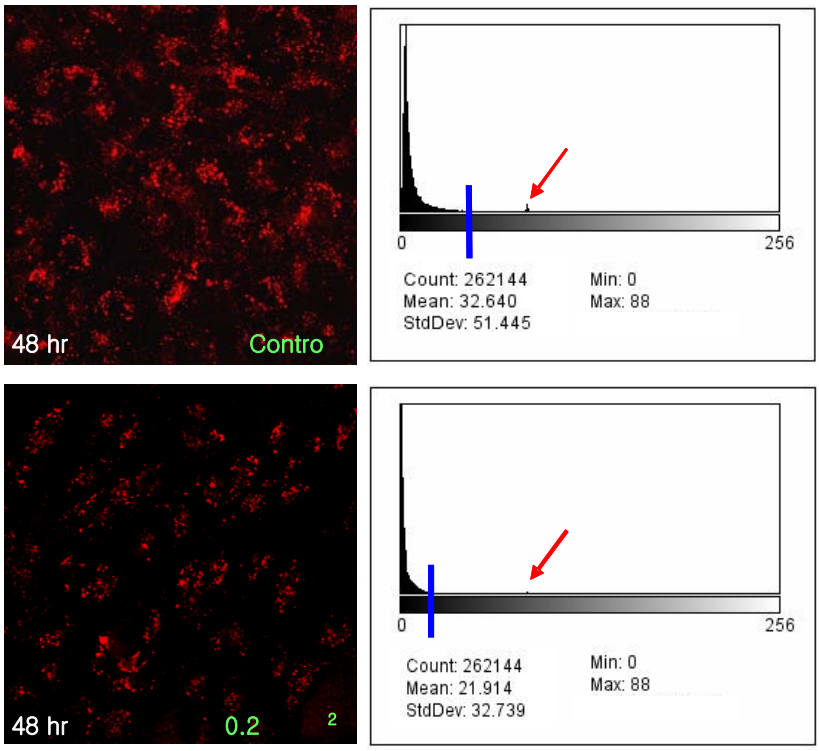

Figure 4. Effect of 0.2 J/cm2 broadband UVB exposure at T48 on the phagocytotic activity of ARPE-19 as revealed by fluorescent microspheres (0.1 um) and flow cytometry. The first images are showing the florescent microspheres in the cytoplasm, and second histograms are representing the intensity of the fluorescence. The number on the right is the average intensity of nine different images.

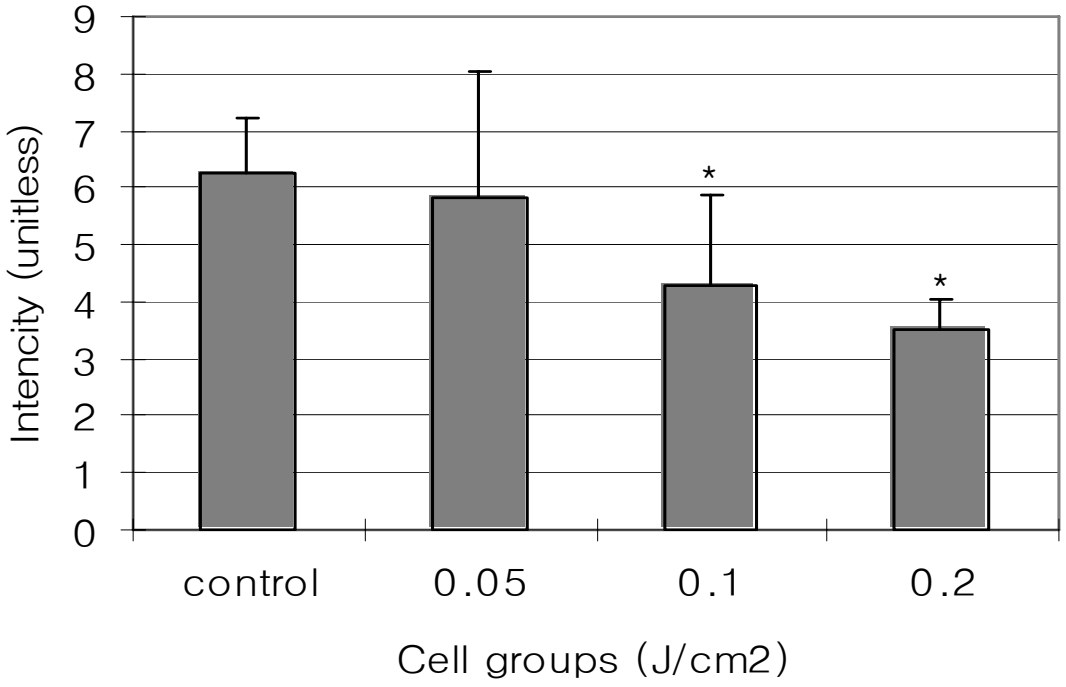

Figure 5. Effect of 0.05, 0.1 and 0.2 J/cm2 broadband UVB exposure at T48 on the phagocytotic activity of ARPE-19 as revealed by fluorescent microspheres (0.1 um) and flow cytometry. Phagocytotic activity was expressed as the average intensity of nine different ARPE-19 images. * indicates significant differences as compared to controls ($p < 0.001$).

2.4 Discussion

The results obtained in this study demonstrate that broadband UV radiation damage of retinal pigment epithelial cells in culture can be quantified using three assays; the Alamar blue assay, confocal microscopy, and a phagocytotic activity assay. The results clearly demonstrate that UV radiation can cause significant decreases in RPE cell viability as well as phagocytotic activity of retinal outer segments by RPE cells. In addition, the results showed that UV radiation can also induce the degradation of DNA/RNA and mitochondria in cultured RPE cells.

A number of studies have demonstrated that UV radiation and visible radiation has the potential to damage the retina and the retinal pigment epithelium [10]. Fortunately, the human retina is protected from short-wavelength radiation, which is particularly damaging, by the cornea which absorbs below 295 nm and the lens which absorbs strongly below 400 nm [20]. Only a very small fraction of UV radiation, therefore, reaches the retina. The depletion of the ozone layer of the stratosphere has, however, led to increased UVB irradiance at the Earth's surface [21]. This, in combination with the increase in the average human life span, may result in an increase in the cumulative lifetime exposure of the retina to UV radiation [8]. Thus, a role for UV radiation in the induction of age-related diseases of the retina, such as age-related macular degeneration (ARMD) becomes a distinct possibility [22,23].

Light exposure may be a factor that plays a role in promoting lipid peroxidation of cellular membranes because light of appropriate wavelength may trigger photo-oxidation reactions, such as the formation of reactive oxygen species (ROS) [24-26]. Furthermore,

the oxygen supply to the photoreceptors via the choroidal and retinal vessels can cause an elevated oxygen tension in the retinal pigment epithelium and photoreceptors [27,28]. Also, UV radiation can cause photosensitized damage to DNA, leading to single strand DNA breaks in the retina [8,29].

RPE cells play an essential role in retinal function, and degeneration of RPE cells may lead to degeneration of the retina and loss of vision [30]. The pigment epithelium is involved in the uptake, process, transport and release vitamin A (retinol) and some of its visual cycle intermediates (retinoids) [31]. Melanin in the RPE is thought to increase photoreceptor efficiency by absorbing excess, scattered light.

It has been reported in a variety of animal models that mitochondria represent a primary site of phototoxicity induced by UV radiation, such as in studies of mitochondrial enzyme activity of human fibroblast cells, mitochondrial function of sperm from sea urchins, and mitochondrial alteration of human RPE cells and intact bovine lenses [32-34]. Also, increases in ROS production after UV radiation exposure correlate well with decreased mitochondrial membrane potential, a marker for mitochondrial function [35-37]. Mitochondrial function can be assessed by staining with Rhodamine 123. Due to the negative potential of the inner membrane, Rhodamine 123 accumulates only in functional mitochondria, causing the mitochondria to produce a red fluorescence [38]. Mitochondria of dead cells are readily distinguishable from those in live cells, since they are not able to retain Rhodamine 123 after washing [38]. In the study of mitochondrial function of sperm cells in sea urchins after UV radiation using Rhodamine 123, the results showed significantly reduced mitochondrial function [33]. Also, these results revealed that UVB is more damaging to the mitochondria than UVA at the same

dose, showing that the level of ROS induced by UVB was much higher than that induced by UVA. Another study using a human fibroblast cell line and mitochondrial enzyme activity assay to test the mitochondrial damage after UV radiation showed loss of activity of mitochondrial NADH dehydrogenase, indicating that mitochondria are among the targets of phototoxicity [32]. Bantseev and Youn also showed that broadband UV irradiation, as a consequence of generation of reactive oxygen species(ROS) and subsequent oxidative stress, causes morphological change and alteration in size and movement of the mitochondria in ARPE-19 cells [34].

In the present study, cells analyzed by confocal microscopy after nuclear staining did not show the typical apoptotic DNA fragmentation. However, apoptosis may not be totally excluded because of the observed mitochondrial dysfunction, which in many cases causes a rapid apoptotic response [39-40]. Also, in the case of UV irradiated cell nuclei were expended in present study and there were bright rings of DNA around the periphery of the nucleus which is regarded as the early stage of apoptosis [45]. More detailed studies are necessary to establish the relative importance of alternative mechanism of cell death (e.g. necrosis, autophagy, etc.) induced by UV radiation. However, increasing the energy level of UV radiation in the current study clearly induced progressive nucleic acid damage, showing reduced fluorescence distribution both on DNA and RNA. In a recent study showing DNA damage of cultured RPE after relatively low doses of UV (between 0 and 0.09 J/cm^2) using the comet assay, the results showed the formation of DNA strand breaks after UV irradiation [8]. Another study using the human Hela (Human cervical carcinoma) cell line and gel electrophoresis to test for DNA fragmentation after UV irradiation showed a ladder-like fragmentation pattern of DNA, indicating that UV

irradiation, using germicidal lamps at dose rate of 1.2 J/cm^2, initiates apoptosis though UV-induced DNA damage [41]. Tratsk and Thanos using the human RPE primary cell culture and TUNEL assay also showed that UV radiation causes DNA fragmentation, indicating cellular apoptosis [9].

In addition to decreased cellular viability and mitochondrial morphological change, UV also caused a reduction in the ability of RPE cells to ingest fluorescent microspheres. Phagocytosis is a critical element in the ability of RPE cells to maintain a healthy retina [1,42]. Retinal degeneration, particularly age-related macular degeneration, results from the loss of specific functions of the RPE cells, particularly their ability to degrade photoreceptor outer segments [43]. The consequence of phagocytotic failure, or alteration, may contribute to outer segment defects, culminating in their degeneration [9]. A classical example of such a disease is seen in the Royal College of Surgeons (RCS) rat strain where photoreceptor cell death is a result of a primary phagocytotic failure of the RPE [44]. Although the cellular and molecular mechanisms remain unclear, the worst consequence would be the death of the RPE, leading to an atrophic process and consequently the death of the photoreceptors [44]. In the present study, the phagocytosis assay used the microbeads to clearly show reduced phagocytotic activity after the UV irradiation. Another study using a human RPE primary cell culture line and fluorescent E. coli BioParticles to test phagocytotic capacity after UV irradiation, showed decreased ability of RPE cells to phagocytose fluorescent bacterial particles [9].

In conclusion, the results of this study have shown that cellular viability, mitochondrial function, nuclei fraction, and phagocytotic activity of human RPE cells were impaired by environmentally relevant levels of UV radiation in a dose-dependent

manner. The three assays (the Alamar blue assay, confocal microscopy, and phagocytotic activity assay) need to examine RPE function may offer a cost effective, sensitive, and meaningful biomarker method for predicting the degree of retinal UV-induced damage and/or oxidative stress *in vitro*. However, further evaluations are needed to assess specificity and confounding factors of these assessment tools [46].

Chapter 3

In Vitro evaluation of the efficacy of intraocular lens material in protecting the retina from UV damage

Hyun-Yi Youn[1], Ralph B. Chou[1], Anthony P. Cullen[1], Niels C. Bols[2], Jacob G. Sivak[1]

[1]School of Optometry/Department of Biology, University of Waterloo, Waterloo, ON, Canada

[2]Department of Biology, University of Waterloo, Waterloo, ON, Canada

Chapter 3 has been submitted for publication. All the data collection and analysis were performed by Hyun-Yi Youn, who was also the primary author. Drs. Chou, Bols and Cullen provided technical support and advice at various points. Dr. Sivak provided supervisory and editorial assistance throughout.

3.1 Introduction

The crystalline lens of the eye is the principal shield against ultraviolet (UV) radiation (between 300 nm and 400 nm), damage to the human retina [1]. Cataract removal is one of the most common operations performed in the United States [2], and generally an intraocular lens (IOL) is replaced in the lens capsule. With the possibility of extending IOL use to phakic eyes for the correction of high myopia, hyperopia, and other nonopacifying conditions, the use of IOLs may increase further still [2]. The first polymethylmethacrylate IOLs transmitted UV in addition to visible light [3]. Ultraviolet radiation is not required for vision but it can harm the retina at acute and intense exposure [4, 5]. Most IOLs incorporated UV blocking chromophores by 1986 [6]. However, spectrophotometric data show that most of the commercially available, UVAbsorbing IOLs currently in use have different properties than the natural crystalline lens in absorbing UV radiation [7-9]. Also, while there are many studies that evaluate the spectral transmission characteristics of various IOLs to verify their anti-UV efficacy [6, 7, 10], studies showing the cytotoxic effects of UV radiation on retinal cells in terms of cell biology and physiology are few in number. UV radiation can generate free radicals including oxygen-derived species [11], which are known to cause lipid peroxydation of cellular membranes [12, 13]. Also, it has been shown that UV can damage DNA, leading to DNA fragmentation [11, 14, 15], and decreased mitochondrial function [6, 16, 17].

The objective of the present study is to evaluate the UVBlocking efficacy of commercially available IOL materials using a retinal cell culture and a biological *in vitro* model that was developed in a previous study [18]. This work involves the exposure of a

retinal cell culture to broadband UVB radiation with and without the protection of IOL material flats. Cellular viability, mitochondrial damage, DNA damage, and phagocytotic activity are quantified after exposure, using the Alamar blue assay, confocal laser scanning microscopy with fluorescent stains, Hoechst 33258 staining and a phagocytotic activity assay.

3.2 Materials and Methods

3.2.1 Human Retinal Pigment Epithelial Cell Culture

The human retinal pigment epithelial (RPE) cell line ARPE-19 was obtained from the American Type Culture Collection (ATCC). The cells were cultured in DMEM/Ham's F-12 with L-glutamine and 15mM HEPES (Mediatech, VA, USA). The medium also contained 10% fetal bovine serum (Hycolone, UT, USA), and insulin-transferrin-sodium selenite media supplement (ITS supplement) (Sigma, MO, USA) [18]. The cells were plated in T75 or T150 flasks (Falcon, NJ, USA), and allowed to grow until the cultures were confluent. The cells were grown at 37°C in a humidified incubator in an atmosphere of 95% air and 5% CO_2. Confluent cell flasks were passaged every two days using the dissociating agent Trypsin/EDTA solution (Cascade Biologics, OR, USA). The culture and conditioned medium were split into three flasks, and an equal volume of fresh medium was added to each flask. Subculturing was usually performed during the log (or exponential) phase when the cells are at their healthiest and are able to adapt to the new environment most efficiently [19].

3.2.2 UV Irradiation of Cultured RPE Cell

The ARPE-19 cells were cultured in 8 groups (two untreated control groups and six treated groups. All treated groups were exposed to two different levels of UVB radiation (see below). The treated groups (6 groups) included four groups of cells that

were shielded from radiation with one of two IOL material flats of either 0.9 mm or 1.5 mm thickness (4 groups) and two control groups that were exposed without being shielded. Eight groups of cells were used for each different assay (4 assays, see below) in this study, and all experiments were repeated twice. Thus, 64 sets of cells and experiments were prepared and carried out for this study.

The IOL flats were supplied by Bausch & Lomb, Rochester New York. They consisted of yellow tinted standard silicone IOL materials (hydrosilylation cured silicone) that were manufactured by cast molding. The flats, measuring 9.0 by 7.0 cm, were large enough to cover 12 cells of a standard 24 cell multi-well plate that contained the cultured cells. Opaque black tape was applied to the periphery of the plate to ensure that only the radiation passing through the silicon flats could reach the cells. The transmittance characteristics of each of the two flats were measured using a Cary 500 Scanning UV-VIS-NIR spectrophotometer (Figure 1a and 1b).

Exposure was produced by UVB fluorescence tubes (cat. No F15T8/UVB; Microlites Scientific, ON, Canada) in a custom designed UV irradiation unit with 4% CO_2 and 96% membrane-filtered air. The spectral distribution of the UVB fluorescent tubes extends from 290 nm to about 370 nm wavelengths, with a peak at around 315 nm. Since the contribution of the wavelengths within the 320 to 370 nm waveband was only 0.1%, this was ignored. Before irradiation, the irradiance of UVB source was calculated with an Instaspec II diode-array spectroradiometer (Oriel Corporation, CT, USA).

After two days of pre-incubation at 37°C to form a confluent cell monolayer, the cells were exposed with 0.2 and 0.4 J/cm² of broadband UVB (280 -315 nm). The cells were incubated for another 48 hours and assays were carried out at 24 and 48 hours after

irradiation. In order to minimize absorption of the radiation by phenol red in the medium, a thin layer of medium (about 1.0 mm) was left above the cells during UV exposure. Thus, a minor phenol red effect may have influenced the results.

Exposure times for two energy levels (0.2 and 0.4 J/cm²) were calculated with the formula: $H_\lambda = t \times E_\lambda$, where H_λ is the energy level (J/cm²), t is the exposure time (second), and E_λ is the irradiance (W/cm²) [20]. The irradiance measured with a spectroradiometer was 0.000306 W/cm^2, and the exposure times were 10 min 54 sec for 0.2 J/cm² and 21 min 48 sec for 0.4 J/cm², respectively. The solar broadband UVB irradiance level (measured in June 1999 @ Waterloo, ON, Canada,) was 0.000276 W/cm^2 [21]. Thus, the irradiance produced by the UVB tubes for this study is comparable to solar spectral irradiance. For comparison to other studies, it was necessary to calculate the biologically effective dose of the two radiant energy levels. Detailed calculation of these doses has been described previously [18]. The calculated biologically effective radiant energy levels were 0.089 and 0.178 J/cm², respectively.

3.2.3 Alamar Blue Assay

The fluorescent indicator dye, Alamar Blue (MEDICORP Inc., Montreal, PQ, Canada) used to evaluate cell viability, is a commercial preparation of the dye resaruzin [22]. It incorporates resazurin and resorufin as a fluometric redox indicator that changes colour in response to reduction resulting from cell metabolism [22]. For experimental use, it was diluted into the culture medium (mentioned above) without serum to 8% (v/v). After two to three days of pre-incubation, the cells were transferred into a sterile flat

bottom multi-well cell culture plate (BD Falcon, Franklin Lakes, NJ, USA) for fluorescence measurements. Cell density was adjusted to 1×10^5 cells/ml for 48-well plates and 5×10^4 cells in 500 $\mu\ell$ of medium were added to each well [23]. After the irradiation, the culture medium was aspirated from each well, and the cells were rinsed once with culture medium with no serum. Then 100 to 150 $\mu\ell$ of assay solution was added to each well containing cells, and the cells were further incubated for one hour to allow the dye to be taken up by the cells. At the end of one hour incubation, the fluorescence measurements were taken with a CytoFluor™ II fluorescence multi-well plate reader (PerSeptive Biosystems Inc., MA, USA). Before the measurements, the excitation / emission wavelengths settings were adjusted to 530 /590 nm, with the sensitivity gain set at 50. An average of 8 readings was obtained for every well. All procedures were carried out under sterile conditions.

3.2.4 Confocal Microscopy

Confocal scanning laser microscopy (Carl Zeiss LSM) and two fluorescent dyes (Hoechst 33342 and Rhodamine 123) (Molecular Probes, OR, USA) were used to observe the changes of RPE cell morphologic features (nucleus and mitochondria of the cells, respectively) after UVB radiation. Hoechst 33342 is a popular cell-permeant nuclear stain that emits blue fluorescence when bound to dsDNA [24]. Rhodamine 123 is a cationic, lipophilic, water-soluble oxonium chloride salt that stains mitochondria in living cells in a membrane potential-dependent fashion [25]. Before irradiation, 1×10^5 cells in 1.5ml of culture medium were transfered into collagen coated glass bottom

culture Petri dishes (MatTek Corp., MA, USA). After the UVB exposure, the cells were then stained for mitochondria and nucleic acid using Rhodamine 123 (20mM) and Hoechst 33342 (10mg/ml) for 20 min at 37ºC. A Zeiss confocal laser scanning microscope (CLSM) 510 system attached to an Axiovert 100 microscope with a 40× water-immersion C-Apochromat objective was used to observe the effects of the two different dyes.

3.2.5 Hoechst 33342 stain

Before the indicated exposure time, cells were plated into 2-well culture slides (BD Falcon, NJ, USA). After the irradiation, cultures were then fixed twice by adding an equal volume (3~4 drops) of Carnoy's fixative (methanol/glacial acetic acid, 3:1), which was prepared fresh with each use, to existing media, exposing the cells for 5 min. The cells were rinsed with 1× PBS (phosphate buffered saline), and allowed to air dry. Following the initial fixation, the cell slides were stained with 0.5 µg/ml Hoechst 33342 (Riedel-de Haen Ag Seetz-Hannover) (Molecular Probes, OR, USA) for 10 min, followed by a rinse in deionized water. After drying, a coverslip was mounted onto the slide with PBS/glycerol (1:1). The fluorescent nuclei were observed using a fluorescence microscope with an ultraviolet (UV) filter (Nikon Optishot microscope, ON, Canada).

3.2.6 Phagocytotic Activity Assay

Phagocytosis is a critical element in the ability of RPE cells to maintain a healthy retina [26]. Confocal scanning laser microscopy (Carl Zeiss Inc., Jena, Germany) and 0.1μm diameter fluorescent carboxylate-modified microbeads (Molecular Probes, OR, USA) were used to observe the effects of UVB radiation on RPE cell phagocytotic activity. The ARPE-19 cells were transfered to collagen-coated glass bottom culture Petri dishes (MatTek Corp., MA, USA) with a density of 1.3×10^5 cells in 2ml of culture medium. After incubating overnight at 37°C, 7×10^{10} microbeads (red fluorescent, excitation 580 nm/emission 605 nm) in culture medium were added at a total volume of 2ml/Petri dish. After one day of incubation to allow the beads to be ingested by cells, the microbeads were removed and the adherent cells were washed carefully with fresh culture medium twice to remove undigested particles before confocal observation. The micobeads in the cells were observed using the confocal microscope, and the intensity of the fluorescent was measured using the Image Analysis toolbox of Matlab 7.1 software package (MathWork Inc., MA, USA).

3.2.7 Statistical Analysis

Statistical calculations were completed using a two-way repeated measures analysis of variance (ANOVA). A probability value of less then or equal to 0.05 was considered significant.

3.3 Results

The transmittance measurements indicate that both IOL thicknesses transmit light at more than the 90% level until about 420 nm when there is a precipitous drop in transmittance to 0% by about 390 nm (figure 1).

3.3.1 Cell Viability

The Alamar Blue assay readings are presented as percent cell viability relative to the non-UVB exposed cells at three time points: 0-hour (before UV exposure), 24 hours (1-day after UV exposure) and 48 hours (2-day after irradiation). These time points were chosen to permit a time-related evaluation. The results for broadband UVB exposed RPE cells (without IOL protection) showed energy level and time – dependent decreases in cell viability in comparison with the control cells (Figure 2a and 2b). Although the measurements for 0.2 and 0.4 J/cm²-exposed cells at the 24-hour time points presented similar loss of cell viability (64.7±1.0% and 61.2±2.0%, respectively), the Alamar blue assay results for both 0.2 and 0.4 J/cm² exposed cells at 48-hour time points clearly showed energy level-dependent decreases in cell viability (55.5±2.8% and 34.6±7.0%, respectively). The IOL covered cells showed similar viability as control cell groups during the entire culture period, showing very effective UV blocking ability for both IOL material thicknesses of 0.9 and 1.5 mm (Figure 2a and 2b).

3.3.2 Mitochondrial Distribution

Non-irradiated cultured RPE cells (control cells) exhibited no morphological change in mitochondria (first column of Figure 3, green fluorescence). Overall, increasing the energy level of UVB radiation from 0.2 to 0.4 J/cm² resulted in sparser mitochondria, indicating degradation of mitochondria (second column of Figure 3, green fluorescence). In the control cells, numerous mitochondria (green fluorescence) could be seen surrounding individual nuclei (blue fluorescence), and mitochondrial lengths were longer (fibre-looking mitochondria in the first column of Figure 3). However, both 0.2 and 0.4 J/cm² UVB-exposed cells showed shorter mitochondria, fewer fibre-looking mitochondria and mostly fragmented and merged mitochondria (see second column of Figure 3). Also, the results for the 0.2 and 0.4 J/cm² exposed cells showed reduced cell populations in comparison with the control group. The results for the 0.9 mm and 1.5 mm thickness IOL covered cell groups also corresponded with the Alamar blue assay results, supporting the lack of significant morphological changes to the mitochondria (long fibre-looking mitochondria in the third and forth column of Figure 3). This inference is based on the common view that the Alamar blue assay is a measure of mitochondrial activity [27, 28].

3.3.3 Morphology of Nuclei

Non-irradiated cultured RPE cells (control cells) exhibited no morphological nuclear changes (first column of Figure 4). Increasing the energy level of UVB radiation from 0.2 to 0.4 J/cm² to the cells, without the protection of IOL material, reduced the

number of cells attached to the slide due to cell death (second column of Figure 4). At a level of 0.2 J/cm² UVB, irradiated cell nuclei seemed expanded in size, and did not show DNA fragmentation (second column, first row of Figure 4). Also, 0.2 J/cm² UVB irradiated cells exhibited bright rings of DNA around the periphery of the nucleus (second column, first row of Figure 4). However, 0.4 J/cm² UVB irradiated cell nuclei seemed condensed and shrunken in size. They did not show DNA fragmentation (second column, second row of Figure 4). The results of 0.9 mm and 1.5 mm thickness IOL material covered cell groups also corresponded to the above Alamar blue assay and confocal microscopy results, showing no significant morphological nuclear changes and showing similar morphology and number of cells as control cell groups in both the 0.2 and 0.4 J/cm² UVB irradiation groups (third and fourth column of Figure 4).

3.3.4 Phagocytotic Activity

Phagocytotic activity is presented as mean intensity of fluorescence of the ingested microspheres in the cells. Nine different spots of each cell plate were randomly selected, and the intensity of each spot was calculated. The final intensity value of each cell group was the average value of the 9 different spots. The ingestion of red fluorescent microbeads (580/605 nm) into RPE cells is shown in the confocal microscopic images (original magnification ×40 oil, ×2 zoom, Z stack) (Figure 5). The images were taken using the Z stack function of the confocal microscope and the middle Z slide image was chosen for analysis. The overall phagocytotic activity assay results are shown in Figure 6. The control cells have significantly greater capacities for uptake than the 0.2 and 0.4

J/cm² UVB exposed cell groups ($p<0.05$), while the IOL material covered cell groups (both 0.9 mm and 1.5 mm thickness) showed no significant differences from the control cell groups (Figure 6). This phagocytotic assay result corresponds with the above 3 assay results, indicating that both IOL materials (0.9 mm and 1.5 mm) block UVB radiation very effectively.

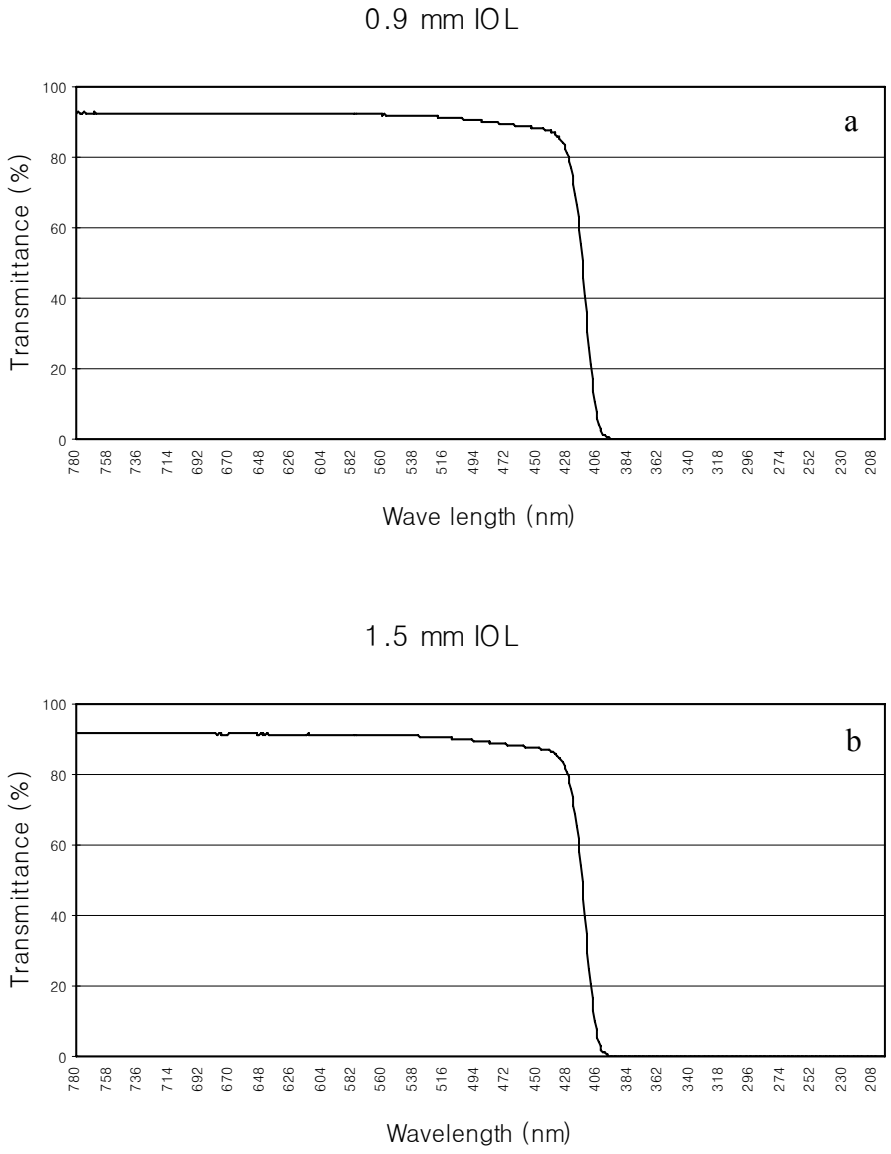

Figure 1. Spectral transmittances of ultraviolet-protective yellow tinted silicone intraocular lens materials (two thicknesses; a = 0.9 mm, and b = 1.5 nm).

0.2 J/cm2 broadband UV-B irradiated ARPE-19

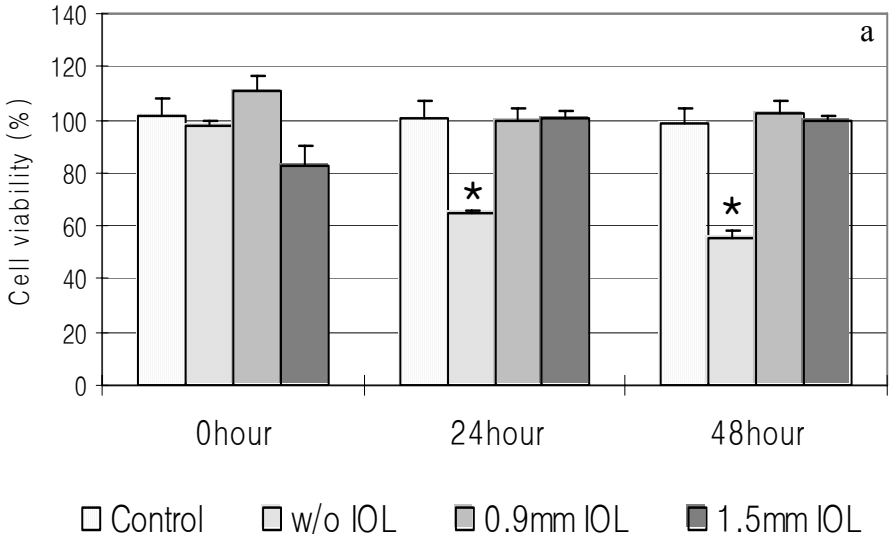

0.4 J/cm2 broadband UV-B irradiated ARPE-19

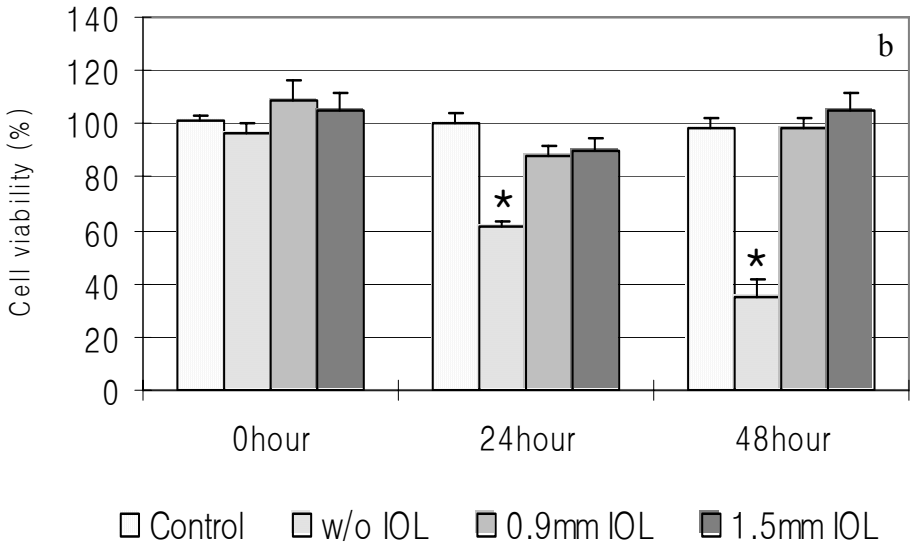

Figure 2. Cell viability results using the Alamar blue assay.

The ARPE-19 cells were cultured in 8 groups (two untreated control groups and six treated groups. All treated groups were exposed to two different levels of UVB radiation. The treated groups (6 groups) included four groups of cells that were shielded from radiation with one of two IOL material flats of either 0.9 mm or 1.5 mm thickness. Two groups of cells were exposed without being shielded (w/o IOL). Cell viability (%) is shown as a function of time (0, 24, and 48 hours) for ARPE-19 cells irradiated with broadband UVB (A: 0.2, and B: 0.4 J/cm2), as revealed by the Alamar blue assay. Cell viability was expressed as a percent of non-UVB exposed cells (% of control). * indicates significant differences as compared to controls ($p < 0.05$).

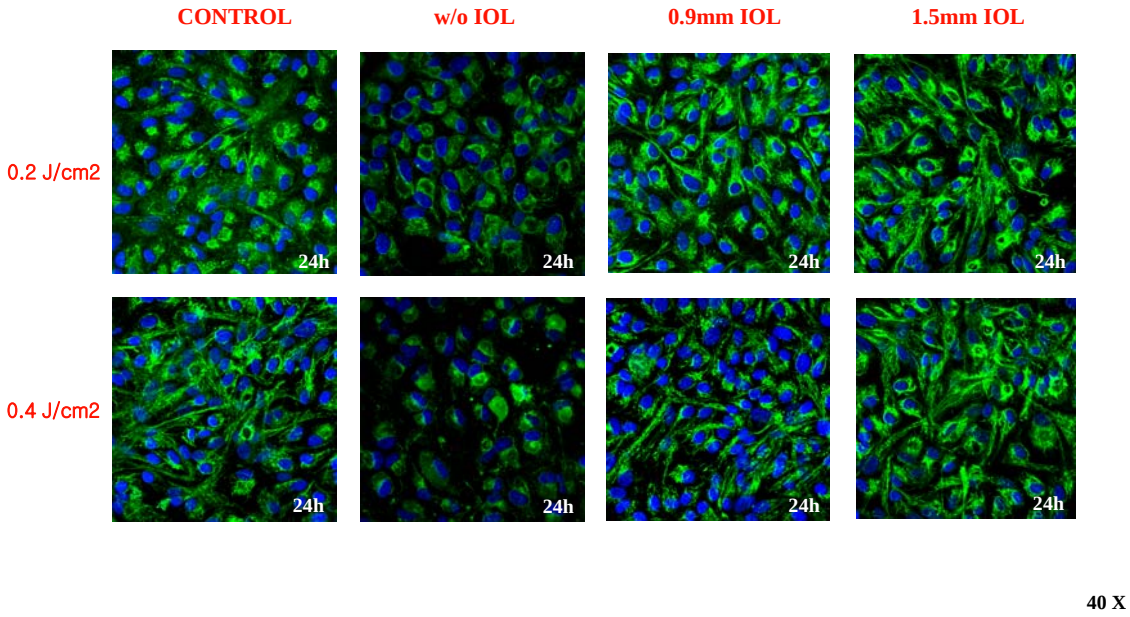

Figure 3. Mitochondrial damage results using confocal laser microscopy.

Eight groups of ARPE-19 cells as figure 2, , with representative confocal laser scanning micrographs showing the effect of UVB (0.2 and 0.4 J/cm2) at 24 hours on distribution of the Rhodamine 123 stained mitochondria (green) and Hoechst 33342 stained nuclei (blue) in ARPE-19 cells. Overall, increasing the energy level of UVB radiation from 0.2 to 0.4 J/cm² resulted in sparser mitochondria, indicating degradation of mitochondria.

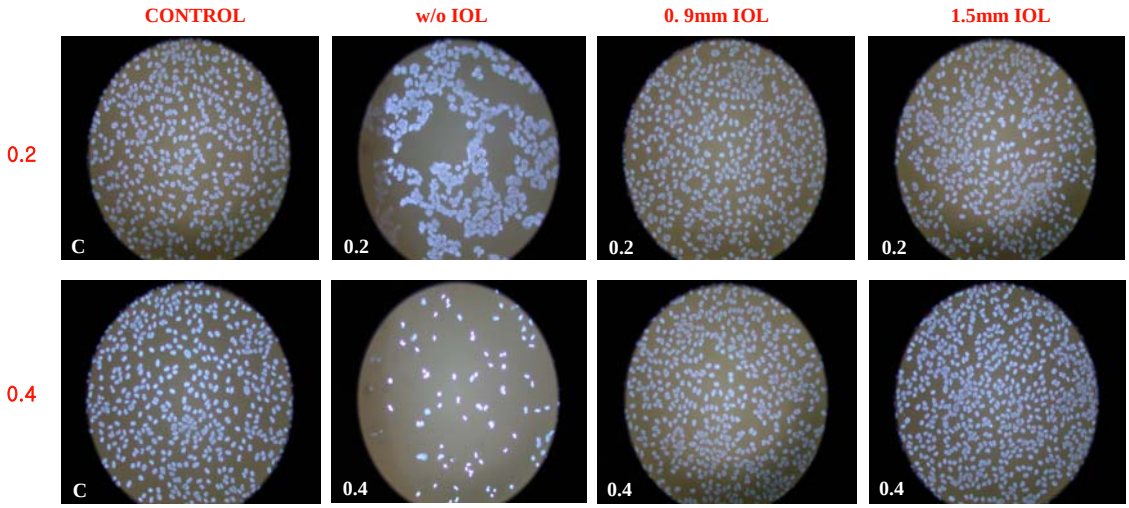

Figure 4. Chromosomal DNA alteration results using the Hoechst assay.

Effect of 0.2 and 0.4 J/cm2 broadband UVB exposure at 24 hours on the nuclear morphology of ARPE-19 cells (eight groups) as revealed by Hoechst 33342 staining and fluorescence microscopy.). At a level of 0.2 J/cm² UVB, irradiated cell nuclei seemed expanded in size, and 0.4 J/cm² UVB irradiated cell nuclei seemed condensed and shrunken in size.

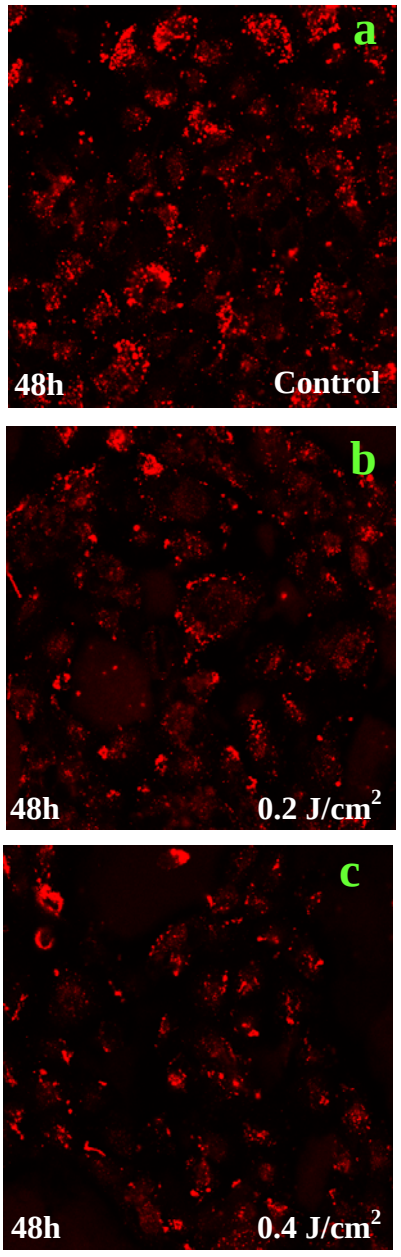

32.7 ± 2.9 *(n = 9)*

23.3 ± 2.5 *(n = 9)*

20.1 ± 2.4 *(n = 9)*

Figure 5. Representative confocal laser scanning micrographs showing the effect of UVB (0.2 and 0.4 J/cm2) at 48 hours on the distribution of red fluorescent microspheres in ARPE-19 cells. Numbers on the right are the average intensity of nine different spots of each cell group.

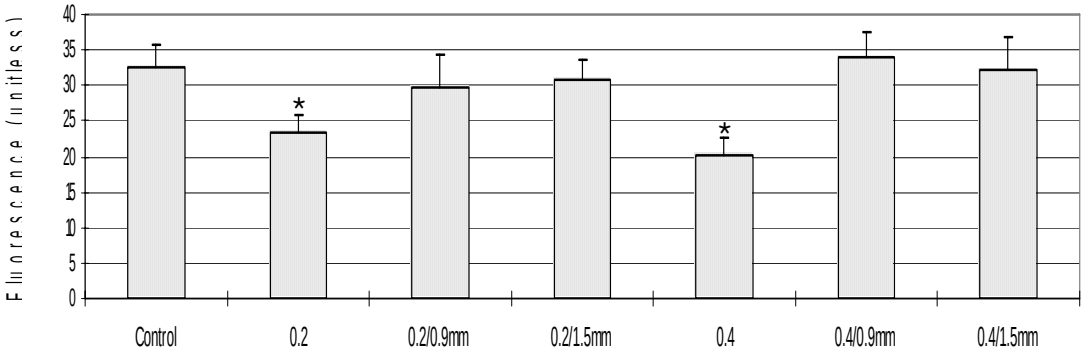

Figure 6. Phagocytotic activity results using the phagocytotic activity assay.

Effect of 0.2 and 0.4 J/cm2 broadband UVB exposure at 48 hours on the phagocytotic activity of ARPE-19 cells as revealed by fluorescent microbeads (0.1 μm) and flow cytometry. Phagocytotic activity was expressed as the average intensity of nine different ARPE-19 images. * indicates significant differences as compared to controls ($p < 0.05$). In this graph, only seven cell groups are shown since two untreated control groups are combined.

3.4 Discussion

3.4.1 Summary of results

The results of this study demonstrate that broadband UVB radiation damage of retinal epithelial cells in culture can be evaluated using four assays; the Alamar blue assay, Rhodamine 123 staining, the Hoestch assay, and a phagocytotic activity assay. Also, the UV blocking efficiency of commercially available IOL materials can be tested using this biological assay model. The results clearly demonstrate that UVB radiation can cause significant decreases in RPE cell viability as well as phagocytotic activity of retinal outer segments by RPE cells. In addition, the results showed that UVB radiation can also induce the degradation of DNA and mitochondria in cultured RPE cells. However, two different thicknesses of IOL material sheets (0.9 mm and 1.5 mm) showed very effective UV blocking ability, allowing no cellular damage at all.

3.4.2 IOL studies and retinal phototoxicity

There have been many studies that have focused only on the spectral transmittance characteristics of various IOLs to verify their anti-UV efficacy. For example, Mainster measured the spectral transmittance (between 300 nm and 500 nm) of 16 implantable intraocular lenses from 12 manufacturers and described the importance of using ultraviolet-absorptive intraocular lenses to protect pseudophakic patients from photic retinopathy [6]. Also, Lin *et al*. analyzed the spectral transmittance (from 200 nm

to 800 nm) of various lenses (spectacle lenses, contact lenses, and intraocular lenses) to clarify their ultraviolet-blocking efficacy [7]. In addition, there are clinical reports involving postoperative measurements of patients who have received intraocular implants. These may include measurements of visual acuity, the occurrence of post operative sight-threatening adverse reactions, and the evaluation of long-term safety and efficacy of implanted ultraviolet absorbing intraocular lenses [29].

It is well known that ultraviolet radiation can produce photochemical lesions in the neural retina and RPE cells, including morphometric cellular changes and DNA damage [15, 30-32]. However, there are fewer studies showing the cytotoxic effects of UV radiation on retina cells in terms of cell biology and physiology. The cellular and molecular mechanisms of ultraviolet-induced retinal cell damage are important to understand how ultraviolet radiation may affect vision.

Although UV-filtered IOL's are an industry standard, some investigators are still concerned because more short wavelength blue light is transmitted by IOLs, as compared to the human crystalline lens [6, 7, 33, 34]. Also, excessive transmission of blue light could degrade perception by creating a colour vision imbalance (cyanopsia) and be hazardous to the long-term health of the retina, such as blue-light induced AMD [9, 35, 60]. Recent research by the authors (unpublished) using the approach described in the current study, has shown that RPE cells can be damaged by wavelengths of 400 nm, although not by wavelengths above 400 nm. The protective results for the IOL material of this study may be, in part due to the fact that the wavelengths filtered include those well into the blue region of the visible spectrum.

3.4.3 In vitro biological assays

Alamar blue is a fluometric indicator of cellular metabolic activity, and it is an ideal test for *in vitro* cell proliferation and cytotoxicity [22]. In the present study, cells analyzed by the Alamar blue assay after UV iradiation showed dose and time dependent decreases in cellular viability. A decrease in the Alamar blue fluorescence readings is a direct measure of the decline in cellular metabolic activity due to loss of appropriate cytoplasmic milieu from the photo-oxidative effect of the UV radiation [36]. Hightower and McCready explained that free radicals are often generated by UV photo-oxidation [37]. The phenomenon of photo-oxidation might have caused the impairment of metabolic activity in the cells. The Alamar blue assay, which is non-radioactive, has been used in *in vitro* photocytotoxicity studies of human RPE, cultured ocular lenses (bovine and porcine), mouse neural crest cells, and human keratinocytes [18, 36, 38-41]. Findings from these studies support the use of the Alamar blue as a sensitive assay for monitoring UV-induced changes in intracellular mitochondrial, cytoplasmic and nuclear integrity, all of which are measures of cellular viability [36].

Rhodamine 123 taken up specifically by mitochondria of living cells can be used as a supravital mitochondrial probe, discriminating between cycling and quiescent cells and having application in sorting functionally distinct cell subpopulations [42]. In the present study, cells analyzed after staining with Rhodamine 123 after UV irradiation showed that by increasing the energy level of UVB radiation, a progressive increase in morphological change, was observed, along with an increased degradation of mitochondria (mostly fragmented and merged mitochondria). Positively charged

Rhodamine 123 seems to bind to the high electronegativity of the intact mitochondrial membranes [42]. Therefore, the intensity of mitochondrial staining may correlate with the activity of the oxidoreductive complexes responsible for the maintenance of the electronegativity of the mitochondrial membrane. Thus, Rhodamine 123 may be a direct marker of energy-supplying metabolic processes [43].

Measurements of mitochondrial deficiencies in living cells by Rhodamine 123 fluorescent micrographs have been used in many *in vitro* photocytotoxicity studies of human corneal epithelial cells, carcinoma cells, RPE cells, and keratinocytes [16-18, 44-46]. Findings from these studies support the use of Rhodamine 123 as a sensitive mitochondrial probe for monitoring UV-induced mitochondrial changes in living cells.

Hoechst 33342 nucleic acid stain is a popular cell-permeant nuclear stain that emits blue fluorescence when bound to dsDNA [47]. This dye is often used to distinguish condensed pycnotic nuclei in apoptotic cells. In the present study, cells analyzed with Hoechst 33342 after UV irradiation showed progressive nuclear morphological change with size expansion for 0.2 J/cm² UVB irradiated cells, and condensation in size for 0.4 J/cm² UVB irradiated cells. Also, 0.2 J/cm² UVB irradiated cells exhibited bright rings of DNA around the periphery of expanded nuclei, which is regarded as the early stage of apoptosis [48]. Apoptosis in animal cells is characterized by chromatin condensation and DNA fragmentation, but in the present study there was no DNA fragmentation (data unavailable) while there was chromatin condensation in the 0.4 J/cm² UVB treated cell group. Furthermore, chromatin pycnosis is a morphological marker for both apoptotic and nonapoptotic programmed cell death (e.g. autophagic cell death) [49]. Thus, more detailed studies are necessary to establish the mechanism of cell

death induced by UV radiation. The measurement of condensed pycnotic nuclei from Hoechst 33342 fluorescent micrographs has been used in *in vitro* photocytotoxicity studies of rat hepatocytes, Chinese hamster ovary cells, Xenopus XTC-2 cells, and B-cell hybridoma [50-53]. Findings from these studies support the use of Hoechst 33342 as a sensitive nuclui morphological marker for monitoring UV-induced apoptotic cells.

The RPE performs several crucial functions important for maintaining the outer retina, including phagocytosis of the distal tips of outer segments, recycling of visual pigment, and transferring nutrients from the choriocapillaris to the neural retina [26, 54, 55]. *In vivo*, approximately 3%–5% of the distal tips of photoreceptor outer segments are shed daily, and proper RPE phagocytosis is necessary to maintain the health and integrity of the neural retina and choriocapillaris [26, 54, 56]. A decrease in phagocytic ability may be associated with an increase in RPE melanogenesis, and clinically, RPE hyperpigmentation is a risk factor for the development of ARMD [57, 58]. In the present study, fluorescent microspheres were used to observe the effects of UVB radiation on RPE cell phagocytotic activity. Increasing the energy level of UVB radiation induced decreased phagocytotic activity of RPE cells. Although it is not clear which molecular change is responsible for a decline in RPE phagocytosis ability, it is known that UV-induced lipofuscin accumulation in RPE cells reduces their phagocytic capacity [57]. Measurements of ingestion by RPE cells using fluorescent microspheres have been used in many *in vitro* photocytotoxicity studies of rabbit, bovine, and human RPE cells [18, 58, 59]. Findings from these studies as well as the current one indicate that the use of fluorescent microspheres may be a sensitive tool for monitoring UV-induced changes in phagocytitic activity of RPE cells.

3.4.4 Conclusion

In conclusion, the results of this study have demonstrated that the Alamar blue assay, confocal microscopy with Rhodamine123 staining, Hoechst assay, and phagocytotic activity assay showed that two thicknesses of an IOL material provide effective RPE cell protection from UVB radiation. These four assays together can be used as a sensitive, and meaningful *in vitro* biomarker method not only for evaluating IOL effectiveness, but also for evaluating RPE function in various conditions such as oxidative stress associated with aging, the retinal effects of blue light, age-related macular degeneration (ARMD) studies, chemical stress from drugs, and genetic stress from altered gene expression.

Chapter 4

Effect of Blue Light (400 nm, 420 nm, and 435.8 nm) on Cultured Human Retinal Pigment Epithelial Cells and Its Application to Blue Light Blocking IOLs

Hyun-Yi Youn[1], Ralph B. Chou[1], Anthony P. Cullen[1], Jacob G. Sivak[1]

[1]School of Optometry/Department of Biology, University of Waterloo, Waterloo, ON, Canada

Chapter 4 has been submitted for publication. All the data collection and analysis were performed by Hyun-Yi Youn, who was also the primary author. Drs Chou and Cullen provided technical support and advice. Dr. Sivak provided supervisory and editorial assistance throughout.

4.1 Introduction

Optical radiation includes ultraviolet radiation (100-400 nm), visible light (400-750 nm), and infrared radiation (750-10,000 nm)[1], and visible light is referred to as short- (blue), medium- (green), and long-wavelength (red) radiation.[2] The ozone layer absorbs wavelengths up to 286 nm, thus we are exposed to wavelengths above 286 nm, most of which falls within the visual light spectrum.[3] Phototoxicity decreases as wavelength increases, and the shorter wavelengths of the visible spectrum pose a potential hazard because they contain more energy.[4] Exposure to these wavelengths has been called the blue light hazard because these wavelengths appear blue to the human eye.[5]

The term blue is often used for the broad range of optical radiation between 400 and 500 nm, and blue-light hazard is defined as the potential for photochemical induced retinal injury resulting from radiation exposure at wavelengths between 400 nm and 500 nm.[6] It has been speculated that blue light may cause retinal damage or contribute to the development of age-related macular degeneration (ARMD).[7,8] Animal experiments show that retinal exposure to excessive levels of blue light induce photochemical damage of photoreceptor and retinal pigment epithelial (RPE) cells.[9,10]

It has been demonstrated that the blue light hazard is mediated through absorption of blue light by fluorophores in the retinal cells, such as rhodopsin, melanin, and lipofuscin.[1,2,7] The high energy photons in the spectrum of blue light radiation create reactive oxygen species (ROS), which are deleterious to DNA and to a variety of cellular organelles, particularly the mitochondria.[1,11,12] The primary lesions in ARMD is in the RPE, where an accumulation of lipofuscin occurs due to the phagocytosis of

photoreceptor disk membranes, and also because it is an oxygen-rich environment.[13] There is considerable evidence that it is the loss of RPE cells caused by blue light that leads to secondary photoreceptor cell degeneration in ARMD.[1]

The most common cause of vision loss in the United States is cataract.[14] Cataract surgery is the most common procedure performed in the medicare population with more than 2,000,000 cataract surgeries performed per year in the United States.[15] Cataract surgery is very successful and considered routine, but there have been some studies that suggest that cataract surgery may accelerate ARMD since removal of the crystalline lens, followed by implantation of an intraocular lens (IOL) that does not attenuate blue light, may cause retinal cell damage.[16-20] This has led to efforts to develop improved, blue light filtering, IOLs, which might provide improved function by more accurately simulating the human crystalline lens.[13] However, currently developed IOLs from various manufacturers have different filtering curves indicating that blue light is only partially blocked or filtered.[21-23]

The objective of this study is to determine more precisely the wavelengths of blue light responsible for photochemical lesions to the retina using *in vitro* biological assays. The information provided can be used in the improved development of blue light absorbing IOLs. This work involves the exposure of a retinal cell culture to narrowband blue light of three different wavelengths using a xenon arc lamp with interference filters. Cellular viability, mitochondrial distribution, and nucleic acid (both DNA and RNA) damage are quantified after exposure, using the Alamar blue assay and confocal laser scanning microscopy with two fluorescent stains (Rhodamine 123 and Acridine Orange).

4.2 Materials and Methods

4.2.1 Human Retinal Pigment Epithelial Cell Culture

An immortalized human RPE cell line, ARPE-19, was obtained from the American Type Culture Collection (Manassas, VA, USA) and cultured in DMEM/Ham's F12 with L-glutamine and 15mM Hepes (Media Tech, VA, USA), supplemented with 10% fetal bovine serum (Hycolone, UT, USA), and insuline-transfferin-sodium selenite (ITS) (Sigma, MO, USA). The cells were incubated in a humidified atmosphere of 5% CO_2 and 95% air at 37˚C, and the culture medium was changed every 24 hours. Cells were plated in T75 or T150 flasks (Falcon, NJ, USA), and allowed to reach confluence (typically 2 to 3 days). Glass bottom Petri culture dishes (MatTek, MA, USA) as well as 48 well plates (Falcon, NJ, USA) were used. Subculturing was carried out using a Trypsin/EDTA solution (Cascade Biolgics, OR, USA) after a confluent monolayer appeared.

4.2.2 Narrowband Blue Light exposure of Cultured RPE cells

The treatments tested were blue visible light of wavelengths at 400 nm, 420 nm, and 435.8 nm. The wavelengths tested were chosen on the basis of commercially available interference filters. Irradiation sources were a Photochemical Research Associates (PRA) integrated arc lamp system using a water cooled 1000 W high pressure xenon arc in reflector fixtures (PRA Inc, ON, Canada). Figure 1 shows a schematic

diagram of the blue light irradiation apparatus. A front surface mirror was used to deflect the beam by 90˚ to impinge on the cells. A quartz-condensing lens (Edmund Scientific Co., NJ, USA) was placed at the entrance, and another quartz-condensing lens at the exit aperture of the mirror housing, respectively. Specific narrow wavebands (400, 420, and 435.8 nm) of blue light were obtained using interference filters (Melles Griot, NY, USA). Table 1 shows general characteristics of each filters. The arc lamp and optical system were enclosed, and purged with nitrogen gas to prevent ozone formation before each use.

Before each irradiation of cells, dosimetry was performed using an 88XL Photodyne radiometer together with a photometric sensor head (Optikon Corp., ON, Canada). To convert the radiometer measurement (μW) to irradiance (W/cm^2), the measured value was divided by the photometric sensor head area (cm^2), multiplied by the area irradiated on the cells (cm^2), and multiplied by the linear multiplication factor (unitless) from the calibration curve. The sensor head area was 0.42 cm^2, and the irradiated area was 5.30 cm^2. The linear multiplication factors were 2.67 for 400 nm, 2.42 for 420 nm, and 2.23 for 435.8 nm, respectively. For example, a radiometer reading of 46 μW for 400 nm would be 0.00155 W/cm^2 as irradiance (e.g. 46 μW ÷ 0.42 cm^2 × 2.67 × 5.3 cm^2 = 0.00155 W/cm^2).

Radiant exposure time (sec) was determined using the following radiometric equation: $t = H_\lambda / E_\lambda$, where t is the exposure duration (sec), H_λ is the radiant energy level (J/cm^2), and E_λ is the measured irradiance (W/cm^2). Table 2 shows the calculated energy levels and exposure durations for this experiment. Radiant exposure time was controlled with a preset electronic counter, which automatically closed the shutter after each predetermined exposure. For comparison to other studies, it was necessary to calculate

the biologically effective dose of the radiant energy levels. Calculation of these doses has been described previously[24], and the calculated biologically effective radiant energy levels are shown in Table 2.

After 2 to 3 days of pre-incubation to form a confluent cell monolayer, the cells were exposed to predetermined energy levels of blue light (see Table 2). The light source was positioned directly above the cells. In order to minimize absorption of the radiation by the phenol red in the medium, a thin layer of medium (about 1.0 mm) was left and thus a minor phenol red effect may have influenced the results. Immediately after exposure, cells were further incubated for 3 to 48 hours under normal conditions (culture medium, 37˚C, 5% CO_2, 95% air) before analysis.

4.2.3 Alamar Blue Assay

After blue light exposure, the fluorescent indicator dye, Alamar blue (Medicorp, PQ, Canada) was used to evaluate cell viability. Alamar blue was diluted into the culture medium to 8% (v/v), and the solution was prepared immediately before each use to avoid possible precipitation. For experimental use, cells were seeded into sterile flat bottom 48-well plates, and cell density was adjusted to 1×10^5 cells/ml. Cells were allowed to settle and form a confluent monolayer for 2 to 3 days in their normal growing condition (culture medium, 37˚C, 5% CO_2, 95% air) before being exposed to the blue light. 24 hours after irradiation, cells were rinsed once with culture medium, and 100-150 μl of 8% Alamar blue working solution was added to each well. Cells were further incubated for one hour to allow the dye to be taken up by the cells. Fluorescent measurements were

performed with the CytoFluor™ II fluorescence multi-well plate reader (PerSeptive Biosystems, MA, USA). The excitation/emission wavelengths settings were adjusted to 530/590 nm, with the sensitivity gain set at 50, and temperature at 37˚C.

4.2.4 Fluorescent Staining and Confocal Microscopy

For evidence of celluar morphological change, cells were evaluated for mitochondrial distribution and nucleic acids damage as assessed by confocal scanning laser microscopy (Carl Zeiss Inc., Jena, Germany) using two fluorescnt stains, Rhodamine 123 and Acridine Orange (Molecular Probes, OR, USA). Positively charged Rhodamine 123 is an mitochondrial inner membrane potential marker that stains electronegative mitochondria in living cells in a membrane potential-dependent fashion.[25] Acridine orange is a nucleic acid selective fluorescent cationic dye which interacts with DNA and RNA by intercalation or electrostatic attractions.[26] When bound to dsDNA and RNA, it emits green fluorescence and red fluorescence, respectively.

Five μl of Rhodamine 123 solution (1.1 mg of Rhodamine 123 per 144 μl of ethanol) was diluted into 10.0 ml of culture medium, and 10.0 μl of Acridine Orange solution (1.3mg of Acridine Orange per 130.0 μl of mili Q water) was diluted into 10.0 ml of culture medium. The solutions were prepaed immediately before each use to avoid possible precipitation. For experimental use, cells were seeded into a collagen coated glass bottom culture Petri dish (MatTek, MA, USA). Cells were allowed to settle and form a confluent monolayer for 2 to 3 days at their normal growing condition (culture medium, 37˚C, 5% CO_2, 95% air) before being exposed to the blue light. After 9 hours

of irradiation, cells were rinsed once with culture medium, and either 2.0 ml of Rhodamine 123 or Acridine Orange working solution was added to each culture dish. Cells were further incubated for 20 minutes to allow the dye to be taken up by cells. Fluorescent measurements were performed with a Zeiss confocal laser scanning microscope (CLSM) 510 system, attached to an Axiovert 100 microscope with a 40 × water-immersion C-Apochromat objective.

4.3 Results

4.3.1 Cell viability

The Alamar blue assay readings were presented as percent cell viability relative to the non-exposed control cells at each exposure time point: 3, 6, and 9 hours after 400 nm of blue light irradiation, 3, 6, 9, and 12 hours after 420 nm of blue light irradiation, and 6, 9 and 12 hours after 435.8 nm of blue light irradiation (Figure 2a, b, and c). Thus, a total of 10 sets of cell cultures and experiments were prepared and carried out for this assay.

Overall, the Alamar blue assay data for 400, 420, and 435.8 nm blue light-exposed RPE cells showed energy level (or exposure time) – dependent decreases in cell viability only at 400 nm blue light exposure (Figure 2a) and not for 420 and 435.8 nm blue light irradiation (Figure 2b and c). All the 400 nm blue light exposed cell groups at each exposure time (3, 6, 9, and 12 hours) showed significant decreases ($p < 0.05$) in fluorescence after irradiation (Figure 2a). Conversely, 420 and 435.8 nm blue light exposed cell groups at each exposure time (3, 6, 9, and 12 hours after 420 nm exposure, and 6 and 12 hours after 435.8 nm exposure) did not show significant changes after irradiation (Figure 2b and c).

4.3.2 Mitochondrial distibution

Mitochondrial distributions in RPE cells are indicated by green fluorescent Rhodamine 123 in the confocal laser scanning micrographs, while blue portions indicate

the Hoechst stained nuclei of the cells (Figure 3).

Overall, the confocal microscopic data of Rhodamine 123 stained RPE cells for 400, 420, and 435.8 nm blue light exposure show increased degradation of mitochondria (sparser mitochondria) only at 400 nm blue light exposures (Figure 3b) in conparison with the control cells (Figure 3a). Cells irradiated with 420 and 435.8 nm blue light do not show mitochondrial damage (Figure 3c and d) and appear similar morphologically to control cells (Figure 3a). The mitochondrial distributions in the case of 400 nm blue light exposed RPE cells are very low and are most pronounsed in the perinuclear region (Figure 3b) while the mitochondria in the control cells are very abundant and longer (fibre-looking mitochondria) (Figure 3a).

4.3.3 Nucleic acid damage

Nucleic acids (DNA and RNA) in RPE cells are indicated by green and red dual-fluorescent Acridine Orange in the confocal laser scanning micrographs. Green portions indicate double stranded DNA, and red portions indicate single stranded RNA (Figure 4).

Overall, the confocal microscopic data for Acridine Orange stained RPE cells for 400, 420, and 435.8 nm blue light exposure show increased degradation (less green and red fluorescences) of nucleic acids (both DNA and RNA), especially red fluoescent RNA, only at 400 nm blue light exposure (Figure 4b) in conparison with the control cells (Figure 4a). Cells irradiated with 420 and 435.8 nm blue light do not show nucleic acids damage (Figure 4c and d) and are morphologically similar to control cells (Figure 4a). The nuclei in 400 nm blue light exposed RPE cells appear to be degraded, showing non-

green fluorescent (black) portions in the nuclei (Figure 4b, blue arrows), and some nuclei seem to be expanded in size (Figure 4b) in comparison to control cell nuclei (Figure 4a). Also, 400 nm blue light exposed RPE cells exhibited bright green rings of DNA around the periphery of the nuclei (Figure 4b, yellow arrows).

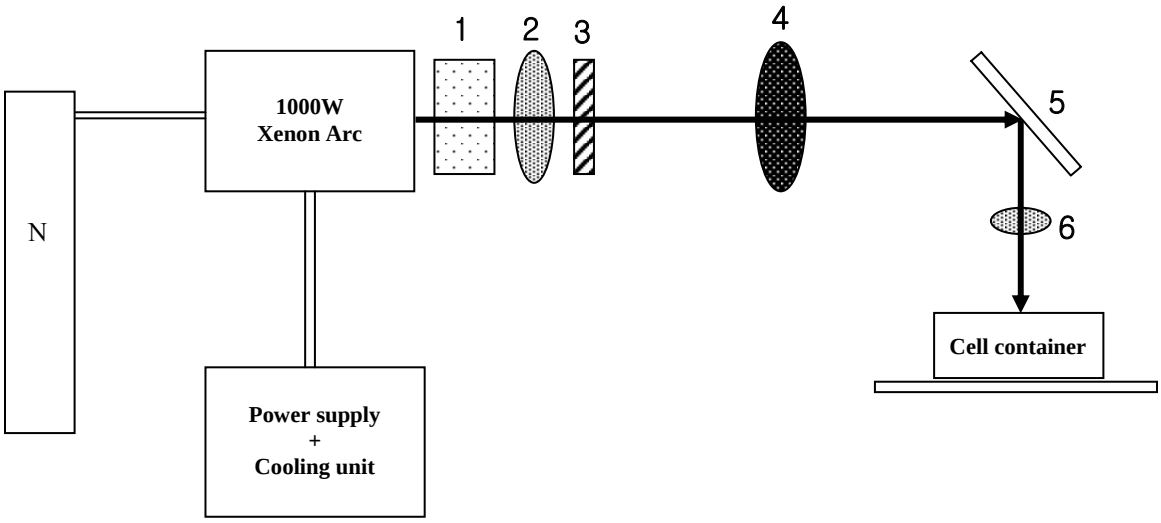

Figure 1. A schematic diagram of the blue light narrow band irradiation system. N: nitrozen gas, 1: De-ionized water chamber, 2: Quartz condensing lens, 3: Electronic shutter controlled by a timer, 4: Interference filter, 5: Front surface mirror, 6: Quartz condensing lens.

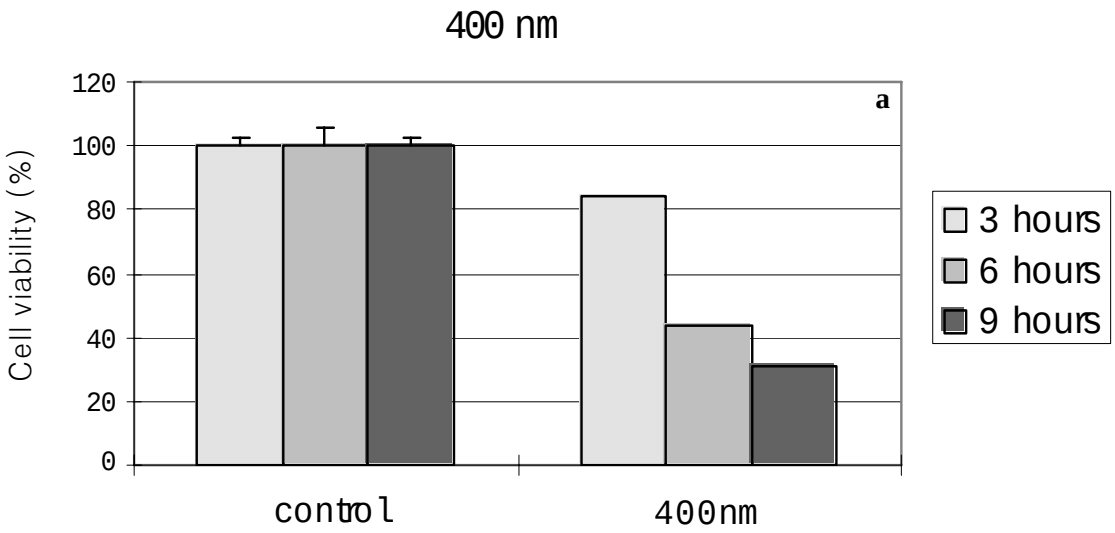
400 nm
a
Cell viability (%)
120
100
80
60
40
20
0
control
400nm
3 hours
6 hours
9 hours

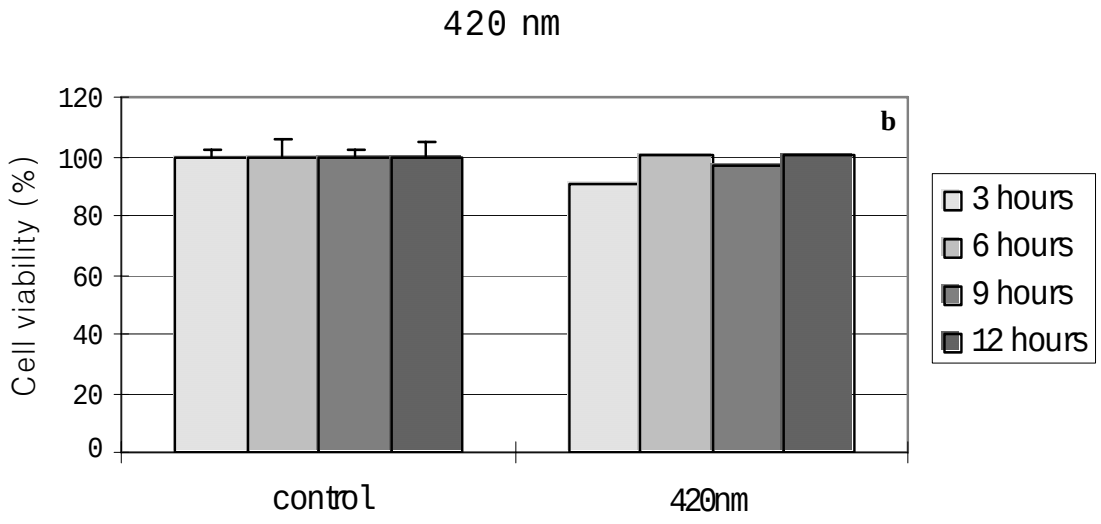
420 nm
b
Cell viability (%)
120
100
80
60
40
20
0
control
420nm
3 hours
6 hours
9 hours
12 hours

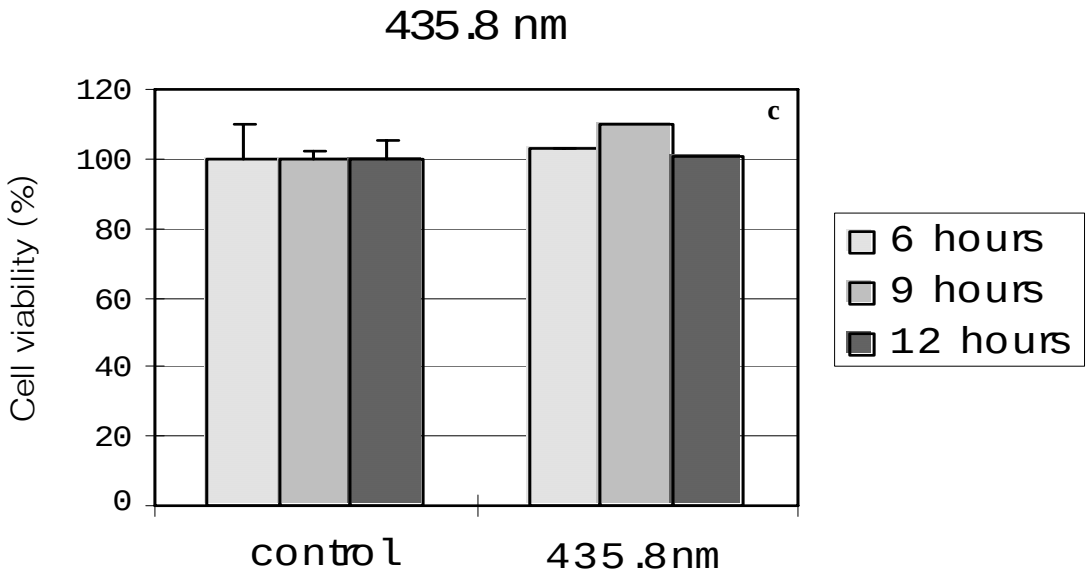

Figure 2. Effects of blue light (a: 400 nm, b: 420 nm, and c: 435.8 nm) 3, 6, 9, and 12 hours after exposure on the cellular viability of ARPE-19 cells as revealed by the Alamar blue assay. Cell viability (%) is expressed as a percent of non-exposed cells (% of control). * indicates significant differences as compared to controls ($p<0.05$).

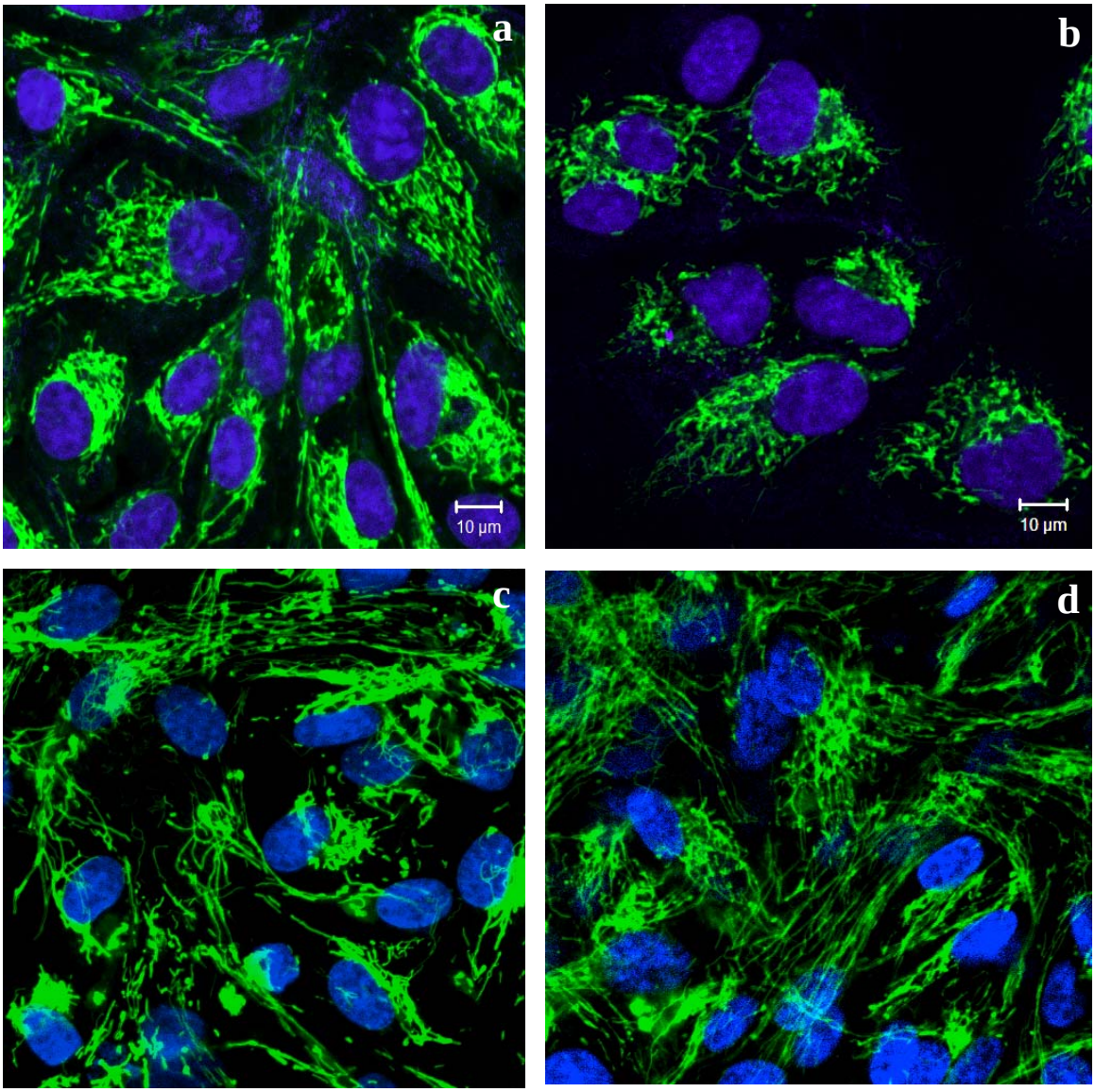

Figure 3. Effects of blue light (a: non-irradiated, b: 400 nm, c: 420 nm, and d: 435.8 nm) 9 hours after exposure on the mitochondrial distribution (green) of ARPE-19 cells as revealed by the Rhodamine123 staining and confocal microscopy. Blue portions are the Hoechst 33342 stained nuclei of ARPE-19 cells.

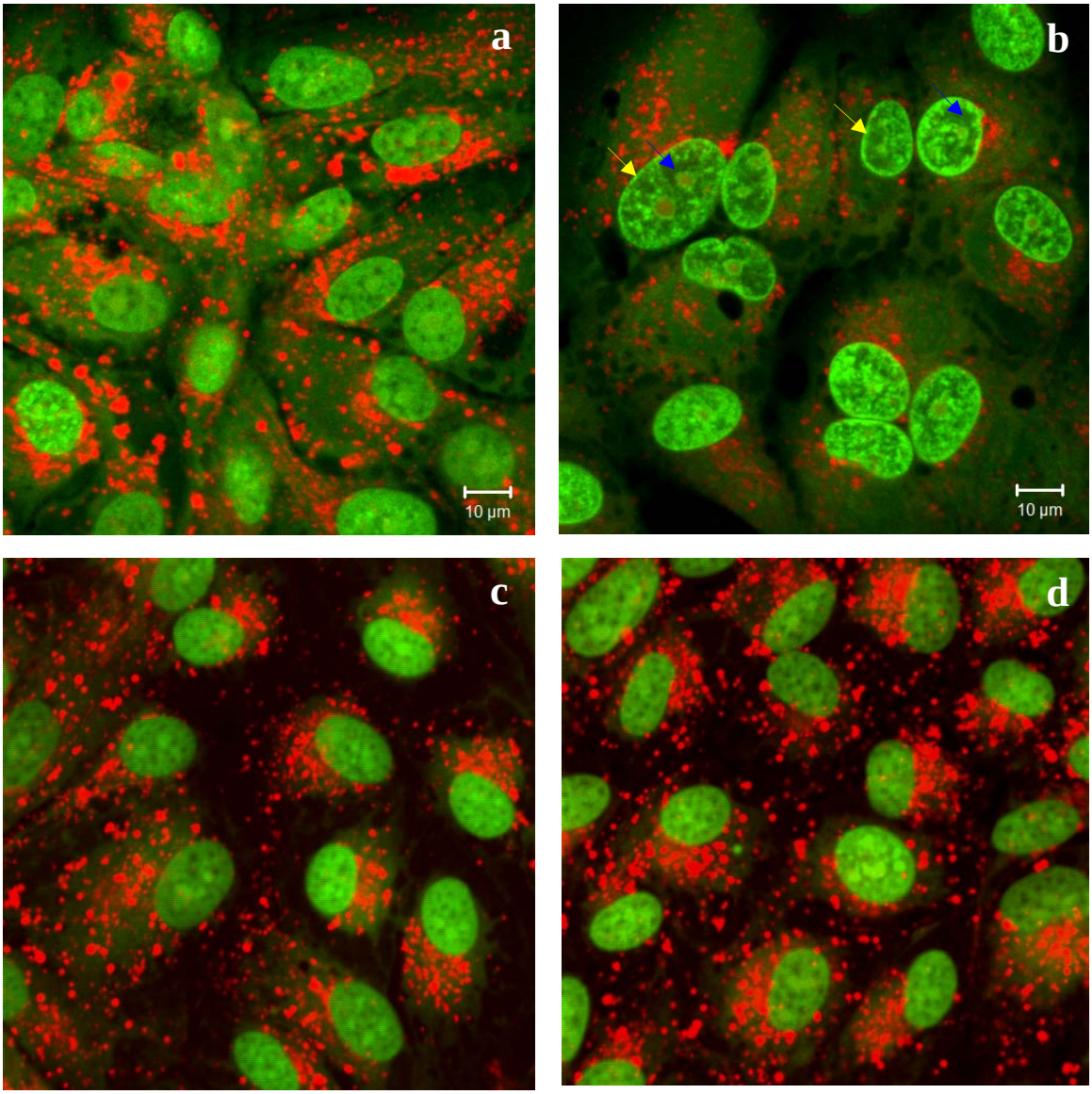

Figure 4. Effects of blue light (a: non-irradiated, b: 400 nm, c: 420 nm, and d: 435.8 nm) 9 hours after exposure on distribution of DNA (green) and RNA (red) in ARPE-19 cells as revealed by the Acridine Orange staining and confocal microscopy.

Table 1. General characteristics for 400nm, 420 nm, and 435.8 nm interference filters adapted from Melles Griot. (* FWHM = full width at half maximum)

Interference filters	Center Wavelength (nm)	Bandwidth (nm)	Peak Transmission (%)	* FWHM (nm)
400nm	401.6	9.2	> 40.0	406.2 ~ 397.0
420 nm	421.3	9.7	> 50.2	416.4 ~ 426.2
435.8 nm	436.9	9.1	> 50.2	432.3 ~ 441.5

Table 2. Descriptive calculations of irradiances (E_λ), exposure durations (t), energy levels (H_λ), and biological effectiveness for 400 nm, 420 nm, and 435.8 nm blue light irradiations of this study.

	E_λ (W/cm^2)	t (hour)	H_λ (J/cm^2)	Biological effectiveness (J/cm^2)
400 nm	0.00155	3	17	7.6
		6	34	15.1
		9	50	22.3
420 nm	0.001466	3	16	7.1
		6	32	14.2
		9	48	21.4
		12	63	28.0
435.8 nm	0.001351	6	29	11.9
		9	44	18.0
		12	58	23.8

4.4 Discussion

4.4.1 Summary of results

The results of this study clearly show that only 400 nm blue light radiation can cause significant decreases in RPE cell viability as well as degradation of DNA/ RNA and mitochondria in RPE cells, while 420 and 435.8 nm blue light radiation is not damaging.

4.4.2 Retinal phototoxicity of blue light

Although the primary function of the retina is to receive and transduce light from the environment, excess exposure to light is hazard to vision.[27] Blue light is the most hazardous component of the visible spectrum,[4] and it is known to generate reactive oxygen species (ROS) in the retina.[28,29] The RPE is especially susceptible to oxidative stress because of its high light, oxygen, fluorophore (e.g. melanin, lipofuscin) and membrane lipid (e.g. polyunsaturated fatty acids) levels.[1,27,30] Several molecules in the retinal cell are implicated in mediating the phototoxicity of blue light.

4.4.2.1 Mitochondrial damage

Mitochondria control numerous metabolic reactions including oxidative processes, and retinal mitochondria offer an additional source of photosensitizers which have the potential to generate ROS as the result of interaction with light.[31-33] ROS is

formed particularly in response to short-wavelength irradiation, and it can be derived from leakage of electrons from mitochondrial aerobic metabolism.[1] An experimental study revealed that mitochondria are an important source of toxic oxygen radicals in blue light exposed RPE cells.[31] The mitochondrial enzyme cytochrome oxidase in the retina absorbs blue light, and this induces morphological changes in the mitochondria[34] and also inhibits mitochondrial respiration.[35,36] It has been shown that the expression of cytochrome oxidase in the retina is irreversibly inhibited when rats are exposed to spectral blue light, leading to retinal damage.[37] Suter et al. also showed that activated fluorophores (e.g. lipofuscin) target mitochondria and induce apoptosis.[9] In this study, the results for rhodamine 123 mediated mitochondrial staining also show blue light (400 nm only, not 420 and 435.8 nm) induced mitochondrial degeneration in the RPE cells (Figure 3b).

4.4.2.2 Apoptotic DNA damage

For tissues that retain the capacity to proliferate, apoptosis provides a mechanism for eliminating a dysfunctional cell,[38,39] but in non-replicating cells such as RPE, cell death has dire implications.[40] There are many studies that reveal blue light induced apoptosis in the RPE cells,[10,31,36,40-42] and the biochemical hallmark of apoptosis is the cleavage of chromosomal DNA into nucleosomal fractions, which marks the final blow in the cell death process.[43] For example, Sparrow et al. showed that blue light illumination in the RPE cells initiates a cell death program that is executed by caspase-3 and regulated by Bcl-2,[36] and DNA is one of the subcellular targets of the photodynamic events initiated by blue light.[40] Blue light leads single strand breaks of DNA, and, at

least some of the DNA lesions are due to the oxidatively modified guanine base.[40] Also, Hafezi et al. and Seko et al. showed that blue light induces apoptosis in the retinal cells, especially revealing DNA fragmentation and nucleic chromatin alteration.[10,41] In the current study, the results of the acridine orange mediated nuclei staining method also showed blue light (400 nm only, not 420 and 435.8 nm) induced nucleic chromatin alteration in the RPE cells (Figure 4b). For example, 400 nm blue light exposed RPE cells exhibited bright green rings of DNA around the periphery of the nuclei (Figure 4b, yellow arrows), and this is corresponds to the electron microscopic observation of Hafezi et al. showing initial peripeheral chromatin clumpingin the RPE cells,[10] which is regarded as the early stage of apoptosis.[44]

4.4.2.3 Age-related macular degeneration

Age-related macular degeneration (ARMD) affects 10 to 20 % of people over the age of 65, and constitutes one of the leading causes of severe visual impairment in the elderly in industrialized nations.[45] Whereas the pathogenesis of ARMD is poorly understood, it is generally believed that the accumulation with age of the pigment lipofuscin and other phagocytotic materials in lysosomes of RPE cells constitutes a precondition for the development of the disease, forming and depositing drusen - extracellular masses of heterogeneous composition[46-48] – between the RPE and Bruch's membrane.[49-51]

Blue light may accelerate the disease process[52,53] since lipofuscin, one of the RPE fluorophores, is responsible for the blue light sensitivity of RPE cells.[54,55] A2E, a hydrophobic constituent of RPE lipofuscin, is maximally excited by light in the blue

region of the spectrum,[54] and blue light exposed A2E generates highly reactive singlet oxygen that induces oxidative cellular damage to the RPE, ultimately resulting in apoptosis.[54,56] The lipofuscin sensitivity to blue light may explain why ARMD has been linked to both RPE lipofuscin[57] and cumulative blue light exposure.[8] Furthermore, the loss of RPE cells due to apoptosis in ARMD may lead to photoreceptor cell degeneration. In this study, blue light irradiation (400 nm only, not 420 and 435.8 nm) reduced the viability of RPE cells (Figure 2a), and this result may also be of significance in relation to the development of ARMD.

4.4.3 Blue light absorbing IOL

4.4.3.1 History of development of IOLs

From the first implantation in 1949 through the early 1980s, IOLs were commercially made from clear polymethyl methacrylate (PMMA) without filtering chromophores.[58] IOLs with UVR blocking chromophores bonded to optic polymers were then introduced in the early 1980s,[59,60] and by 1986, almost all IOLs available in the U.S. market came with UVR filtering even though some IOLs still have inadequate UVR protection.[61,62] In addition, nonfoldable PMMA IOLs that absorb blue as well as UVR were introduced in the 1990s,[63] and the first foldable blue light absorbing IOLs were introduced in 2003.[22]

4.4.3.2 Spectral transmittance curves of IOLs

Unfortunatley, UVR protection in contemporary IOLs is inconsistent, and some manufacturers still produce IOLs that transmit potentially phototoxic near-UVR to the retina.[21,62-64] For example, IOLs from different manufacturers have various cutoff points ranging in wavelength from 350 nm to 393 nm.[21,62] IOLs of different powers also have different cutoff points with low plus power lenses showing less UV blocking effect.[62] While these IOLs provided some UV absorption, none absorbed blue light.

Furthermore, the spectral transmittance for blue blocking IOLs were studied,[22,23,64,65] but older and even some modern IOLs transmit much more potentially hazardous blue light than the crystalline lens does. Mainster showed different photoprotection percentages of blue blocking IOLs, ranging from 1% to 94%.[23] This implies that there is still no agreement as to how much blue light an IOL should transmit. In this study, the results clearly show that only 400 nm (not 420 and 435.8 nm) blue light radiation can cause significant cellular damage to the RPE.

4.4.4 Potential long-term side effects of blue light absorbing IOLs

Despite the benefits of blocking blue light, a yellow tinted IOL may modify visual performance. It is expected that the blue cone and rod photoreceptors, which have a spectral sencitivity range between approximately 430 nm and 555 nm, may be significantly affected by a yellow filter that blocks wavelengths below approximately 400 ~ 500 nm.[22,23,64,65] This may result in changes in scotopic vision and colour perception although many case reports indicate that there are no adverse effects of blue light filtering IOLs.[23,30,64,66-70]

4.4.4.1 Scotopic sensitivity

Vision in darkness that is only mediated by rods is known as scotopic vision.[71] Blue light is more important for scotopic than photopic vision because of the Purkinje shift.[30] The Purkinje shift is the change in peak spectral sensitivity from longer (555 nm) to shorter (507 nm) wavelengths as illumination decreases - from photopic vision to scotopic vision.[72] Thus, rod-mediated scotopic sensitivity is much more dependent on blue light than photopic sensitivity.[30]

Previous studies reported that yellow tinted IOLs induce a reduction in scotopic sensitivity.[1,30,64] For example, subjects with blue light blocking IOL's exhibit a significant decrease in scotopic vision threshold (less sensitivity) at 410 nm and 450 nm, while no significant differences in scotopic visual performance were found at 500 nm or 560 nm between patients implanted with a yellow IOL as compared to those implanted with a IOL.[1] Mainster and Sparrow propose that blue blocking IOL's (AcrySof Natural IOL, Alcon Laboratories, Inc.) may decrease rod-mediated scotopic vision by 27 %, compared to conventional IOLs[64] since this IOL blocks 50 % of blue light at 450 nm and 25 % at 480 nm (product information by Alcon Laboratories Inc.).

4.4.4.2 *Blue colour perception*

Too little transmission of blue light or excessive transmission of yellow colour due to the blue light filtering of IOL's with a yellow chromophore, may also degrade perception by creating a colour vision imbalance.[67,70,73,74] For example, Shar and Miller reported that a 50-year-old woman complained of binocular imbalance and "yellow

vision" in her left eye after implantation of a blue light–filtering yellow IOL.[70] Mester et al. also showed that a blue light filtering IOL with a yellow chromophore induced significant impairment of colour perception for blue.[67] However, many case reports also noted that the impairment of colour perception did not exceed the normal range and did not induce subjective disturbance of colour vision.[66,68,75-78]

4.4.5 Conclusion

The results of this study have demonstrated using the Alamar blue assay and confocal microscopy with Rhodamine123 and Acridine orange staining, that only 400 nm blue light induced decreased cell viability, mitochondrial degeneration, and nucleic damage in RPE cells, while 420 nm and 435.8 nm blue light did not have an influence on the RPE cells at all. Thus, blue light wavelengths between 400 nm and 420 nm represent the critical wavelength range responsible for photochemical lesion to RPE cells. These results may be of value in future IOL design efforts.

General Conclusions

All five *in vitro* bioassays used in these experiments – mitochondrial dynamics, Alamar blue assay, confocal microscopy with two fluorescent (Rhodamine123 and Acridine Orange) staining methods, Hoechst assay, phagocytotic activity assay – proved to be useful for examining ultraviolet and blue light-induced retinal pigment epithelial (RPE) cell damage.

The results described in chapter 1 show that the optical analysis of organ cultured bovine lenses showed energy level-dependent increases in back vertex distance variability (loss of lens focusing ability) from 0.39 ± 0.04 mm for untreated control lenses (n = 11), to 1.63 ± 0.33 mm for lenses treated with 1.0 J/cm^2 UVB irradiation (n = 10) and 0.63 ± 0.13 mm for lenses treated with 0.5 J/cm^2 UVB irradiation (n = 9). Also, confocal laser scanning microscopy analysis of both bovine lenses and cultured human RPE cells (ARPE-19 cells) showed that following treatment with 0.5 J/cm^2 of UVB radiation the mitochondria stopped moving immediately, whereas at 1.0 J/cm^2 not only did the mitochondria stop moving, but fragmentation and swelling of mitochondria was seen. Untreated control tissue exhibited up to 15 micrometer/min of movement of the mitochondria. This could represent healthy mitochondrial movement, presumably allowing energy transmission across the cell from regions of low to regions of high ATP demand. Thus, lack of mitochondrial movement, fragmentation, and swelling of mitochondria may represent early morphological damage following oxidative stress that may lead to activation of apoptotic pathways.[12]

The results obtained in chapter 2 show that environmentally relevant levels of UVB radiation can cause significant decreases in RPE cell viability, as well as phagocytotic activity of RPE cells, in a dose-dependent manner. In addition, the results show that UVB radiation can also induce the degradation of nuclei, including DNA/RNA (as in the early stage of apoptosis), and mitochondria in cultured RPE cells in a dose-dependent manner. The lowest dose used in this chapter, 0.05 J/cm^2 broadband UVB, did not show any phototoxic damage, and the highest energy level of 0.2 J/cm^2 broadband UVB showed the most damage with all three assays. Thus, these assays together provide a valuable *in vitro* model for UV radiation-induced retinal toxicology research.

Chapter 3 shows that two different thicknesses of commercially available IOL material (0.9 mm and 1.5 mm) showed very effective UV blocking ability, allowing no cellular damage with the use of the *in vitro* approach that is developed in chapter 2. The results demonstrate that UVB radiation can be completely blocked by IOL material sheets while IOL uncovered RPE cells show significant decreases in viability and phagocytotic activity. The findings suggest that these *in vitro* assays can be used as a sensitive and meaningful biomarker method for evaluating IOL effectiveness. Also, while there are many studies that evaluate the spectral transmission characteristics of various IOLs to verify their anti-UV efficacy,[8,25,27] studies showing the cytotoxic effects of UV radiation on retinal cells in terms of cell biology and physiology are few in number. This work represents an effort to improve this situation.

Finally, the effect of blue light (400 nm, 420 nm, and 435.8 nm) on RPE cells and its application to blue light blocking IOLs was investigated in chapter 4 by also using the *in vitro* approach developed in chapter 2. The results clearly show that only blue light radiation of 400 nm can cause significant decreases in cell viability as well as degradation of nuclei (DNA/RNA) and mitochondria in RPE cells, while 420 and 435.8 nm blue light radiation cause no cellular damage at all. Thus, blue light wavelengths between 400 nm and 420 nm represent the critical wavelength range responsible for phototoxic damage to RPE cells. These results may be of value in future IOL design efforts.

In conclusion, the purpose of this dissertation is to develop an *in vitro* approach to the study of retinal UVR and blue light protection using sensitive and meaningful bioassays for the evaluation of not only RPE function after oxidative/chemical stress, but also IOL effectiveness.

The Alamar blue assay for evaluating cell viability is a proper assay designed to quantify cell proliferation, cytotoxicity, and metabolic activity. Mitochondria represent a primary site of phototoxicity induced by UV and blue light radiation in a variety of animal models,[29-31] and mitochondrial dysfunction causes a rapid apoptotic response in many cases.[32,33] The study of mitochondrial motion described in this thesis, and its possible use in evaluating RPE cell function, is the first study of this kind involving RPE cells. Also the evaluation of nucleic (DNA/RNA) damage is significant since UV-induced DNA damage can iniciate cellular apoptosis.[34,35] In addition to these assays, the phagocytotic activity assay, a novel method developed for the studies carried out in this

thesis, is an appropriate tool for examining RPE cells since phagocytosis is one of the main functions of RPE.

In summary, this approach and these assays provide a valuable *in vitro* model for UVR and blue light induced retinal toxicology research.

References to General Introduction and General Conclusions

1. Marmor M. F. and Wolfensberger T. J. (1998). The retinal pigment epithelium: function and disease. Oxford University press, New York.
2. Reme C., Reinboth J., Clausen M. and Hafezi F. (1996). Light damage revisited: converging evidence, diverging views? Graefes Arch Clin Exp Ophthalmol. 234, 2-11.
3. Algvere PV, Marshall J, Seregard S. Age-related maculopathy and the impact of blue light hazard. Acta Ophthalmol Scand 2006; 84:4-15
4. McCarty C. A. and Taylor H. R. (1996). Recent developments in vision research: light damage in cataract. Invest Ophthalmol Vis Sci. 37(9), 1720-1723.
5. Wu J, Seregard S, Algvere PV. Photochemical damage of the retina. Surv Ophthalmol 2006; 51:461-481
6. Norren D. V. and Vos J. J. (1974). Spectral transmission of the human ocular media. Vision Res. 14(11). 1237-1244.
7. Patton W. P., Charavarthy U., Davies R. J. H. and Archer D. B. (1999). Comet assay of UV-induced DNA damage in retinal pigment epithelial cells. Invest. Ophthalmol. Vis. Sci. 40, 3268-3275.
8. Mainster M. A. (1986). The spectra, classification, and rationale of ultraviolet-protective intraocular lenses. Am J Ophthalmol. 102(6), 727-732.
9. American National Standard Institute/ Illuminating Engineering Society of North America. “ANSI/IESNA RP-27.1-05: Recommended Practice for Photobiological Safety for Lamp and Lamp Systems – General Requirements.” Illuminating

Engineering Society of North America Web Store 10 June. 2007 <https://www.iesna.org/shop/>.

10. Braunstein RE, Sparrow JR. A blue-blocking intraocular lens should be used in cataract surgery. Arch Ophthalmol 2005; 123:547-549

11. Taylor HR, West S, Muñoz B, Rosenthal FS, Bressler SB, Bressler NM. The long-term effects of visible light on the eye. Arch Ophthalmol 1992; 110:99-104.

12. Suter M, Remé C, Grimm C, Wenzel A, Jäättela M, Esser P, Kociok N, Leist M, Richter C. Age-related macular degeneration. The lipofusion component N-retinyl-N-retinylidene ethanolamine detaches proapoptotic proteins from mitochondria and induces apoptosis in mammalian retinal pigment epithelial cells. J Biol Chem 2000; 275:39625-39630

13. Hafezi F, Marti A, Munz K, Remé CE. Light-induced apoptosis: differential timing in the retina and pigment epithelium. Exp Eye Res 1997; 64:963-970

14. Rahmani B, Tielsch JM, Katz J, Gottsch J, Quigley H, Javitt J, Sommer A. The cause-specific prevalence of visual impairment in an urban population. The Baltimore Eye Survey. Ophthalmology 1996; 103:1721-1726

15. Ederer F., Hiller R., and Taylor H. R. (1981). Senile lens changes and diabetes in two population studies. Am J Ophthalmol. 91(3), 381-395.

16. Stambolian D. Galactose and cataract. Surv Ophthalmol. 1988 Mar-Apr;32(5):333-49

17. Lipman R. M., Tripathi B. J., and Tripathi R. C. (1988). Cataracts induced by microwave and ionizing radiation. Surv Ophthalmol. 33(3), 200-210.

18. Lerman S. (1986). Photosensitizing drugs and their possible role in enhancing ocular toxicity. Ophthalmology. 93(3), 304-318.

19. Lerman S., Hockwin O., and Dragomirescu V. (1980). In vivo fluorescence photography. Opthal. Res. 12, 303-314.

20. Ridley H. Intra-ocular acrylic lenses; a recent development in the surgery of cataract. Br J Ophthalmol 1952; 36:113-122

21. Mainster M. A. (1978). Spectral transmittance of intraocular lenses and retinal damage from intense light sources. Am J Ophthalmol. 85(2), 167-170.

22. Clayman HM. Ultraviolet-absorbing intraocular lenses. J Am Intraocul Implant Soc 1984; 10:429-432

23. Peyman GA, Sloan HD, Lim J. Ultraviolet radiation absorbing pseudophakos. J Am Intraocul Implant Soc 1982; 8:357-360

24. Lindstrom RL, Doddi N. Ultraviolet radiation absorption in intraocular lenses. J Cataract Refract Surg 1986; 12:285-289

25. Lin KK, Lin YC, Lee JS, Chao AN, Chen HSL. Spectral transmission characteristics of spectacles, contact, and intraocular lenses. Ann Opthalmol 2002; 34:206-215

26. Niwa K, Yoshino Y, Okuyama F, Tokoro T. Effects of tinted intraocular lens on contrast sensitivity. Ophthalmic Physiol Opt 1996; 16:297-302

27. Ernest PH. Light-transmission-spectrum comparison of foldable intraocular lenses. J Cataract Refract Surg 2004; 30:1755-1758

28. Werner J. S. and Spillmann L. (1989). UVAbsorbing intraocular lenses: safety, efficacy, and consequences for the cataract patient. Graefes Arch Clin Exp Ophthalmol. 227(3), 248-256.

29. Bastianon C., Zanoni R., Miolo G., Caffieri S., and Reddi E. (2005). Mitochondria and plasma membrane as targets of UVA-induced toxicity of neuroleptic drugs fluphenazine, perphenazine and thioridazine. Int J Biochem Cell Biol. 37(4), 901-908.

30. Lu X. Y. and Wu R. S. (2005). Ultraviolet damages sperm mitochondrial function and membrane integrity in the sea urchin Anthocidaris crassispina. Ecotoxicol Environ Saf. 61(1), 53-59.

31. Bantseev V. and Youn H. Y. (2006). Mitochondrial "movement" and lens optics following oxidative stress from UVB irradiation: Cultured bovine lenses and human retinal pigment epithelial cells (ARPE-19) as examples. Annals of the New York Academy of Sciences.

32. Green DR, Kroemer G. (2004). The pathophysiology of mitochondrial cell death. Science. 305(5684), 626-629.

33. Orrenius S. (2004). Mitochondrial regulation of apoptotic cell death. Toxicol Lett. 149(1-3), 19-23.

34. Sasai K, Yajima H, Suzuki F. (2002). Suppression of postmitochondrial signaling and delayed response to UV-induced nuclear apoptosis in HeLa cells. Jpn J Cancer Res. 93(3), 275-283.

35. Tratsk K. S. and Thanos S. (2003). UV irradiation causes multiple cellular changes in cultured human retinal pigment epithelium cells. Graefes Arch Clin Exp Ophthalmol. 241(10), 852-859.

References to Chapter 1

1. Frey, T. G. & C. A. Mannella. 2000. The internal structure of mitochondria. TIBS. 25: 319-324.
2. Wallace, D. C., M. D. Brown, S. Melov, B. Graham & M. Lott. 1998. Mitochondrial biology, degenerative diseases and aging. Biofactors. 7: 187-90.
3. McAvoy, J. W. 1978. Cell division, cell elongation and the co-ordination of crystallin gene expression during lens morphogenesis in the rat. J Embryol Exp Morphol. 45: 271-81.
4. Kuwabara, T. 1975. The maturation of the lens cell: a morphologic study. Exp Eye Res. 20: 427-43.
5. Kinsey, V. A. & V. N. Reddy. 1965. Studies of the crystalline lens. XI. The relative role of the epithelium and capsule in transport. Invest Ophthalmol. 4: 104-116.
6. Bantseev, V., K. L. Herbert, J. R. Trevithick & J. G. Sivak. 1999. Mitochondria of rat lenses: distribution near and at the sutures. Curr Eye Res. 19: 506-16.
7. Bantseev, V., K. L. Moran, D. G. Dixon, J. R. Trevithick & J. G. Sivak. 2004. Optical properties, mitochondria and sutures of lenses of fishes: a comparative study of nine species. Can J Zool. 82: 86-93.
8. Bantseev, V., A. P. Cullen, J. R. Trevithick & J. G. Sivak. 2003. Optical function and mitohondrial metabolic properties in damage and recovery of bovine lens after in vitro carbonyl cyanide m-chlorophenylhydrazone treatment. Mitochondrion. 3: 1-11.

9. Bantseev, V., D. McCanna, A. Banh, W. W. Wong, K. L. Moran, D. G. Dixon, J. R. Trevithick & J. G. Sivak. 2003. Mechanisms of ocular toxicity using the in vitro bovine lens and sodium dodecyl sulfate as a chemical model. Toxicol Sci. 37: 98-107.

10. Skulachev, V. P. 2001. Mitochondrial filaments and clusters as intracellular power-transmitting cables. Trends Biochem Sci. 26: 23-9.

11. Bantseev, V. & J. G. Sivak. 2005. Confocal laser scanning microscopy imaging of dynamic TMRE movement in the mitochondria of epithelial and superficial cortical fibre cells of bovine lenses. Mol Vis. 11: 518-23.

12. Robman, L. & H. Taylor. 2005. External factors in the development of cataract. Eye. 19: 1074-82.

13. Lin, K., Y. Lin, J. Lee, A. Chao & H. S. Chen. 2002. Spectral transmission characteristics of spectacle, contact, and intraocular lenses. Ann Ophthalmol. 34: 206-215.

14. Stuart, D. D., A. P. Cullen, J. G. Sivak & M. J. Doughty. 1994. Optical effects of UVA and UVB radiation on the cultured bovine lens. Curr Eye Res. 13: 371-6.

15. Youn, H. Y., K. L. Moran, O. M. Oriowo, N. C. Bols & J. G. Sivak. 2004. Surfactant and UVB-induced damage of the cultured bovine lens. Toxicol In Vitro. 18: 841-52.

16. Patton, W. P., U. Chakravarthy, R. J. Davies & D. B. Archer. 1999. Comet assay of UV-induced DNA damage in retinal pigment epithelial cells. Invest Ophthalmol Vis Sci. 40: 3268-75.

17. Johnson, G. J. 2004. The environment and the eye. Eye. 18: 1235-50.

18. Ligon, L. A. & O. Steward. 2000. Movement of mitochondria in the axons and dendrites of cultured hippocampal neurons. J Comp Neurol. 427: 340-50.

19. Neutzner, A. & R. J. Youle. 2005. Instability of the mitofusin Fzo1 regulates mitochondrial morphology during the mating response of the yeast Saccharomyces cerevisiae. J Biol Chem. 280: 18598-603.

20. Knowles, M. K., M. G. Guenza, R. A. Capaldi & A. H. Marcus. 2002. Cytoskeletal-assisted dynamics of the mitochondrial reticulum in living cells. Proc Natl Acad Sci U S A. 99: 14772-7.

21. Tseng, C. J., Y. J. Wang, Y. C. Liang, J. H. Jeng, W. S. Lee, J. K. Lin, C. H. Chen, I. C. Liu & Y. S. Ho. 2002. Microtubule damaging agents induce apoptosis in HL 60 cells and G2/M cell cycle arrest in HT 29 cells. Toxicology. 175: 123-42.

22. Lo, W. K., X. J. Wen & C. J. Zhou. 2003. Microtubule configuration and membranous vesicle transport in elongating fibre cells of the rat lens. Exp Eye Res. 77: 615-26.

23. Bereiter-Hahn, J. 1990. Behavior of mitochondria in the living cell. Int Rev Cytol. 122: 1-63.

24. Rintoul, G. L., A. J. Filiano, J. B. Brocard, G. J. Kress & I. J. Reynolds. 2003. Glutamate decreases mitochondrial size and movement in primary forebrain neurons. J Neurosci. 23: 7881-8.

25. Desagher, S. & J. C. Martinou. 2000. Mitochondria as the central control point of apoptosis. Trends Cell Biol. 10: 369-77.

26. Frank, S., B. Gaume, E. S. Bergmann-Leitner, W. W. Leitner, E. G. Robert, F. Catez, C. L. Smith & R. J. Youle. 2001. The role of dynamin-related protein 1, a mediator of mitochondrial fission, in apoptosis. Dev Cell. 1: 515-25.

27. Filiano, J. J., M. J. Goldenthal, A. C. Mamourian, C. C. Hall & J. Marin-Garcia. 2002. Mitochondrial DNA depletion in Leigh syndrome. Pediatr Neurol. 26: 239-42.

28. Dubinsky, J. M. & Y. Levi. 1998. Calcium-induced activation of the mitochondrial permeability transition in hippocampal neurons. J Neurosci Res. 53: 728-41.

29. Kristal, B. S. & J. M. Dubinsky. 1997. Mitochondrial permeability transition in the central nervous system: induction by calcium cycling-dependent and -independent pathways. J Neurochem. 69: 524-38.

30. Amchenkova, A. A., L. E. Bakeeva, Y. S. Chentsov, V. P. Skulachev & D. B. Zorov. 1988. Coupling membranes as energy-transmitting cables. I. Filamentous mitochondria in fibroblasts and mitochondrial clusters in cardiomyocytes. J Cell Biol. 107: 481-95.

31. Herbert, K. L., D. G. Dixon & J. G. Sivak. 1998. Effects of age on the sensitivity of the rat lens to hexanol *in vitro*. J Toxicol-Cut & Ocular Toxicol. 17: 127-13

References to Chapter 2

1. Marmor M. F. and Wolfensberger T. J. (1998). The retinal pigment epithelium: function and disease. Oxford University press, New York.
2. Reme C., Reinboth J., Clausen M. and Hafezi F. (1996). Light damage revisited: converging evidence, diverging views? Graefes Arch Clin Exp Ophthalmol. 234, 2-11.
3. McCarty C. A. and Taylor H. R. (1996). Recent developments in vision research: light damage in cataract. Invest Ophthalmol Vis Sci. 37(9), 1720-1723.
4. Kerr J. B. and McElroy C. T. (1993). Evidence for large upward trends of UVB radiation linked to ozone depletion. Science. 262, 1032-1034.
5. Noell W. K. (1980). Possible mechanisms of photoreceptor damage by light in mammalian eyes. Vision Res. 20(12), 1163-71.
6. Gorgels T. G. M. F. and van Norren D. (1995). Ultraviolet and green light cause difference types of damage in rat retina. Invest. Ophthalmol. Vis. Sci. 36, 851-863.
7. Van Kuijk F. J. G. M. (1991). Effect of ultraviolet radiation on the eye: role of protective glasses. Environ Health Perspet. 96, 177-195.
8. Patton W. P., Charavarthy U., Davies R. J. H. and Archer D. B. (1999). Comet assay of UV-induced DNA damage in retinal pigment epithelial cells. Invest. Ophthalmol. Vis. Sci. 40, 3268-3275.

9. Tratsk K. S. and Thanos S. (2003). UV irradiation causes multiple cellular changes in cultured human retinal pigment epithelium cells. Graefes Arch Clin Exp Ophthalmol. 241(10), 852-859.

10. Noell W. K., Walker V. S., Kang B. S., and Berman S. (1966). Retinal damage by light in rats. Invest. Ophthalmol. Vis. Sci. 5, 450-473.

11. Beatty S., Koh H., Phil M., Henson D., and Boulton M. (2000). The role of oxidative stress in the pathogenesis of age-related macular degeneration. Surv Ophthalmol. 45(2), 115-134.

12. Norren D. V. and Vos J. J. (1974). Spectral transmission of the human ocular media. Vision Res. 14(11). 1237-1244.

13. Mainster M. A. (1986). The spectra, classification, and rationale of ultraviolet-protective intraocular lenses. Am J Ophthalmol. 102(6), 727-732.

14. Sparrow J. R., Nakanishi K., and Parish C. A. (2000). The lipofuscin fluorophore A2E mediates blue light-induced damage to retinal pigment epithelium. Invest Ophthalmol Vis Sci. 41(7), 1981-1989.

15. Godley B. F., Shamsi F. A., Liang F. Q., Jarrett S. G., Davies S., and Boulton M. (2005). Blue light induces mitochondrial DNA damage and free radical production in epithelial cells. J Biol Chem. 280(22), 21061-21066.

16. American Conference of Governmental Industrial Hygienists (ACGIH), 2006. Threshold limit values for chemical substances and physical agents and biological exposure indices. Cincinnati, OH., USA, pp. 164-170.

17. Dayeh V. R., Schirme K., Lee L. E. J., and Bols N. C. (2003). The use of fish- derived cell lines for investigation of environmental contaminants. Current Protocols in Toxicology. Wiley, New York, pp. 1–17.

18. Triel C., Vestergaard M. E., Bolund L., Jensen T. G., and Jensen U. B. (2004). Side population cells in human and mouse epidermis lack stem cell characteristics. Experimental cell research. 295(1), 79-90.

19. Lampidis T. J., Bernal S. D., Summerhayes I. C., and Chen L. B. (1983). Selective toxicity of rhodamine 123 in carcinoma cells in vitro. Cancer Res. 43(2), 716-720.

20. Margrain T. H., Boulton M., Marshall J., and Sliney D. H. (2004). Do blue light filters confer protection against age-related macular degeneration? Prog Retin Eye Res. 23(5), 523-531.

21. Meyer-Rochow V. B. (2000). Risks, especially for the eye, emanating from the rise of solar UV-radiation in the Arctic and Antarctic regions. Int J Circumpolar Health. 59(1), 38-51.

22. Sadun A. C., Sadun A. A., and Sadun L. A. (1984). Solar retinopathy. A biophysical analysis. Arch Ophthalmol. 102(10), 1510-1512.

23. Young R. W. (1988). Solar radiation and age-related macular degeneration. Surv. Ophthalmol. 32, 252-269.

56(3), 353-356.

24. Hiramitsu T. and Armstrong D. (1991). Preventive effect of antioxidants on lipid peroxidation in the retina. Ophthalmic Res. 23(4), 196-203.

25. Wihlmark U., Wrigstad A., Roberg K., Brunk U. T., and Nilsson S. E. (1996). Formation of lipofuscin in cultured retinal pigment epithelial cells exposed to pre-oxidized photoreceptor outer segments. APMIS. 104(4), 272-279.

26. Augustin A. J., Hunt S., Breipohl W., Boker T., and Spitznas M. (1996). Influence of oxygen free radicals and free radical scavengers on the growth behaviour and oxidative tissue damage of bovine retinal pigment epithelium cells in vitro. Graefes Arch Clin Exp Ophthalmol. 234(1), 58-63.

27. Weiter J. J. (1987). Phototoxic changes in the retina. Clinical light damage to the eye (D. Miller, Ed.), Springer-Verlag, New York, pp. 79-125.

28. Bynoe L. A., Gottsch J. D., Pou S., and Rosen G. M. (1992). Light-dependent generation of superoxide from human erythrocytes. Photochem Photobiol. 56(3), 353-356.

29. Kielbassa C., Roza L., and Epe B. (1997). Wavelength dependence of oxidative DNA damage induced by UV and visible light. Carcinogenesis. 18(4), 811-816.

30. Liang Y. G., Jorgensen A. G., Kaestel C. G., Wiencke A. K., Lui G. M., la Cour M. H., Ropke C. H., and Nissen M. H. (2000). Bcl-2, Bax, and c-Fos expression correlates to RPE cell apoptosis induced by UV-light and daunorubicin. Curr Eye Res. 20(1), 25-34.

31. Bok D. (1990). Processing and transport of retinoids by the retinal pigment epithelium. Eye. 4, 326-332.

32. Bastianon C., Zanoni R., Miolo G., Caffieri S., and Reddi E. (2005). Mitochondria and plasma membrane as targets of UVA-induced toxicity of neuroleptic drugs

fluphenazine, perphenazine and thioridazine. Int J Biochem Cell Biol. 37(4), 901-908.

33. Lu X. Y. and Wu R. S. (2005). Ultraviolet damages sperm mitochondrial function and membrane integrity in the sea urchin Anthocidaris crassispina. Ecotoxicol Environ Saf. 61(1), 53-59.

34. Bantseev V. and Youn H. Y. (2006). Mitochondrial "movement" and lens optics following oxidative stress from UVB irradiation: Cultured bovine lenses and human retinal pigment epithelial cells (ARPE-19) as examples. Annals of the New York Academy of Sciences. 1091, 17–33.

35. Wang X., Sharma P. K., Gupta A., George V., Thomas A. J., Falcone T., and Agarwal A. (2003). Alterations in mitochondria membrane potential and oxidative stress in infertile men: a prospective observational study. Fertil. Steril. 80, 844-850.

36. Sreekumar P. G., Kannan R., Yaung J., Spee C. K., Ryan S. J., and Hinton D. R. (2005). Protection from oxidative stress by methionine sulfoxide reductases in RPE cells. Biochem Biophys Res Commun. 334(1), 245-253.

37. Wong Y. T., Ruan R., and Tay F. E. H. (2006). Relationship between levels of oxidative DNA damage, ipid peroxidation and mitochondrial membrane potential in young and old F344 rats. Free Radical Research. 40(4), 393-402.

38. Graham J. K., Kunze E., and Hammerstedt R. H. (1990). Analysis of sperm cell viability, acrosomal integrity, and mitochondrial function using flow cytometry. Biol Reprod. 43(1), 55-64.

39. Green DR, Kroemer G. (2004). The pathophysiology of mitochondrial cell death. Science. 305(5684), 626-629.

40. Orrenius S. (2004). Mitochondrial regulation of apoptotic cell death. Toxicol Lett. 149(1-3), 19-23.

41. Sasai K, Yajima H, Suzuki F. (2002). Suppression of postmitochondrial signaling and delayed response to UV-induced nuclear apoptosis in HeLa cells. Jpn J Cancer Res. 93(3), 275-283.

42. Ershov A. V., Parkins N., Lukiw W. J., and Bazan N. G. (2000). Modulation of early response gene expression by prostagelandins in cultured rat retinal pigment epithelium cells. Curr Eye Res. 6, 968-974.

43. Godar D. E. (1996). Pre-programmed and programmed cell death mechanisms of apoptosis: UV-induced immediate and delayed apoptosis. Photochem Photobiol 63, 825-830.

44. Strauss O, Stumpff F, Mergler S, Wienrich M, Wiederholt M. (1998). The Royal College of Surgeons rat: an animal model for inherited retinal degeneration with a still unknown genetic defect. Acta Anat (Basel). 162(2-3), 101-111.

45. Kressel M., Groscurth P. (1994). Distinction of apoptotic and necrotic cell death by in situ labeling of fragmented DNA. Cell Tissue Res. 278, 549-556

46. Au D. W. T. (2004). The application of histo-cytopathological biomarkers in marine pollution monitoring: a review. Mar. Pollut. Bull. 48, 817-834.

47. Nielsen L. K., Reid S., Greenfield P. F. (2000). Cell cycle model to describe animal cell size variation and lag between cell number and biomass dynamics. Biotechnology and Bioengineering. 56(4), 372-379.

48. Oriowo O. M., Cullen A. P., Sivak J. G. (2002). Impairment of eye lens cellphysiology and optics by broadband ultraviolet A-ultraviolet B radiation. Photochemistry and Photobiology. 76(3), 361-367.

References to Chapter 3

1. Boettner EA, Wolter JR: Transmission of the ocular media. Investigative ophthalmology & visual science 1962;1:776-783.
2. Ellerin BE, Nisce LZ, Roberts CW, Thornell C, Sabbas A, Wang H, Li PM, Nori D: The effect of ionizing radiation on intraocular lenses. International journal of radiation oncology, biology, physics 2001;51:184-208.
3. Mainster MA: Spectral transmittance of intraocular lenses and retinal damage from intense light sources. American journal of ophthalmology 1978;85:167-170.
4. Ham WT Jr, Ruffolo JJ Jr, Mueller HA, Guerry D 3rd: The nature of retinal radiation damage: dependence on wavelength, power level and exposure time. Vision research 1980;20:1105-1111.
5. Mainster MA, Ham WT Jr, Delori FC: Potential retinal hazards. Instrument and environmental light sources. Ophthalmology 1983;90:927-932.
6. Mainster MA: The spectra, classification, and rationale of ultraviolet-protective intraocular lenses. American journal of ophthalmology 1986;102:727-732.
7. Lin KK, Lin YC, Lee JS, Chao AN, Chen HSL: Spectral transmission characteristics of spectacle, contact, and intraocular lenses. Annals of ophthalmology 2002;34:206-215.
8. Mainster MA: Intraocular lenses should block UV radiation and violet but not blue light. Archives of ophthalmology 2005;123:550-555.
9. Mainster MA: Violet and blue light blocking intraocular lenses: photoprotection versus photoreception. The British journal of ophthalmology 2006;90:784-792.

10. Thoms M, Fishman GA, Meulen DV: Spectral transmission characteristics of intraocular and aphakic contact lenses. Archives of ophthalmology 1983;101:92-93.

11. Alapetite C, Wachter T, Sage E, Moustacchi E: Use of the alkaline comet assay to detect DNA repair deficiencies in human fibroblasts exposed to UVC, UVB, UVA and gamma-rays. International journal of radiation biology 1996;69:359-369.

12. Hiramitsu T, Armstrong D: Preventive effect of antioxidants on lipid peroxidation in the retina. Ophthalmic research 1991;23:196-203.

13. Augustin AJ, Hunt S, Breipohl W, Böker T, Spitznas M: Influence of oxygen free radicals and free radical scavengers on the growth behaviour and oxidative tissue damage of bovine retinal pigment epithelium cells in vitro. Graefe's archive for clinical and experimental ophthalmology 1996;234:58-63.

14. Kielbassa C, Roza L, Epe B: Wavelength dependence of oxidative DNA damage induced by UV and visible light. Carcinogenesis 1997;18:811-816.

15. Patton WP, Chakravarthy U, Davies RJ, Archer DB: Comet assay of UV-induced DNA damage in retinal pigment epithelial cells. Investigative ophthalmology & visual science 1999;40:3268-3275.

16. Shimmura S, Tsubota K: Ultraviolet B-induced mitochondrial dysfunction is associated with decreased cell detachment of corneal epithelial cells in vitro. Investigative ophthalmology & visual science 1996;38:620-626.

17. Bantseev V, Youn HY: Mitochondrial "movement" and lens optics following oxidative stress from UVB irradiation: cultured bovine lenses and human retinal

pigment epithelial cells (ARPE-19) as examples. Annals of the New York Academy of Sciences 2006;1091:17-33.

18. Youn HY, Bantseev V, Bols NC, Cullen AP, Sivak JG: In vitro assays for evaluating the ultraviolet B-induced damage in cultured human retinal pigment epithelial cells. Journal of photochemistry and photobiology B 2007;88:21-28.

19. Nielsen LK, Reid S, Greenfield PF: Cell cycle model to describe animal cell size variation and lag between cell number and biomass dynamics. Biotechnology and bioengineering 2000;56:372-379.

20. American Conference of Governmental Industrial Hygienists (ACGIH): Threshold limit values for chemical substances and physical agents and biological exposure indices. Cincinnati, OH., USA, 2006, pp. 164-170.

21. Oriowo OM, Cullen AP, Schirmer K, Chou BR, Bols NC, Sivak JG: Evaluation of a porcine lens and fluorescence assay approach for in vitro ocular toxicological investigations. Alternatives to laboratory animals 2002;30:505-513.

22. O'Brien J, Wilson I, Orton T, Pognan F: Investigation of the Alamar Blue (resazurin) fluorescent dye for the assessment of mammalian cell cytotoxicity. European journal of biochemistry 2000;267:5421-5426.

23. Dayeh VR, Schirmer K, Lee LEJ, Bols NC: The use of fish-derived cell lines for investigation of environmental contaminants. Curr. Protocols Toxicol., Wiley, New York, 2003, pp. 1-17.

24. Durand RE, Olive PL: Cytotoxicity, Mutagenicity and DNA damage by Hoechst 33342. The journal of histochemistry and cytochemistry 1982;30:111-116.

25. Darzynkiewicz Z, Traganos F, Staiano-Coico L, Kapuscinski J, Melamed MR:

Interaction of rhodamine 123 with living cells studied by flow cytometry. Cancer research 1982;42:799-806.

26. Young RW, Bok D: Participation of the retinal pigment epithelium in the rod outer segment renewal process. The Journal of cell biology 1969;42:392-403.

27. Abu-Amero KK, Bosley TM: Detection of mitochondrial respiratory dysfunction in circulating lymphocytes using resazurin. Archives of pathology & laboratory medicine 2005;129:1295-1298.

28. Zhang HX, Du GH, Zhang JT: Assay of mitochondrial functions by resazurin in vitro. Acta pharmacologica Sinica 2004;25:385-389.

29. Steinert RF, Giamporcaro JE, Tasso VA: Clinical assessment of long-term safety and efficacy of a widely implanted silicone intraocular lens material. American journal of ophthalmology 1997;123:17-23.

30. Noell WK: Possible mechanisms of photoreceptor damage by light in mammalian eyes. Vision research 1980;20:1163-1171.

31. Gorgels TGMF, van Norren D: Ultraviolet and green light cause difference types of damage in rat retina. Investigative ophthalmology & visual science 1995;36:851-863.

32. Tratsk KS, Thanos S: UV irradiation causes multiple cellular changes in cultured human retinal pigment epithelium cells. Graefe's archive for clinical and experimental ophthalmology 2003;241:852-859.

33. Pons A, Delgado D, Campos J: Determination of the action spectrum of the blue-light hazard for different intraocular lenses. Journal of the Optical Society of America A 2007;24:1545-1550.

34. Laube T, Apel H, Koch HR: Ultraviolet radiation absorption of intraocular lenses. Ophthalmology 2004;111:880-885.

35. Mainster MA, Sparrow JR: How much blue light should an IOL transmit? The British journal of ophthalmology 2003;87:1523-1529.

36. Oriowo OM: AlamarBlue bioassay for cellular investigation of UV-induced crystalline lens damage. Ophthalmic & physiological optics 2003;23:307-314.

37. Hightower K, McCready J: Mechanisms involved in cataract development following near-ultraviolet radiation of cultured lenses. Current eye research 1992;11:679-689.

38. Youn HY, Moran KL, Oriowo OM, Bols NC, Sivak JG: Surfactant and UVB-induced damage of the cultured bovine lens. Toxicology in vitro 2004;18:841-52.

39. Oriowo OM, Cullen AP, Sivak JG: Impairment of eye lens cell physiology and optics by broadband ultraviolet A-ultraviolet B radiation. Photochemistry and photobiology 2002;76:361-367.

40. Hosaka E, Soma Y, Kawa Y, Kaminaga H, Osumi K, Ooka S, Watabe H, Ito M, Murakami F, Mizoguchi M: Effects of ultraviolet radiation on melanocyte differentiation: studies with mouse neural crest cells and neural crest-derived cell lines. Pigment cell research 2004;17:150-157.

41. Reid L, Clothier RH, Khammo N: Hydrogen peroxide induced stress in human keratinocytes and its effect on bithionol toxicity. Toxicology in vitro 2001;15:441-445.

42. Darzynkiewicz Z, Staiano-Coico L, Melamed MR: Increased mitochondrial uptake

of rhodamine 123 during lymphocyte stimulation. Proceedings of the National Academy of Sciences of the United States of America 1981;78:2383-2387.

43. Schneckenburger H, Gessler P, Pavenstädt-Grupp I: Measurements of mitochondrial deficiencies in living cells by microspectrofluorometry. The journal of histochemistry and cytochemistry 1992;40:1573-1578.

44. Shimmura S, Tadano K, Tsubota K: UV dose-dependent caspase activation in a corneal epithelial cell line. Current eye research 2004;28:85-92.

45. Shea CR, Wimberly J, Hasan T: Mitochondrial phototoxicity sensitized by doxycycline in cultured human carcinoma cells. The Journal of investigative dermatology 1986;87:338-342.

46. Banerjee G, Gupta N, Kapoor A, Raman G: UV induced bystander signaling leading to apoptosis. Cancer letters 2004;223:275-284.

47. Mocharla R, Mocharla H, Hodes ME: A novel, sensitive fluorometric staining technique for the detection of DNA in RNA preparations. Nucleic acids research 1987;15:10589

48. Kressel M, Groscurth P: Distinction of apoptotic and necrotic cell death by in situ labeling of fragmented DNA. Cell and tissue research 1994;278:549-556.

49. Ricci MS, Zong WX: Chemotherapeutic approaches for targeting cell death pathways. The oncologist 2006;11:342-357.

50. Worner W, Schrenk D: Influence of liver tumor promoters on apoptosis in rat hepatocytes induced by 2-acetylaminofluorene, ultraviolet radiation, or transforming growth factor beta 1. Cancer research 1996;56:1272-1278.

51. Baumstark-Khan C, Hentschel U, Nikandrova Y, Krug J, Horneck G: Fluorometric

analysis of DNA unwinding (FADU) as a method for detecting repair-induced DNA strand breaks in UV-irradiated mammalian cells. Photochemistry and photobiology 2000;72:477-484.

52. Davis SK, Bardeen CJ: Cross-linking of histone proteins to DNA by UV illumination of chromatin stained with Hoechst 33342. Photochemistry and photobiology 2003;77:675-679.

53. Souvannavong V, Lemaire C, Brown S, Adam A: UV irradiation of a B-cell hybridoma increases expression of alkaline phosphatase: involvement in apoptosis. Biochemistry and cell biology 1997;75:783-788.

54. La Vail MM: Rod outer segment disk shedding in rat retina: relationship to cyclic lighting. Science 1976;194:1071-1074.

55. Young RW: The renewal of photoreceptor cell outer segments. The Journal of cell biology 1967;33:61-72.

56. Young RW: The daily rhythm of shedding and degradation of cone outer segment membranes in the lizard retina. Journal of ultrastructure research 1977;61:172-185.

57. Sundelin S, Wihlmark U, Nilsson SE, Brunk UT: Lipofuscin accumulation in cultured retinal pigment epithelial cells reduces their phagocytic capacity. Current eye research 1998;17:851-857.

58. Nilsson SE, Sundelin SP, Wihlmark U, Brunk UT: Aging of cultured retinal pigment epithelial cells: oxidative reactions, lipofuscin formation and blue light damage. Documenta ophthalmologica 2003;106:13-16.

59. Seagle BL, Gasyna EM, Mieler WF, Norris JR Jr: Photoprotection of human retinal

pigment epithelium cells against blue light-induced apoptosis by melanin free radicals from Sepia officinalis. Proceedings of the National Academy of Sciences of the United States of America 2006;103:16644-16648.

60. Werner JS: Night vision in the eldery: consequences for seeing through a “blue filtering” intraocular lenses. The British journal of ophthalmology 2005;89:1518-1521.

References to Chapter 4

1. Algvere PV, Marshall J, Seregard S. Age-related maculopathy and the impact of bluelight hazard. Acta Ophthalmol Scand 2006; 84:4-15

2. Wu J, Seregard S, Algvere PV. Photochemical damage of the retina. Surv Ophthalmol 2006; 51:461-481

3. Bass AM, Paur RJ. Ultraviolet absorption crosssectionsof ozone: measurements, results, and analysis. Quadrienniel Ozone Symposium, Reidel, Halkidiki, Greece 1984; pp. 606–610

4. Ham WT Jr., Mueller HA, Sliney DH. Retinal sensitivity to damage from short wavelength light. Nature 1976; 260:153-155

5. Okuno T, Saito H, Ojima J. Evaluation of blue-light hazards from various light sources. Dev Ophthalmol 2002; 35:104-112.

6. American National Standard Institute/ Illuminating Engineering Society of North America. “ANSI/IESNA RP-27.1-05: Recommended Practice for Photobiological Safety for Lamp and Lamp Systems – General Requirements.” Illuminating Engineering Society of North America Web Store 10 June. 2007 <https://www.iesna.org/shop/>.

7. Braunstein RE, Sparrow JR. A blue-blocking intraocular lens should be used in cataract surgery. Arch Ophthalmol 2005; 123:547-549

8. Taylor HR, West S, Muñoz B, Rosenthal FS, Bressler SB, Bressler NM. The long-term effects of visible light on the eye. Arch Ophthalmol 1992; 110:99-104.

9. Suter M, Remé C, Grimm C, Wenzel A, Jäättela M, Esser P, Kociok N, Leist M, Richter C. Age-related macular degeneration. The lipofusion component N-retinyl-N-retinylidene ethanolamine detaches proapoptotic proteins from mitochondria and induces apoptosis in mammalian retinal pigment epithelial cells. J Biol Chem 2000; 275:39625-39630

10. Hafezi F, Marti A, Munz K, Remé CE. Light-induced apoptosis: differential timing in the retina and pigment epithelium. Exp Eye Res 1997; 64:963-970

11. Rózanowska M, Pawlak A, Rózanowski B, Skumatz C, Zareba M, Boulton ME, Burke JM, Sarna T, Simon JD. Age-related changes in the photoreactivity of retinal lipofuscin granules: role of chloroform-insoluble components. Invest Ophthalmol Vis Sci 2004; 45:1052-1060

12. Boulton M, Dontsov A, Jarvis-Evans J, Ostrovsky M, Svistunenko D. Lipofuscin is a photoinducible free radical generator. J Photochem Photobiol B 1993; 19:201-204

13. Davison JA, Patel AS. Light normalizing intraocular lenses. Int Ophthalmol Clin 2005; 45:55-106

14. Rahmani B, Tielsch JM, Katz J, Gottsch J, Quigley H, Javitt J, Sommer A. The cause-specific prevalence of visual impairment in an urban population. The Baltimore Eye Survey. Ophthalmology 1996; 103:1721-1726

15. Leaming DV. Practice styles and preferences of ASCRS members--2000 survey. American Society of Cataract and Refractive Surgery. J Cataract Refract Surg 2001; 27:948-955

16. Blair CJ, Ferguson J Jr. Exacerbation of senile macular degeneration following cataract extraction. Am J Ophthalmol 1979; 87:77-83

17. van der Schaft TL, Mooy CM, de Bruijn WC, Mulder PG, Pameyer JH, de Jong PT. Increased prevalence of disciform macular degeneration after cataract extraction with implantation of an intraocular lens. Br J Ophthalmol 1994; 78:441-445

18. Pollack A, Marcovich A, Bukelman A, Oliver M. Age-related macular degeneration after extracapsular cataract extraction with intraocular lens implantation. Ophthalmology 1996; 103:1546-1554

19. Hawkins WR. AMD after ECCE with IOL implant. Ophthalmology 1997; 104:900

20. Chaine G, Hullo A, Sahel J, Soubrane G, Espinasse-Berrod MA, Schutz D, Bourguignon C, Harpey C, Brault Y, Coste M, Moccatti D, Bourgeois H. Case-control study of the risk factors for age related macular degeneration. France-DMLA Study Group. Br J Ophthalmol 1998; 82:996-1002

21. Pons A, Delgado D, Campos J. Determination of the action spectrum of the blue-light hazard for different intraocular lenses. J Opt Soc Am A 2007; 24:1545-1550

22. Ernest PH. Light-transmission-spectrum comparison of foldable intraocular lenses. J Cataract Refract Surg 2004; 30:1755-1758

23. Mainster MA. Violet and blue light blocking intraocular lenses: photoprotection versus photoreception. Br J Ophthalmol 2006; 90:784-792

24. Youn HY, Bantseev V, Bols NC, Cullen AP, Sivak JG. In vitro assays for evaluating the ultraviolet B-induced damage in cultured human retinal pigment epithelial cells. J Photochem Photobiol B 2007; 88:21-28

25. Lampidis TJ, Bernal SD, Summerhayes IC, Chen LB. Selective toxicity of rhodamine 123 in carcinoma cells in vitro. Cancer Res 1983; 43:716-720

26. Lerman LS. The structure of the DNA-acridine complex. Proc Natl Acad Sci U S A 1963; 49:94-102

27. Siu TL, Morley JW, Coroneo MT. Toxicology of the retina: advances in understanding the defence mechanisms and pathogenesis of drug- and light-induced retinopathy. Clin Experiment Ophthalmol 2008; 36:176-185

28. Ruffolo JJ Jr, Ham WT Jr, Mueller HA, Millen JE. Photochemical lesions in the primate retina under conditions of elevated blood oxygen. Invest Ophthalmol Vis Sci 1984; 25:893-898

29. Crockett RS, Lawwill T. Oxygen dependence of damage by 435 nm light in cultured retinal epithelium. Curr Eye Res 1984; 3:209-215

30. Mainster MA. Intraocular lenses should block UV radiation and violet but not blue light. Arch Ophthalmol 2005; 123:550-555

31. King A, Gottlieb E, Brooks DG, Murphy MP, Dunaief JL. Mitochondria-derived reactive oxygen species mediate blue light-induced death of retinal pigment epithelial cells. Photochem Photobiol 2004; 79:470-475

32. Godley BF, Shamsi FA, Liang FQ, Jarrett SG, Davies S, Boulton M. Blue light induces mitochondrial DNA damage and free radical production in epithelial cells. J Biol Chem 2005; 280:21061-21066

33. Kroemer G, Reed JC. Mitochondrial control of cell death. Nat Med 2000; 6:513-519

34. Pautler EL, Morita M, Beezley D. Hemoprotein(s) mediate blue light damage in the retinal pigment epithelium. Photochem Photobiol 1990; 51:599-605

35. Schütt F, Davies S, Kopitz J, Holz FG, Boulton ME. Photodamage to human RPE cells by A2-E, a retinoid component of lipofuscin. Invest Ophthalmol Vis Sci 2000; 41:2303-2308

36. Sparrow JR, Cai B. Blue light-induced apoptosis of A2E-containing RPE: Involvment of Caspase-3 and protection by Bcl-2. Invest Ophthalmol Vis Sci 2001; 42:1356-1362

37. Chen E. Inhibition of cytochrome oxidase and blue-light damage in rat retina. Graefes Arch Clin Exp Ophthalmol 1993; 231:416-423

38. Bürkle A. Mechanisms of ageing. Eye 2001; 15:371-375

39. Zhang Y, Herman B. Ageing and apoptosis. Mech Ageing Dev 2002; 123:245-260

40. Sparrow JR, Zhou J, Cai B. DNA is a target of the photodynamic effects elicited in A2E-laden RPE by blue-light illumination. Invest Ophthalmol Vis Sci 2003; 44:2245-2251

41. Seko Y, Pang J, Tokoro T, Ichinose S, Mochizuki M. Blue light-induced apoptosis in cultured retinal pigment epithelium cells of the rat. Graefes Arch Clin Exp Ophthalmol 2001; 239:47-52

42. Rezai KA, Gasyna E, Seagle BL, Norris JR Jr, Rezaei KA. AcrySof Natural filter decreases blue light-induced apoptosis in human retinal pigment epithelium. Graefes Arch Clin Exp Ophthalmol 2008; 246:671-676

43. Remé CE, Grimm C, Hafezi F, Wenzel A, Williams TP. Apoptosis in the Retina: The Silent Death of Vision. News Physiol Sci 2000; 15:120-124

44. Kressel M, Groscurth P. Distinction of apoptotic and necrotic cell death by in situ labelling of fragmented DNA. Cell Tissue Res 1994; 278:549-556

45. Klein R, Meuer SM, Moss SE, Klein BE. Detection of drusen and early signs of age-related maculopathy using a nonmydriatic camera and a standard fundus camera. Ophthalmology 1992; 99:1686-1692

46. Crabb JW, Miyagi M, Gu X, Shadrach K, West KA, Sakaguchi H, Kamei M, Hasan A, Yan L, Rayborn ME, Salomon RG, Hollyfield JG. Drusen proteome analysis: an approach to the etiology of age-related macular degeneration. Proc Natl Acad Sci U S A 2002; 99:14682-14687

47. Malek G, Li CM, Guidry C, Medeiros NE, Curcio CA. Apolipoprotein B in cholesterol-containing drusen and basal deposits of human eyes with age-related maculopathy. Am J Pathol 2003; 162:413-425

48. Mullins RF, Russell SR, Anderson DH, Hageman GS. Drusen associated with aging and age-related macular degeneration contain proteins common to extracellular deposits associated with atherosclerosis, elastosis, amyloidosis, and dense deposit disease. FASEB J 2000; 14:835-846

49. Hogan MJ. Role of the retinal pigment epithelium in macular disease. Trans Am Acad Ophthalmol Otolaryngol 1972; 76:64-80

50. Ishibashi T, Patterson R, Ohnishi Y, Inomata H, Ryan SJ. Formation of drusen in the human eye. Am J Ophthalmol 1986; 101:342-353

51. Gass JD. Drusen and disciform macular detachment and degeneration. Trans Am Ophthalmol Soc 1972; 70:409-436

52. Cruickshanks KJ, Klein R, Klein BE. Sunlight and age-related macular degeneration. The Beaver Dam Eye Study. Arch Ophthalmol 1993; 111:514-518

53. Taylor HR, Muñoz B, West S, Bressler NM, Bressler SB, Rosenthal FS. Visible light and risk of age-related macular degeneration. Trans Am Ophthalmol Soc 1990; 88:163-173

54. Sparrow JR, Nakanishi K, Parish CA. The lipofuscin fluorophore A2E mediates blue light-induced damage to retinal pigmented epithelial cells. Invest Ophthalmol Vis Sci 2000; 41:1981-1989

55. Schütt F, Davies S, Kopitz J, Holz FG, Boulton ME. Photodamage to human RPE cells by A2-E, a retinoid component of lipofuscin. Invest Ophthalmol Vis Sci 2000; 41:2303-2308

56. Ben-Shabat S, Parish CA, Vollmer HR, Itagaki Y, Fishkin N, Nakanishi K, Sparrow JR. Biosynthetic studies of A2E, a major fluorophore of retinal pigment epithelial lipofuscin. J Biol Chem 2002; 277:7183-7190

57. Holz FG, Bellman C, Staudt S, Schütt F, Völcker HE. Fundus autofluorescence and development of geographic atrophy in age-related macular degeneration. Invest Ophthalmol Vis Sci 2001; 42:1051-1056

58. Ridley H. Intra-ocular acrylic lenses; a recent development in the surgery of cataract. Br J Ophthalmol 1952; 36:113-122

59. Clayman HM. Ultraviolet-absorbing intraocular lenses. J Am Intraocul Implant Soc 1984; 10:429-432

60. Peyman GA, Sloan HD, Lim J. Ultraviolet light absorbing pseudophakos. J Am Intraocul Implant Soc 1982; 8:357-360

61. Lindstrom RL, Doddi N. Ultraviolet light absorption in intraocular lenses. J Cataract Refract Surg 1986; 12:285-289

62. Lin KK, Lin YC, Lee JS, Chao AN, Chen HSL. Spectral transmission characteristics of spectacles, contact, and intraocular lenses. Ann Opthalmol 2002; 34:206-215

63. Niwa K, Yoshino Y, Okuyama F, Tokoro T. Effects of tinted intraocular lens on contrast sensitivity. Ophthalmic Physiol Opt 1996; 16:297-302

64. Mainster MA, Sparrow JR. How much blue light should an IOL transmit? Br J Ophthalmol 2003; 87:1523-1529

65. Mencucci R, Mercatelli L, Fusi F, Ponchietti C, Monici M, Menchini U. AcrySof Natural intraocular lens optical characteristics during and after different doses of ultraviolet-visible light illumination. J Cataract Refract Surg 2006; 32:1961-1965

66. Greenstein VC, Chiosi F, Baker P, Seiple W, Holopigian K, Braunstein RE, Sparrow JR. Scotopic sensitivity and color vision with a blue-light-absorbing intraocular lens. J Cataract Refract Surg 2007; 33:667-672

67. Mester U, Holz F, Kohnen T, Lohmann C, Tetz M. Intraindividual comparison of a blue-light filter on visual function: AF-1 (UY) versus AF-1 (UV) intraocular lens. J Cataract Refract Surg 2008; 34:608-615

68. Muftuoglu O, Karel F, Duman R. Effect of a yellow intraocular lens on scotopic vision, glare disability, and blue color perception. J Cataract Refract Surg 2007; 33:658-666

69. Schwiegerling J. Blue-light-absorbing lenses and their effect on scotopic vision. J Cataract Refract Surg 2006; 32:141-144

70. Shah SA, Miller KM. Explantation of an AcrySof Natural intraocular lens because of a color vision disturbance. Am J Ophthalmol 2005; 140:941-942

71. Werner JS. Night vision in the elderly: consequences for seeing through a "blue filtering" intraocular lens. Br J Ophthalmol 2005; 89:1518-1521

72. Lipetz LE. A neural mechanism of the Purkinje shift. Am J Optom Arch Am Acad Optom 1962; 39:188-194

73. Mayer S, Wirbelauer C, Pham DT. [Functional results after intraocular lens implantation with or without blue light filter: an intraindividual comparison] Klin Monatsbl Augenheilkd 2006; 223:142-146

74. Olson MD, Miller KM. Implanting a clear intraocular lens in one eye and a yellow lens in the other eye: a case series. Am J Ophthalmol 2006; 141:957-958

75. Cionni RJ, Tsai JH. Color perception with AcrySof natural and AcrySof single-piece intraocular lenses under photopic and mesopic conditions. J Cataract Refract Surg 2006; 32:236-242

76. Bhattacharjee H, Bhattacharjee K, Medhi J. Visual performance: Comparison of foldable intraocular lenses. J Cataract Refract Surg 2006; 32:451-455

77. Rodríguez-Galietero A, Montés-Micó R, Muñoz G, Albarrán-Diego C. Comparison of contrast sensitivity and color discrimination after clear and yellow intraocular lens implantation. J Cataract Refract Surg 2005; 31:1736-1740

78. Marshall J, Cionni RJ, Davison J, Ernest P, Lehmann R, Maxwell WA, Solomon K. Clinical results of the blue-light filtering AcrySof Natural foldable acrylic intraocular lens. J Cataract Refract Surg 2005; 31:2319-2323